A STUDY ON AGENT-BASED MODELING AND SIMULATION FOR ANALYZING PEDESTRIAN URBAN SPATIAL SAFETY

歩行者の都市空間安全性分析のためのエージェント・ベースド・モデリングとシミュレーションに関する研究

by

LIU YUANYUAN

M. Arch, Tongji University, 2018
M. Eng, Nagoya Institute of Technology, 2018

A DISSERTATION

submitted in partial fulfillment of the requirements for the degree

DOCTOR OF ENGINEERING

Field of Architecture and Design
Architecture, Civil Engineering and Industrial Management Engineering

NAGOYA INSTITUTE OF TECHNOLOGY
Nagoya, Japan

2021

Approved by:

Supervisor
Kaneda Toshiyuki

Committee
Natsume Yoshinori
Moriyama Koichi
Oki Takuya

To my parents, who raised me with love and patience.

ACKNOWLEDGEMENTS

This work could not have been accomplished without generous help from the below individuals and organizations:

First, I would like to thank my Ph.D supervisor, Dr. Eng. Kaneda Toshiyuki, Professor in the Department of Architecture, Graduate School of Engineering, Nagoya Institute of Technology. I have been studying under his guidance since pursuing my master's degree. As a result, I developed my research interests in pedestrian empirical studies and simulations. The research habits and analytical methods I developed under his instruction will be a treasure for my entire life.

Next, my sincere gratitude goes to my dissertation committee members: Natsume Yoshinori, Associate Professor in the Department of Architecture; Moriyama Koichi, Associate Professor in the Department of Computer Science, Graduate School of Engineering, Nagoya Institute of Technology; and Oki Takuya, Associate Professor in the Department of Architecture and Building Engineering, School of Environment and Society, Tokyo Institute of Technology.

I am sincerely grateful to China Scholarship Council, China, for providing the financial support which made this study possible.

Further heartful appreciation goes to Tongji University, China, for providing a double degree master program, which facilitated my arrival at Nagoya Institute of Technology and allowed me to pursue my study here till today. Furthermore, a special thanks go to my supervisor during my master's study, Zhu Xiaoming, Professor from the Department of Architecture, College of Architecture and Urban Planning, Tongji

University, who has shown sincere concern for my academic and personal development throughout these years.

I also extend my gratitude to all the Kaneda Laboratory members for their sincere help: special thanks to Dr. Cui Mingji, who offered a lot of generous support ever since I was a master's student; special thanks to Dr. Cui Qinglin, his dedicated works deeply inspired me while constructing this dissertation; special thanks to Mizuno Takayuki, chapter 4 would not be possible without his precious video recordings from another study conducted in 2015. Many thanks to Iwata Ayumi and Shimoji Miyu for attending the pedestrian seminar and contributing inspiring ideas. Many thanks to Ishihara Koki for helping with the contact work with the local government. Thanks to Zhang Yufan, Hao Shuqi, Biya Girma Hirpo, Li Guangyu, Liu Wei and Wu Xiaonan, your companionship makes the time in the lab enjoyable. Finally, I'm grateful to the office members, Hirata Keiko and Higashi Mio, for maintaining our daily affairs so efficiently.

I want to thank the seniors from Nagoya Institue of Technology in different laboratories, Dr. Chen Ye and Dr. Xiong Xi. They offered not only great suggestions during my study period but also great friendships and the passing of much enjoyable time together.

A special thanks to Dr. Edward Scruggs and his family, who makes the stay in Japan feel like home.

My heartful thanks go to my parents, Liu Risheng and Liu Huaying. I feel constantly blessed for being their child, and their love and support always make me fearless.

TABLE OF CONTENTS

ACKNOWLEDGEMENTS **I**

LIST OF TABLES **V**

LIST OF FIGURES **VII**

LIST OF ACRONYMS AND ABBREVIATIONS **IX**

SUMMARY **XI**

CHAPTER 1. INTRODUCTION **14**
1.1 Background **14**
1.2 Statement of the Problem **15**
1.3 Purpose of the Study **16**
1.4 Significance of the Study **17**
1.5 Scopes of the Study **17**
1.6 Structure of the Study **18**
1.7 Definition of Terms **20**

CHAPTER 2. EXISTING PEDESTRIAN STUDIES AND SPATIAL SAFETY PROBLEMS 23
2.1 Existing Studies on Crowd Accidents **23**
2.1.1 Crowd Motions and Phenomena 23
2.1.2 Mechanism of Crowd Accidents 26
2.1.3 Triggers of Crowd Accidents 27
2.1.4 Case Study: Duisburg Love Parade Disaster (Germany, July 2010) 29
2.1.5 Case Study: the Hajj Experience (Saudi Arabia, 1975 - 2013) 32
2.1.6 Case Study: Akashi Citizens' Summer Festival Disaster (Japan, July 2001) 36
2.2 Existing Studies on Public Health Under the COVID-19 Pandemic **39**
2.2.1 The Transmission Characteristics of the COVID-19 39
2.2.2 Physical Distancing Policies and Advice Worldwide 39
2.2.3 Pedestrian Avoidance Behavior 40
2.3 Evaluation Schema for Safe Pedestrian Spaces **41**
2.3.1 Static and Dynamic Crowd Density 41
2.3.2 Considering Items of Safe Urban Public Spaces 49
2.3.3 Considering Items of Pedestrian Encounter 51
2.4 Rule-Driven Agent-Based Models and Other Model Types **52**
2.4.1 Models and Simulations of Crowd Behaviors 52
2.4.2 Types of Crowd Simulation Models 53
2.4.3 Evacuation Validation Guidelines and Tests 56
2.4.4 Qualitative and Quantitative Validation Assessments 58
2.4.5 Microscopic Pedestrian Simulation Software 62
2.5 Development of an Agent-Based Modeling and Simulation Framework for Analyzing Pedestrian Spatial Problems **65**
2.5.1 A Categorized Framework of Agent-Based Modeling 65
2.5.2 Spatial Coordinate System and Parameter Setting 67
2.5.3 Development of Agent Behavioral Rulesets 71

2.6 Chapter Conclusions 72

CHAPTER 3. AN ANALYSIS ON RELATIVELY HIGH-DENSITY SPATIAL SAFETY: USING AGENT-BASED SIMULATION FOR ANALYZING PUBLIC SPACE DESIGN BASED ON A CROWD DISASTER 74
3.1 Overview of the Shanghai Bund Crowd Accident 74
3.2 Site Survey: Pedestrian Flow Data 79
3.3 Development of an Agent-Based Simulator for Crowd Safety Analysis 80
3.3.1 Pedestrian Agent Algorithm 80
3.3.2 Pedestrian Behavior Rulesets: ASPFver4.0 81
3.4 Development of Simulation Scenarios 84
3.5 Simulation Results and Discussion 87
3.6 Chapter Conclusions 95

CHAPTER 4. AN ANALYSIS ON LOW-DENSITY SPATIAL SAFETY: USING AGENT-BASED SIMULATION FOR ESTIMATING PEDESTRIAN PROXIMITY PROBABILITY DURING THE COVID-19 PANDEMIC 97
4.1 Overview of the COVID-19 Pandemic 97
4.2 Site Survey: Pedestrian Avoidance Behavior Before and During the COVID-19 Pandemic 98
4.2.1 Data Collection 98
4.2.2 Measured Speed in Each Density Level 101
4.2.3 Personal Spacing Avoidance (PSA) and Long Range Avoidance (LRA) 103
4.3 Development of an Agent Simulator of Contagious Pedestrian Proximity 108
4.3.1 Pedestrian Agent Algorithm 108
4.3.2 Pedestrian Behavior Rulesets: ASCPP 110
4.3.3 Variable Settings 111
4.3.4 Model Validation 112
4.4 Development of Simulation Scenarios 113
4.5 Simulation Results and Discussion 114
4.5.1 Influence of Pedestrians' 'Distancing' Awareness 116
4.5.2 Influence of Mask-Wearing Population 116
4.5.3 Influence of Standing Pedestrians 117
4.5.4 Violation of Physical Distancing with A Contagious Person 117
4.6 Chapter Conclusions 117

CHAPTER 5. CONCLUSIONS 120
5.1.1 Evaluation Scheme for Pedestrian Spatial Safety Problems 120
5.1.2 ABMS Framework for Analyzing Two Specific Spatial Safety Problems 121
5.1.3 Case Study: Shanghai Bund Crowd Accident 122
5.1.4 Case Study: Pedestrian Encounter Under COVID-19 123

APPENDIX A. ANTHROPOMETRIC DATA 125

APPENDIX B. LEVEL OF SERVICES 126

REFERENCES 128

LIST OF TABLES

Chapter 2

Table 1	– Pedestrian density terms.	43
Table 2	– Pedestrian walking stages.	48
Table 3	– Evaluation items for pedestrian facilities.	49
Table 4	– Evaluation items for mass gathering events.	50
Table 5	– Pedestrian proximity zones.	51
Table 6	– Existing verification and validation guidelines.	58
Table 7	– Diagram for chapter conclusions.	73

Chapter 3

Table 8	– Timeline of the Bund crowd accident.	78
Table 9	– Average entrance visitor number of the surveyed area (people/minute).	80
Table 10	– Explanations of ASPF rulesets and rule adapt priorities.	82
Table 11	– Simulation scenario settings.	84
Table 12	– Agent amount in different scenarios.	91

Chapter 4

Table 13	– Pedestrian origin-destination matrix measured in 2015 and 2020.	101
Table 14	– Analysis of covariance on speed.	103
Table 15	– Analysis of variance on avoidance distance (PSA).	106
Table 16	– Analysis of variance on avoidance distance (LRA).	106
Table 17	– Analysis results of personal spacing avoidance (PSA) behavior and long-range avoidance (LRA) behavior.	107
Table 18	– Model validation results.	112
Table 19	– Scenario design.	113

Table 20 – Simulation results of the agent distribution in each proximity zone. 115

Table 21 – T-test of Sc.000 and Sc.100 simulation results. 116

Appendix

Table 22 – Anthropometric sizes of the world's population (adults). 125

Table 23 – Relationships between pedestrian status and density in Level-of-Services. 127

LIST OF FIGURES

Chapter 1

Figure 1 – Structure of the dissertation. 20

Chapter 2

Figure 2 – Venue layout of the Love Parade, 2010 (map redrawn by the author based on Helbing et al., 2012). 30

Figure 3 – Comparison of the old and the new Jamarat Bridge (Imam & Alamoudi, 2014). 33

Figure 4 – Asagiri Overpass at Okura Beach (photo by the author). 38

Figure 5 – Illustration of the crowd density between 1 – 6 people/m2 (world population). 42

Figure 6 – Illustration of the crowd density of fewer than 1 person/m2. 43

Figure 7 – Dynamic crowd density experiment with Japanese adults (age 20 – 25, male, indoor clothes). 45

Figure 8 – Dynamic crowd density experiment with Chinese adults (age 20 – 35, male, winter clothes). 47

Figure 9 – Agent's proximity zones. 51

Figure 10 – Geometric layout of NIST verif.2.9. test: group behaviors. 57

Figure 11 – A categorized framework of agent-based modeling. 67

Figure 12 – The simulation process. 67

Figure 13 – Illustration of the absolute and relative coordinate systems (draw based on Kaneda et al., 2010). 68

Figure 14 – Outline of conversion between coordinate systems (draw based on Kaneda & Okayama, 2007). 69

Figure 15 – Illustration of the routing. 71

Chapter 3

Figure 16 – The Bund Scenic Area, A: Chen Yi Square, B: Waitan-Yuan, the actual event location (drawn by one of the authors based on the detailed plan of the urban design & site plan Shanghai Bund Waterfront by Xi & Xu, 2011). 75

Figure 17 – The three elevations of the road, square, and viewing platform of Chen Yi Square (snapshot from the survey video by one of the authors). 76

Figure 18 – Simulation area, agent generation areas (from A to J), and the waypoint network (drawn by one of the authors based on satellite map). 79

Figure 19 – Pedestrian agent's algorithm. 81

Figure 20 – Explanation of pedestrian behavior rules of ASPFver4.0 (Kaneda & Okayama, 2007). 83

Figure 21 – Scenario settings (a. the original space layout in 2014; b. use separation facilities to form rotary traffic; c. add pillars to divide pedestrian traffic; d. add belt separation facilities after the crowd accident; e. set capacity reserve area and the viewing platform; f. the route control plan implemented after the crowd accident). 85

Figure 22 – Local density simulation results shown by density measurement areas. 89

Figure 23 – Local density simulation results shown by scenarios. 89

Figure 24 – Snapshots of simulations in two-times surveyed pedestrian flow-in value in different scenarios. 90

Chapter 4

Figure 25 – Spatial layout of the atrium in Nagoya Station. 100

Figure 26 – Sight field from the video-recording spot in 2020. 100

Figure 27 – Measured speed in each density level. 102

Figure 28 – Pedestrian’s personal spacing avoidance (PSA) behavior and long-range avoidance (LRA) behavior. 104

Figure 29 – Pedestrians’ avoidance distance in each density level. 105

Figure 30 – Pedestrian agent’s algorithm. 109

Figure 31 – ASCPP pedestrian behavior rulesets. 111

Figure 32 – Waypoint network and simulation snapshot. 114

Figure 33 – Agent number in each proximity zone. 115

Appendix

Figure 34 – Fruin Body Ellipse. 126

LIST OF ACRONYMS AND ABBREVIATIONS

ABM	Agent-based modeling
ABMs	Agent-based models
ABMS	Agent-based modeling and simulation
ACS	Absolute coordinate system
ANOVA	Analysis of variance
ANCOVA	The analysis of variance
ASCPP	Agent Simulator of Contagious Pedestrian Proximity
ASPFver4.0	Agent Simulator of Pedestrian Flow version 4.0
BG	Big gesture avoidance behavior
CA	Cellular automata model
CDC	Centers for Disease Control and Prevention of the United States
CV	Covariates
DV	Dependent variable
IV	Independent variable
LRA	Long-range avoidance behavior
MAS	Multi-agent simulation
MG	Mass gathering event
OD	The origin-destination pairs
PSA	Personal spacing avoidance behavior
RCS	Relative coordinate system
SF	Social force model
V & V	Verification and validation
WHO	World Health Organization
NIST	National Institute of Standards and Technology

IMO International Maritime Organization

SUMMARY

Agent-based modeling and simulation (ABMS) research of pedestrians is expected to solve spatial safety problems. Evacuation studies, focusing on unidirectional flows and evacuation time, have entered the practical stage of commercial software development and have built evaluation guidelines of verification and validation (V&V). However, for spatial safety problems where bi-directional flows and multi-directional flows are involved, such as crowd accident prevention and infection risk reduction, a research framework is still being formed. After the Shanghai Bund crowd accident in 2014, architects' discussion of improvement proposals has highlighted the importance of spatial design and management. The prevalence of COVID-19 adds a new challenge in addition to the above aspects with the requirements of physical distancing policies.

This dissertation explores an ABMS framework for analyzing two specific spatial safety problems in urban public spaces related to crowd accidents and the COVID-19 pandemic infection. This dissertation adds its significance in (1) summarizing an evaluation scheme for the above problems based on the review of crowd accidents, public health, and ABMS studies (2) describing structures and characteristics of the behavioral rule-driven pedestrian agent (3) conducting an ABMS based on the records of the Shanghai Bund accident to study the spatial design and crowd management strategies and (4) conducting an ABMS based comparative study of pedestrian avoidance behavior before and during the COVID-19 pandemic to estimate the proximity probability between pedestrians. The scope of this dissertation covers a general review of existing pedestrian-related problems and corresponding simulation development, and utilizing a developed ABMS framework for problem-solving.

Chapter one presents the research background, problem, purposes, significance, scope, structure, and explanation of the terminology.

Chapter two reviews existing studies on crowd accidents, public health under a pandemic condition, and the situation of ABMS. An evaluation scheme for the targeted spatial problems is then summarized. In addition, a general ABMS framework with the behavioral rule-driven pedestrian agent is explored.

In chapter three, the Shanghai Bund crowd accident is analyzed using publicly available videos and documents. A model is constructed reproducing a relatively high-density situation of 3 to 5 people/m^2. By comparing five replacement scenarios, including three improvement designs and two crowd management strategies in addition to the basic scenario, this chapter: 1) identifies several possible causes of the accident, 2) generalizes some common points to be avoided in designing public spaces, and 3) clarifies the importance of efficient crowd management.

In chapter four, an ABMS is applied to estimate pedestrian proximity probability during the COVID-19 pandemic in a station atrium. A video comparison analysis is conducted before and during the pandemic focusing on pedestrian avoidance behavior in a low-density space of 0.1 to 0.5 people/m^2. The result shows that the average starting distance of pedestrians' avoidance behavior is longer during a pandemic, which may reflect people's awareness of 'distancing'. Therefore, avoidance behavior is divided into two categories, personal spacing avoidance (PSA) and long-range avoidance (LRA). Based on the findings, the chapter develops Agent Simulator of Contagious Pedestrian Proximity (ASCPP), reflecting those two types of avoidance and has 16 behavioral rules. We simulate the counter flows in the atrium with five scenarios that deal with the ‘distancing’ awareness, facial masks, and the obstruction of flow by the presence of

people standing still, and estimates the effect of each scenario on the probability of proximity assuming a ratio of 1% contagious people in the population.

Chapter five summarizes the research and findings, and discusses future issues.

CHAPTER 1. INTRODUCTION

1.1 Background

Agent-based modeling and simulation (ABMS) research, including agent-based modeling (ABM) and multi-agent simulation (MAS) research, has shown unique advantages for solving spatial safety problems. On the one hand, evacuation studies, focusing on unidirectional flows and evacuation time, have entered the practical stage of commercial software development and built evaluation guidelines of verification and validation (V and V). On the other hand, for spatial safety problems where bi-directional flows and multi-directional flows are involved, such as crowd accident prevention and infection risk reduction, a research framework is still being formed.

Complex Systems are a discipline studying how parts of a system and their relationships lead to the collective behaviors of the system and how the system interrelates with its environment (Bar-Yam, 2002). The pedestrian system is a typical example of a complex system: individuals interact and influence each other and form a pedestrian system, where the characteristics of the system emerge and affect the individuals in this system in turn. It is 'complex' because the characteristics of those interactions are spontaneously generated, nonlinear, and emerged with a series of complex phenomena.

The complexity of the pedestrian system determines that the understanding and reproduction of complex pedestrian phenomena demand sophisticated autonomous models. Even though many pedestrian data can be acquired through empirical and experimental observation, computer simulation is still a complementary technique for hypothesis testing and scenario analysis (Helbing & Balietti, 2011).

1.2 Statement of the Problem

The pedestrian urban spatial safety problems considered in this dissertation is the safety issues arising from pedestrian gathering and interactions in urban public spaces. Countermeasures of such problems are two-folded: spatial design and crowd management. When the problem cannot be solved or alleviated through those measures, it usually means that space is not suitable for the intended function. The spatial safety problems are closely related to crowd formation: unidirectional, bidirectional, and multi-directional flow.

In places of public assembly, the design of an effective evacuation strategy is one of the first safety concerns. Evacuation studies, focusing on unidirectional flows and evacuation time, have developed many analysis systems, such as pedestrian flow analysis, crowd analysis, and egress analysis systems. Many computer simulation models based on those systems have entered the practical stage of commercial software development and built evaluation guidelines of verification and validation (V and V). Most of those models treat human traffic as uniform individuals that follow the mathematics of fluid dynamics or other formulas defined by empirical observations. Those evacuation models may suit well most basic architectural space layout but cannot work well in complex space layouts nor provide a comprehensive range of scenario testing. Besides, in spaces with special functional requirements, outdoor urban public spaces, and mass gathering events, it is necessary to anticipate the problems that may occur during an emergency, especially considering the complexity of human behaviors.

Another problem related to the pedestrian gathering is the crowd accidents associated with the mass gatherings held worldwide. Almost every year, hundreds or even thousands of lives have been claimed in crowd accidents or other secondary

injuries. A crowd accident can happen during an emergency evacuation process (unidirectional flow) or cause by other different situations that lead to trampling or crushing (bidirectional or multi-directional flow). Various festivals, religious events, football matches have always been a high incidence of crowd accidents. In the recent decade, researchers tend to understand the failure of a crowd gathering as a 'systematic failure', where different crowd factors fail to balance and eventually lead to the system stability collapse. When we analyze those past failed crowds in detail, some accidents are primarily attributed to design flaws (or venue suitability), others are primarily attributed to a lack of understanding of crowd dynamics (inappropriate or insufficient crowd management). However, while many studies have focused on fact-findings or releasing the mechanism of a crowd accident, unexpectedly, less discussion has been made on keeping the density low and plan a safe public space for crowd assembly.

COVID-19, an undergoing worldwide pandemic that emerged since the end of 2019, brings new challenges to crowd safety. Crowd density not only needs to satisfy the requirement of safe evacuation and crowd gathering but fulfill the requirement of physical distancing. The capacity of a public space where people are static is easy to calculate, but for space with dynamic pedestrians, pedestrian flow rate and the interpersonal encounter is not in a linear relationship. Besides, public space's opening strategy is also constantly being adjusted to balance life safety and economic affordability. Countermeasures under such circumstances need analytical tools.

1.3 Purpose of the Study

With the background of the described pedestrian spatial safety problems, this study contains the following purposes:

(1) Summarize an evaluation scheme for pedestrian spatial safety problems;

(2) Explore an ABMS framework for analyzing two specific spatial safety problems in urban public spaces crowd accidents and pandemic infection.

1.4 Significance of the Study

This study has its significance in different aspects. First of all, an evaluation scheme for spatial safety problems was summarized based on reviewing crowd accidents, public health, and ABMS studies. This scheme lists the considered factors for public space evaluation towards various problems and gives some quantitive reference standards.

In recent decades, different types of agent-based models (ABMs) have been developed. Comparing to all the other ABMs, behavioral rule-driven pedestrian agents have their unique advantages. We summarize and discuss the structures and characteristics of behavioral rule-driven pedestrian agents. Based on the findings, an ABMS framework for analyzing spatial safety problems is explored.

Two detailed case studies corresponding to the aimed two spatial safety problems are provided utilizing the ABMS framework we developed. For the crowd gathering problem, thorough research on the records of the Shanghai Bund accident is conducted to study the spatial design and crowd management strategies. For the infection risk problem, we compare pedestrian behaviors before and during the COVID-19 pandemic in an atrium in Nagoya Station and estimate the pedestrian encounter with a 'proximity probability' concept we proposed. The later research also has its value in facilitating studies towards the emerging low-density pedestrian field.

1.5 Scopes of the Study

The scopes of this study include:

(1) Review the existing pedestrian studies: When reviewing the existing studies on pedestrian crowd accidents, the completion of understanding crowd dynamics is stressed. A few previous happened crowd accidents that profoundly impact this research field are analyzed through literature surveys. When reviewing the public health studies under the pandemic, the transmission characteristics of the COVID-19 and physical distancing policies worldwide are stressed.

(2) Summarize safe pedestrian space evaluation schema: We conduct two simple groups of pedestrian experiments to help understanding crowd status under different density levels. Based on the experiment result and findings of the review mentioned above, the factors that should be considered for a safe pedestrian space are summarized. For the factors that can be valued quantitively, we try to give reference values from previous researches.

(3) Explore an ABMS framework: We discussed the structure and characteristics of the behavioral rule-driven pedestrian agent. The differences and advantages of rule-driven ABM comparing with other ABMs are explained. We also summarized the qualitative and quantitative validation assessments being applied in the recent decade and discussed the principles of validating an ABM. An ABMS framework is developed for the upcoming case studies in this dissertation.

(4) Utilization of the ABMS framework and evaluation schema: a case study of the Shanghai Bund crowd accident and a case study of an atrium in Nagoya Station for infection risk reduction are analyzed separately.

1.6 Structure of the Study

This dissertation is composed of five chapters, and the considerations of each chapter will be introduced one by one.

Chapter one presents the research background, purpose, structure, and explanation of the terminology used in this dissertation.

Chapter two reviews existing studies on crowd accidents, public health under pandemic conditions, and ABMS. An evaluation scheme for the targeted spatial problems is then summarized. In addition, a general ABMS framework with the behavioral rule-driven pedestrian agent is explored.

In chapter three, the Shanghai Bund crowd accident is analyzed using publicly available videos and documents. A model is constructed reproducing a relatively high-density situation of 3 – 5 people/m^2. By comparing five scenarios, including three improvement designs and two crowd management strategies in addition to the basic scenario, the author 1) identifies several possible causes of the accident, 2) generalizes some common points to be avoided in designing public spaces, and 3) clarifies the importance of efficient crowd management.

In chapter four, the author applies an ABMS to estimate pedestrian proximity probability to contagious pedestrians during the COVID-19 pandemic in a transit station atrium. The author conducted a video comparison analysis before and during the pandemic focusing on pedestrian avoidance behavior in a low-density space (0.1 – 0.5 people/m^2). The result shows that pedestrians have different avoidance awareness in ordinary and pandemic situations, and their avoidance behaviors were different between personal spacing avoidance (PSA) and long-range avoidance (LRA). Based on the findings, the author develops Agent Simulator of Contagious Pedestrian Proximity (ASCPP), reflecting those two types of avoidance as behavioral rules. The simulation

results show that the factors affecting pedestrian proximity probability are the mask-wearing rate, the awareness of physical distancing, and the presence of stationary pedestrians, in that order.

Chapter five summarizes the research and findings, and discusses future issues.

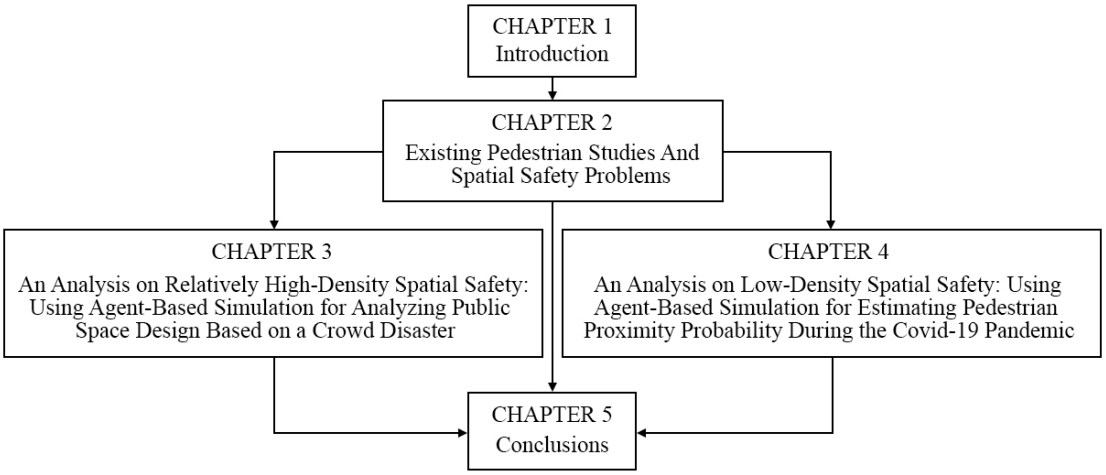

Figure 1 – Structure of the dissertation.

1.7 Definition of Terms

Capacity: The maximum number of people that a venue or facility can accommodate.

Crowd density: The number of people per unit area. In this dissertation, we use people per square meter as the unit.

Crowd dynamics: It can be defined as the study of how and where crowds form, and move, above the critical density threshold of more than one person per square meter (Still, 2000). Crowd dynamics can be analogies with gases, fluids, and granular media at different densities, and despite those simplifications, many self-organization phenomena are also observed (Helbing & Johansson, 2010).

Crowd turbulence: Unanticipated and unintended irregular motion of people into different directions due to strong and rapidly changing forces in crowds of extreme density. The definition is adapted based on (Helbing & Johansson, 2010). Crowd turbulences have been observed from many previous accidents, and crowd accidents are already happening when it happens.

Crushing: People suffering from the high compress pressure in a high-density crowd and the fatalities may occur from asphyxiation while still standing. The definition is adapted based on (Lee & Hughes, 2005).

Mass gathering (MG) event: A MG event is defined by WHO as "any occasion, either organized or spontaneous, that attracts a sufficient number of people to strain the planning and response resources of the community, city or nation hosting the event" (Alshammari & Mikler, 2015). Common MG events include sports, music, religious and political events, and at least 1000 people must attend the event to be qualified as an MG event (Owaidah et al., 2019).

Panic: Refers to the anxious state of people unable to act rationally during an emergency. It also indicates the behavior of people pushes each other to escape the pressure. Survival behaviors of people under extreme crowd conditions are often misused as panic by the media. It is a controversial word to use because, in most crowd accidents, people did not lose their rationality. The definition is adapted based on (Helbing et al., 2007a)(Helbing & Johansson, 2010).

Pedestrian flow rate: The number of pedestrians passing a point per unit time (Fruin, 1971). Flow is the most crucial characteristic for pedestrian planning because it determines the width of pedestrian facilities. It is often expressed as pedestrians per meter per minute or pedestrians per meter per second.

Self-organized phenomenon: The spontaneously organized pedestrian movement patterns that are not induced by initial or boundary conditions, by regulations or constraints (Helbing & Johansson, 2010).

Shockwave: A compression wave happens when the crowd density allows no space between individuals (Still, 2014). Shockwaves have been observed from many previous accidents and are dangerous.

Stampede: It is an inaccurate description of a crowd accident and is often related to crowd panic, often seen in the media reports. 'Stampede,' to some extent, blames the brutality of the crowd instead of analyzing the causal relationships of a crowd accident. In this dissertation, we use the terminology reflecting the mechanism of crowd accidents, such as 'trampling,' 'crushing,' 'shockwave,' and 'crowd turbulence' instead.

Trampling: People fall and cannot stand up again in a moving crowd, usually in a relatively high density of 3 – 5 people/m^2. The fatalities may occur from the percussion by others' feet or by asphyxiation by others tripping and falling on top. Trampling will occur before crushing, but it does not occur in static crowds. The definition is adapted based on (Lee & Hughes, 2005).

CHAPTER 2. EXISTING PEDESTRIAN STUDIES AND SPATIAL SAFETY PROBLEMS

2.1 Existing Studies on Crowd Accidents

The Broad meaning of the word ‘crowd’ can mean any situation that involves two individuals interacting with each other. While for specific researches, the precise definition should be discussed case by case. A few key criteria characterise a crowd: size, density, time, collectivity, and novelty (Challenger et al., 2010). The crowd consist of individuals but also includes the interactions between them. The interactions are partially fluid, partially granular and partially psychological related (Still, 2000).

To ensure a safe crowd gathering, understanding pedestrian and crowd behaviors, the reasons for formation, and formation patterns are necessary. This section first reviews crowd motions and self-organization phenomena and then reviews the mechanism and triggers of crowd accidents. Studies of three previous crowd accidents are reviewed: the Love Parade, the Hajj experience, and the Akashi accident. We introduce each case by order of the government accident investigation report, expert report, and modeling and simulation studies.

2.1.1 Crowd Motions and Phenomena

2.1.1.1 Crowd Motions

Pedestrian flows can be roughly divided into unidirectional, bidirectional, and crossing flows. Unidirectional flow is a benchmark for calculating the capacity of roads. Furthermore, safe evacuation design is usually assumed to be unidirectional flow. The probability of conflict in unidirectional flow is low. Crowd motions under

unidirectional flow include 1) straight flow, 2) rounding a corner, 3) entering a bottleneck, and 4) exiting a bottleneck (Duives et al., 2013). In bidirectional flows, people head in two directions facing each other. Bidirectional flows can be observed on the staircase, pedestrian streets, and crosswalks. Crowd motions under crossing flows include 1) intersecting flows, 2) more than two flows crossing, and 3) random flows (Duives et al., 2013).

2.1.1.2 Self-Organization Phenomena

Self-organization phenomena are spatio-temporal patterns that are not externally planned, prescribed, or organized. Instead, they emerge due to the non-linear interactions of pedestrians (Helbing & Johansson, 2013). Understanding self-organization phenomena is helpful to understand how the crowd density accumulated before a crowd disaster. In the following, we will summarize the phenomena that can be commonly observed with different cultural backgrounds (Helbing et al., 2002)(Helbing et al., 2005)(Helbing & Johansson, 2013).

Lane formation: Oppositely moving pedestrians are forming segregation (lanes) to reduce walking conflicts. Lane formation increases the efficiency of walking, and the desired walking speed is maximized.

Oscillatory flows at bottlenecks: At bottlenecks, bidirectional flows of moderate density oscillatory change the control of flow direction. The existence of oscillatory flows will reduce pedestrian speed and pedestrian flow rate. A long bottleneck has a more severe blockage of flow than a short bottleneck. In extreme density, there will be clogging instead of oscillatory flows.

Strip formation in intersecting flows (the zipper-effect): The pedestrian flow often appears to be irregular in intersection areas. However, in some density situations, where pedestrian flows cross each other only in two directions, the strip formation phenomenon is observed. Strip formation is a segregation phenomenon. The pedestrian strip extends in a direction perpendicular to its desired direction. Strip formation phenomenon allows pedestrians to continue walking without having to stop.

Herding and ignorance of available exits: People tend to imitate the behavior of others when they are not sure what to do (Helbing et al., 2005)(Helbing & Johansson, 2013).

The faster-is-slower effect: The evacuation process will take more time if performed at high speed (Helbing & Johansson, 2013).

Queueing behavior: During the queuing process, if the front queue is not moving for a long time, people will continuously reduce the distance between them to create an illusion of advancement. As the waiting time increases, the crowd pressure will increase.

Stop and go waves (shock wave): Stop and go waves are a very dangerous symptom that indicates a crowd accident is about to happen. This phenomenon can happen on flat ground and is related to a significant drop in pedestrian traffic. This phenomenon was observed in the Hajj crowd accident video analysis on January 12, 2006 (Helbing et al., 2007b). The maximum density reaches about 7 people/m^2, lasting 20 minutes (Helbing et al., 2007a). In a pedestrian experiment conducted by Still and colleges, six or seven (depending on the body size) people were asked to stay in a one-meter square. They then gave the person on the corner a diagonally push across the group. The whole group moved, and the person on the opposite side corner is often pushed out of the square (Still, 2004). They name this phenomenon 'compression wave' or 'shock wave'

when the crowd density allows no space between individuals. There are many accidents where shock waves have been observed, such as Love Parade, Hajj, the Jamarat Bridge, Shanghai Bund.

Crowd turbulence: Crowd turbulence, or crowd quake, refers to the crowd situation when balancing high-density breaks and people show the unintended irregular motion in multiple directions. It happens at extreme densities with random flow characteristics, and it is a determining warning sign in advance of crowd disasters. It is observed in the Hajj crowd accident on January 12, 2006, following the stop and go wave. The reason for this phenomenon is still under discovery (Helbing et al., 2007b). The current understanding is that crowd turbulence will occur only under a density of 10 people/m^2 or more (Okada, 2011). The Akashi crowd accident mechanism is more appropriately described as 'crowd turbulence' instead of 'tramping' (Akashi Citizen's Summer Festival Accident Investigation Committee, 2002).

2.1.2 Mechanism of Crowd Accidents

Understanding the mechanism of crowd accidents is helpful to analyze the spatial safety of crowd activities. Crowd accidents may occur due to an emergency evacuation, irrational behavior of the crowd, lack of site design and management, or caused simply by overloaded crowd capacity.

A few researchers have concluded the key factors that lead to crowd disasters. Fruin used the acronym ‘FIST’ to provide a basic understanding of crowd disasters: the crowd force (F), the information (I), the physical space (S), and time (T) (Fruin, 1993). Dickie concluded that inadequate planning, excited crowd, lack of crowd management and a flaw or hazard in a facility are the common threads that lead to a crowd accident (Dickie, 1995). However, most of the time, there is more than a single reason that breaks

down the crowd system's coordinate (Helbing & Mukerji, 2012). Different self-organization phenomena can explain why pedestrians accumulate an unusually high density in some spots. One of the fatal consequences of crowd accidents comes from asphyxia, lead by trampling or crushing. Even though it is statistical whether a crowd accident will occur in a particular situation, the probability is closely related to the crowd density. Also, the initiation densities for trampling, crushing are different (Lee & Hughes, 2005).

2.1.2.1 Trampling

Trampling occurs only in moving crowds and usually happens before crushing. On the other hand, the Domino effect is related to trampling, and it refers to the crowd accident that occurs when someone falls and people are pushed down. When a domino effect happens, people scroll from the back to the front linearly, and it usually occurs under a density of between 3 to 5 people/m^2 (Okada, 2011).

2.1.2.2 Crushing

Crushing can occur in a static or a dynamic crowd after trampling. Research shows that when people stand still in a density of 7 people/m^2, they start to feel constant pressure from others, and people may lift their arms to create space for their chests (Okada, 2011). For moving crowds, the density of 7 people/m^2 is close to a fluid mass (Helbing & Mukerji, 2012). It should be noted that because of the difference of anthropometric data over the countries, as shown in Table 22 in Appendix A, related density for the initiation of crushing varies largely.

2.1.3 Triggers of Crowd Accidents

Crowd disasters are usually triggered by one or more factors, adapted based on Okada, 2011. These triggering factors can be classified as spatial design and crowd management problems, and irrational psychology. Because the suitability of a spatial layout is closely related to the event function, we put triggers in spatial design and crowd management problems together in this discussion.

1) Triggers in spatial design and crowd management problems :

Group conflict: Different pedestrian groups have to push each other to move forward.

Construction collapse: Walls or handrails collapse and cause accidents because of crowd pressure or collisions. Construction collapse can happen when the strength of walls or handrails is insufficient, and the high-density crowd tries to push forward.

Accident fall: Someone falls and triggers a domino effect. Even though a pedestrian can fall because of an inappropriate spatial design, a certain density (usually 3 to 5 people/m^2) is needed for a domino effect, attributed to the crowd management problem.

Crowd turbulence: In extreme crowd density, people fall in different directions. If the crowd condition does not allow to fall around, the crowd will collapse internally because of space felt people left. Crowd turbulence occurs on flat ground.

2) Triggers of pedestrian irrational psychology include:

Break limitation: Facilities used to limit the crowd fails to restrict pedestrians. For example, ropes, wooden, or metal fences can be broken easily.

Penetration: Other people entered the pedestrian flow suddenly.

Panic: Irrational behavior caused by people who want to escape the situation caused due to danger or false information.

Aggressive crowd: The crowd is aggressive because of anger or excitement, mostly seen in football matches.

2.1.4 Case Study: Duisburg Love Parade Disaster (Germany, July 2010)

Overview of the situation Love Parade was a famous music festival in Germany first held in Berlin in 1989 for many years until 2003. From 2004 to 2009, Love Parade was moving between different cities, and in many years, it was cancelled for various reasons. The last Love Parade was held in Duisburg on July 24, 2010, and a crowd accident occurred, causing 21 death and more than 500 injuries. Compared to other terrible crowd accidents, the Love Parade stands out because seven security cameras have well documented it.

Venue description Figure 2 shows the venue layout of the 2010 event and the surveillance camera screens. The event venue for the 2010 Love Parade is an abandoned train station with a usable area of around 96,000 m^2. The main stage area is located north of the venue, surrounded by a circle of music trucks. Most audiences come to the venue through a highway from the west side of the site. Karl-lehr street is the only path for entering the venue. There were crowd control points at the east and west ends of that street. The Karl-lehr street passes through the bottom of three bridges, making a naturally two-storey height difference in the site. After passing through the crowd control points, pedestrians enter the main stage area through the main ramp. There is a narrower secondary ramp planned as an evacuation exit.

The accident The event was initially planned to open at 11:00 but was delayed by one hour. During this waiting time, the crowd piled up at the entrance. Approximately 105,000 people arrived at the venue before 14:00, and the crowd density can be calculated, which is around 1 person/m^2. Severe congestion was formed at the north end of the main ramp around 13:00. The police established a human cordon at each end of Karl-lehr street and the bottom of the main ramp, around 16:00, to control the increasing density. This move is very controversial. Those cordons were released one by one in about 20 minutes. One crowd accident happened at about 16:30 at the southern end of the main ramp cordon. The evacuation ramp was locked at the beginning but was opened after the situation becomes urgent. However, very few people have noticed there was an evacuation road available.

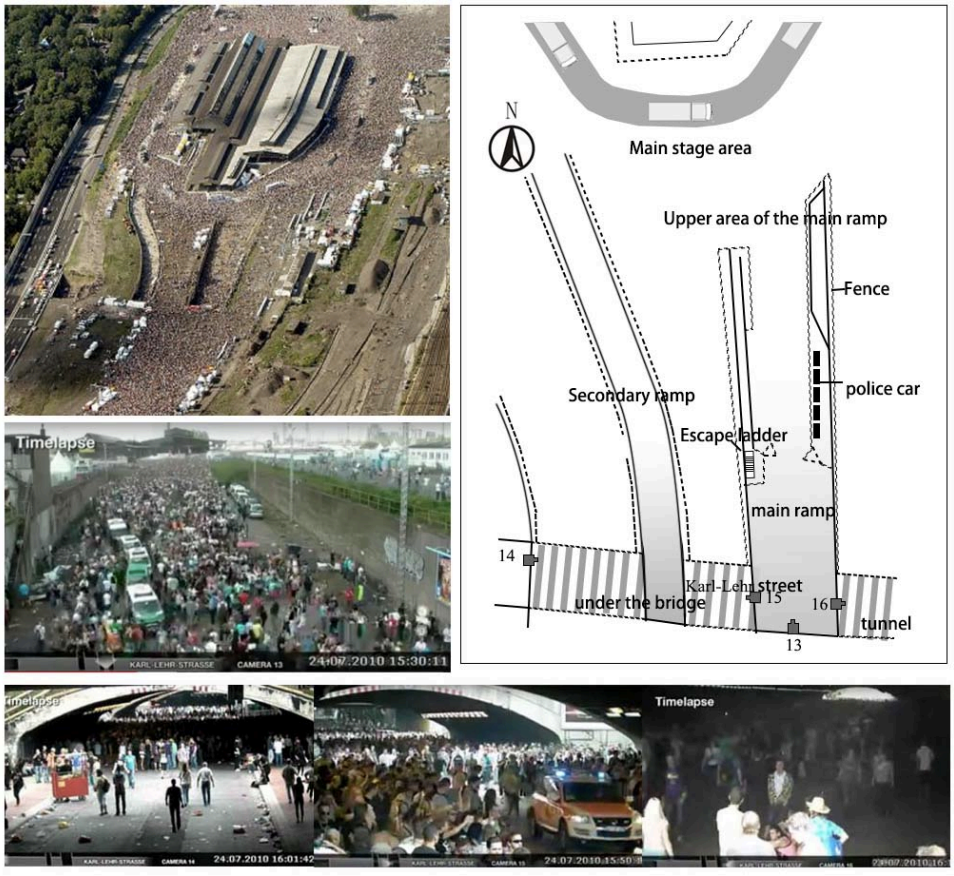

Figure 2 – Venue layout of the Love Parade, 2010 (map redrawn by the author based on Helbing et al., 2012).

We reviewed the studies on the fact-findings and simulation and modeling studies on Love Parade crowd accident in the followings:

Helbing & Mukerji, 2012 revisited this accident's causality and revealed several misunderstandings through qualitative analysis of the video recordings. They attributed the accident to the domino effect resulting from crowd turbulence phenomena. Their analysis indicated that in Duisburg, crowd turbulence is the consequence of systemic instabilities. They also introduced a new scale to assess the criticality of crowd conditions.

Krausz & Bauckhage, 2012 presented an automatic, video-based analysis of the Love Parade event. Their automatic vision system can detect motion patterns that characterize crowd behavior in crowd accidents.

Pretorius et al., 2015 utilized a fine mesh evacuation model, buildingEXODUS, combining the data of pedestrian flow and space utilisation to indicate the onset of potentially dangerous population densities for large crowd modeling. To predict the onset of crowd crush conditions, they first identified the criteria that might lead to crushing conditions and then allow those conditions to be identified within a simulation. The limitation of this approach is that pedestrian characteristics are oversimplified.

Summary of the findings The reason analysis of the Love Parade crowd accident shows 1) The fatal factors rarely happen alone but have interdependent system coordination; 2) The crowd system needs to be planned with a certain resilience to resist the systemic instabilities. A resilient pedestrian system considers factors that include capacity reserve, separation of in- and outflows, and a separate route for emergency vehicles; 3) There are several methods to stop the cascading effects of unfavourable crowd factors, including choosing a more suitable venue, adapting higher

organizational standards, preparing superior emergency plans at bottlenecks, avoiding obstacles, considering the location of rescue units, and cordon locations, consider the location for information stand and so on.

2.1.5 Case Study: the Hajj Experience (Saudi Arabia, 1975 - 2013)

Overview of the situation The Hajj is an Islam pilgrimage and the largest annual gathering worldwide. An increasing number of pilgrims travel to Makkah, Saudi Arabia, challenging the site with overcrowding and other problems each year. The whole pilgrim involves four main holy sites and needs to finish in five days. The pilgrims complete their ritual at one site and then move to the following site, bringing enormous crowd movement challenges. The Hajj management authorities have great input in introducing state-of-the-art technologies to modify pedestrian facilities and crowd management. However, despite the Hajj authorities' tremendous efforts, a few thousand people have died, mainly caused by crowd accidents.

Tawaf and Sayee rituals are the first day rituals in the pilgrimage. Pilgrims need to circumambulate the Ka'bah seven times anticlockwise and often create overcrowding problems.

Mina is a valley and neighborhood located in Makkah city, and it consists of city tents and Aljamarat Bridge.

Al-Jamarat Bridge is the site for the 'Stoning the devil' ceremony, where the pilgrims need to throw stones at the pillars to finish the journey. The Al-Jamarat Bridge was originally built in 1975, and three pillars extend through openings in the bridge, allowing the pilgrims to throw stones from the ground or the bridge. Between 1994 to 2006, five major crowd accidents happened, and more than 1000 people were killed on

the Jamarat Bridge(Alaska et al., 2017). Those accidents mainly were attributed to the lack of organization in the 'Stoning the devil' ceremony and the construction of temporary shelters nearby.

The new Jamarat Bridge After the crowd accident in 2006, the Saudi Arabia government decided to reconstruct the Aljamarat Bridge to solve the long-term overcrowding problem. The new Aljamarat Bridge was completed and put into use in 2010. It is featured with five-level floors, multi entrances, and exits, together with an integrated cooling system and CCTV cameras, and can accommodate 300,000 pilgrims per hour. The pedestrian flow is unidirectional in this new bridge (Imam & Alamoudi, 2014). The authority implemented strict time schedules and specific route plans with the newly built Jamarat Bridge and achieved a seven-year history of no crowd accidents.

However, in 2015, due to some pilgrims not following the schedule, another large-scale crowd accident caused 769 deaths and more injuries. A lesson was taught from this tragedy that unidirectional flow and high time accuracy arrangements might not enhance the system's resilience: It makes the system's fault tolerance smaller.

Figure 3 – Comparison of the old and the new Jamarat Bridge (Imam & Alamoudi, 2014).

We reviewed the studies on the fact-findings and simulation and modeling studies on the Hajj experience in the followings:

Helbing & Johansson, 2007 conduct a video analysis study of the crowd disaster during the Hajj 2006 to fill in the lack of experimental data of crowd disasters. The analysis reveals that: 1) the motion of crowd is not entirely stopped even in extreme density up to 10 people/m^2; 2) two sudden transitions, from laminar to stop-and-go flows and turbulent flows, have been observed; 3) the local density can vary considerably compared to the average density due to dynamical patterns in the crowd; 4) analysis of the velocity field, in addition to the local density evaluation, is necessary, to identify the critical times and locations. Al-Kodmany, 2013 presented a summary of research and efforts toward Hajj crowd management. It explained that software could contribute to crowd management in three areas: diagnosing problems, testing designs, and setting operational plans. ABMs, CA models, and fluid mechanics models were employed in their study. Owaidah et al., 2019 conducted a detailed review of the Hajj experience modeling and simulation studies covering 75 full-text articles for qualitative synthesis.

Kurdi, 2017 analyzed the behavior of crowd flows in the Sayee ritual utilizing an ABM addressed with disabled persons and tracking data from real-life videos. Khan & McLeod, 2012 developed a comprehensive Tawaf simulator that calculates metrics including throughput, satisfaction, health, and safety. The simulation experiments generated emergent, tipping point, expected, and counter-intuitive behaviors and concluded a set of Tawaf crowd management guidelines. Kim et al., 2015 reproduced the Tawaf ritual with a MAS that combines velocity-based collision-avoidance algorithms with external physical forces. A series of behaviors are specified using finite-state machines. This simulator can simulate 35,000 agents with a density of up to 8 people/m^2 and generate many emergent behaviors. Sarmady et al., 2008 proposed a multi-layer model that a behavior model simulates the individual's actions while a C.A.

model simulates their small-scale movements. Zainuddin et al., 2009 simulated the circumambulation of the Ka'aba using the pedestrian simulation computer software, SimWalk, which adopts the social force model. Their research mainly focuses on two problems: overcrowding and bi-directional entries in the area. They simulated two alternative spatial plans to mitigate crowd congestion: adapt the spiral path and an underground tunnel or add waiting points around the Ka'ba. The simulation results show that the spiral path plan effectively ensures a smooth flow, but the authors also address that this plan may not be realistic due to costs and historical reasons.

Mahmood et al., 2017 proposed an ABM crowd simulation and analysis framework using the Anylogic platform and integrate the Anylogic simulation environment with the external modules for optimization and analysis. Their framework consists of three layers: 1) a simulation layer for modeling crowd simulation in Anylogic; 2) an interface layer to combine Anylogic with external modules; 3) an optimization and analysis layer. Different crowd evacuation strategies of Hajj are assessed with this framework as a case study. The result shows that the evacuation strategies may vary according to the complexity level of physical and behavioral details. Ilyas, 2013 developed a simulation model in NetLogo to simulate Ramy ('stoning the devil ritual') on Jamrat bridge. They analyzed various shapes of the pillars, including circle, ellipse, and deformed ellipse. Their model analyzed the effect of parameters such as percentage of aggressive and considerate people, view range and hitting a range of the pillars, and time to perform the ritual. Fayoumi et al., 2011 used a microscopic simulation tool. STEPS, to simulate the relationship between the Jamarat basin length and the stoning performance, and the influence of organizing pilgrims in three rows.

Dridi, 2014 has discussed different verification and validation approaches to microscopic simulation models using data collected during Hajj 2009. Their methods include: compare the simulation result with the video recording, compare the simulation results with other models, parameter variability and sensitivity analysis, and compare with optical flow results. The calibrate and validate the PedFlow simulation model is shown compared to other simulation model results, such as Simulex/Myriad. They concluded that PedFlow could produce realistic crowd motion of pedestrians with different speeds, believable trails, and sensible avoidance at medium to high pedestrian densities.

Summary of the findings: The Hajj practice has provided many research materials and laid the foundation for research in this field. The new Jamarat Bridge plan is a notable example of utilizing ABMS to aid pedestrian safety space design. ABMS is useful when answering quantitative questions in a design, such as a bottleneck width or the impact of changing some spatial layouts. When utilizing ABMS for making event schedules and countermeasures, system resilience should also be considered. No matter what design layout is adopted, the on-the-ground assistance measures for MG events are still necessary.

2.1.6 Case Study: Akashi Citizens' Summer Festival Disaster (Japan, July 2001)

Overview of the situation Akashi citizens' summer festival was held at Okura Beach, Akashi City, on July 21, 2001. A crowd accident happened at about 20:45, causing 11 death and 247 injuries. According to the Akashi Citizen's Summer Festival Accident Investigation Committee, the main reason for this accident is that visitors enter and leave the venue met on the Asagiri Overpass and led to the tragedy. In addition, the accident investigation report shows a few judgments on the cause of the accident: 1)

failed to estimate the projected visitor number and did not take enough measures to prevent crowd congestion; 2) unrestricted inflow of people caused overcrowding during fireworks, and by the time the firework ended, there was no flow separation of entering and leaving flows; 3) did not have adequate crowd evacuation plan; 4) did not pay effective real-time attention to the visitors present (Akashi Citizen's Summer Festival Accident Investigation Committee, 2002).

The Asagiri Overpass Figure 4 shows the spatial layout of the Asagiri Overpass. The overpass has a width of 6 meters but was halved to 3 meters at the south end stairs and formed a bottleneck. On the event night, some visitors stopped at the south-end observation deck to watch the fireworks. Also, there were many night stalls just below the overpass that further exacerbated the congestion. The accident investigation report calculated the visitor number by dividing the venue into 12 zones and estimated the crowd density at the peak period. The number of people who stayed during the peak hour was about 83,000, less than the 120,000-150,000 expected in the planning stage. However, it must be noted that the high density of 7 people/m^2 in the aisle of the night stalls is one of the factors leading to the accident. This high density was accumulated from three factors: 1) the width of the stairs is only 3m compared to the 6m width overpass; 2) visitors stopped at the observation deck as the firework starts that stopped the flow; 3) there were night stalls close to the bottom of the stairs that blocked the pedestrian flow.

Kaitsuji & Hokugo, 2014 analyzed a few crowd disasters at mass gathering events by examining their event and security planning. They attribute the failure of these events to three venue-suitability factors: 1) projected visitor number, 2) venue space

planning, and 3) access route for crowd flow. They address the importance of judging venue suitability during the event planning stage.

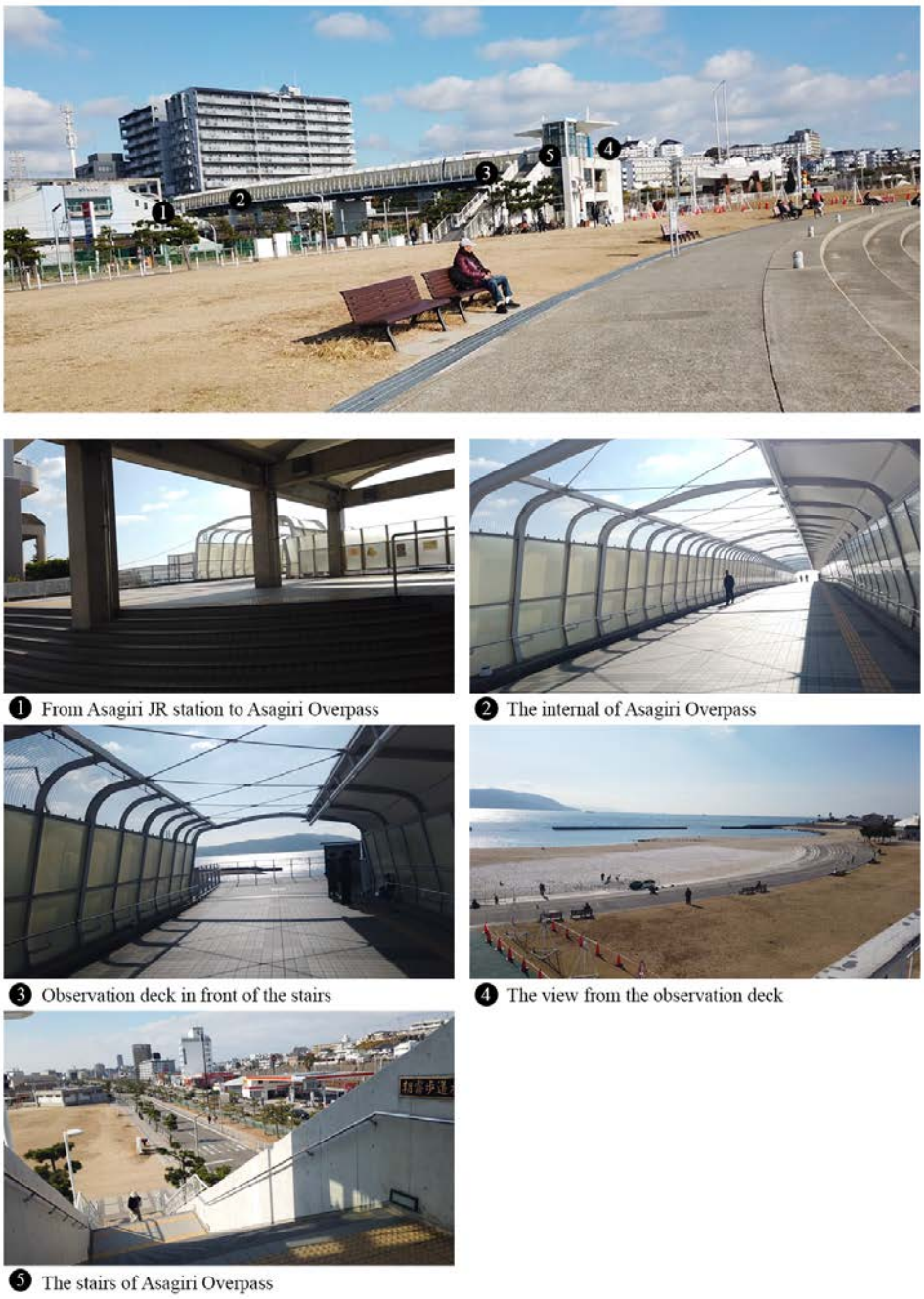

Figure 4 – Asagiri Overpass at Okura Beach (photo by the author).

Kaneda et al., 2003 analyzed the Asagiri Overpass accident through agent-based simulation under an assumption of confrontation flows' hypothesis. They verified pedestrian behavioral rules in the low-density case and then verified the triggering point

of the accident with simulation results. Their simulation results suggest that the collision of the bidirectional flow triggered the increase of density on the overpass and caused the accident.

Summary of the findings Akashi crowd accident offered a highly detailed investigation report and played an educational role in accident prevention following mass gathering events in Japan.

2.2 Existing Studies on Public Health Under the COVID-19 Pandemic

2.2.1 The Transmission Characteristics of the COVID-19

Respiratory infectious diseases, including COVID-19, are transmitted via large droplets and small droplets (aerosols) (Singhal, 2020). Exhalations, sneezes, and coughs are made of a multiphase turbulent gas cloud carrying pathogen-bearing droplets. The gas cloud allows droplets to travel as far as 23 to 27 feet (7.01 to 8.23 m) when sneezing (Bourouiba, 2020). Recent experimental research shows that a heavy cough jet can reach 3.66 m, and the average cough jet can reach 2.44 m when the face is uncovered(Verma et al., 2020). This research also reveals that the average air leak can travel 0.20 m, even wearing a non-woven mask. Those studies prove the necessity of personal protection equipment and address that the exposure degree varies tremendously according to the proximity degree. In the general understanding, transmission probability is decided by the proximity and exposure time to a contagious individual (D'Orazio et al., 2020ab)(Fang et al., 2020).

2.2.2 Physical Distancing Policies and Advice Worldwide

Physical distancing policies and advice vary worldwide under different considerations. In the WHO Coronavirus disease advice for the public, people are

advised to maintain at least 1 m distance (World Health Organization, 2021). The Centers for Disease Control and Prevention of the United States (CDC) recommends a physical distance of about six feet (2 m) (Centers for Disease Control and Prevention, 2021). In Japan, people are advised to keep at least a 2 m distance from others and avoid the three Cs: crowded places, close-contact settings, and closed spaces (Ministry of Health, Labour and Welfare, 2021).

2.2.3 Pedestrian Avoidance Behavior

To distinguish conscious avoidance behavior because of the pandemic, we reviewed studies on human distances. The previous studies have studied many influential factors for avoidance behaviors. A unidirectional walking experiment study shows the avoidance distance from pedestrians to an obstacle or a standing pedestrian is determined by the sum of the distance to keep personal space, the distance caused by the pedestrian's forward movement, and the distance exerted by the forecasted movement of an obstacle (Tatebe & Nakajima, 1990). A following unidirectional empirical study shows that selecting the point where the curvature in the walking trajectory is the biggest defines the beginning point of avoidance behavior (Tatebe et al., 1994). Tang et al. found that direction and time period are essential correlative factors of people-to-people avoidance distance. Other correlative factors include general variables like speed, density, space characteristics, and personal variables like gender, age, and stature. The concept of avoidance behavior ahead of time is also mentioned in this study (Tang et al., 2012a). The following study revealed that avoidance behavior shows significant differences between pedestrians moving in the opposite direction and the same direction (Tang et al., 2012b).

Personal distance, ranging from 0.46 to 1.22 m, provides a small protective sphere around the human body. Social distance, ranging from 1.22 to 3.66 m, provides the "limit of domination" (Hall, 1966). Fruin also gives a definition of social distance: "Social distance, or the circle of personal involvement, begins at an inter-person spacing of 12 feet (3.66 m)" (Fruin, 1971). In this dissertation, we define personal spacing avoidance (PSA) as the avoidance behavior starting at a distance of fewer than 3.66 m, and corresponding to PSA, the avoidance behavior that begins at a distance longer than 3.66 m is defined as long-range avoidance (LRA). In prior work, Golas et al., 2014 proposed a hybrid algorithm for collision avoidance with transitions between continuum and discrete representations for crowd simulation. This algorithm aims to save computational costs by clustering distant agents. There is no current study considering LRA behavior for physical distancing analysis.

All the physical distancing policies are consistent with the distance of PSA. We distinguish between PSA and LRA mainly by considering the reason for avoidance. In a conventional concept, avoidance prevents physical contact and keeps the pedestrian in a comfortable zone. Along with the physical distancing policies and concern about infections, we want to know if pedestrians have manifested their awareness in daily movement. People's avoidance awareness is reflected as the increased avoidance rate and distance in this paper caused by COVID-19, and it can be both PSA and LRA.

2.3 Evaluation Schema for Safe Pedestrian Spaces

2.3.1 Static and Dynamic Crowd Density

2.3.1.1 Static Crowd Density

Static and moving crowds in public spaces require different space areas. Therefore, defining static and moving crowd density is essential and differentiating static and dynamic spaces when considering crowd accidents (Still, 2014). To illustrate crowd density, we illustrate crowd density between 1 – 6 people/m^2 in Figure 5. The body's breadth and depth are the basic dimensions designers should consider when designing space and relative facilities. The breadth, in particular, affects the capacity of design elements such as entrances, walkways, and stairs. The body size we choose in our illustration is 0.46 × 0.27 m, approximately the average of 95% of the world population (Pheasant, 2003).

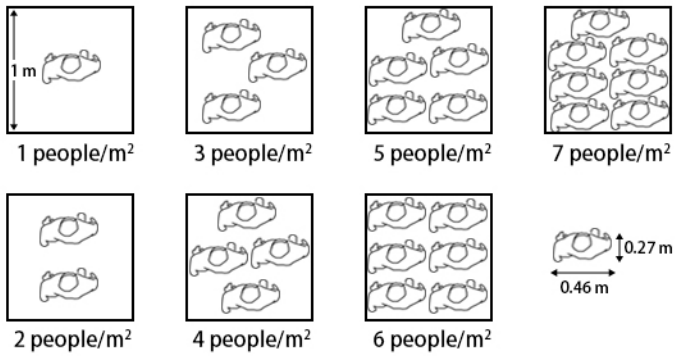

Figure 5 – Illustration of the crowd density between 1 – 6 people/m^2 (world population).

Human boundaries do not limit to their skins (Hall, 1966). The space occupied by the body contracts and expands with a person's emotions and state of mind, sense of self, social relations, and cultural predispositions (Low, 2003). Hall established the field of proxemics, studying how culture influences people's spatial perception and behavior. This theory assumes that human has an innate distancing mechanism that modified by culture to regulate contact in social situations (Low, 2003). Hall distinguished and termed human distances as intimate (0 – 0.46 m), personal (0.47 – 1.22 m), social (1.23 – 3.66 m), and public (3.67 m or more). In Figure 6, we illustrate the crowd density of

fewer than 1 person/m^2. We use this illustration to give an intuitive understanding of the relationship (roughly) between interpersonal distance and crowd density: intimate distance (1 person/m^2), personal distance (0.4 – 1 people/m^2), social distance (less than 0.4 people/m^2), and public distance (much less than 0.1 people/m^2). When discussing the physical distancing policies worldwide (1 – 2 m), the density range is roughly between 0.1 - 0.5 people/m^2. Still, 2014 refers to the density of 5 – 6 people/m^2 as higher-density and 6 – 7 people/m^2 as high density.

In Table 1 we expand still's density division to unify the terminology of the full text. The actual situation of different densities will be related to the characteristics of the population.

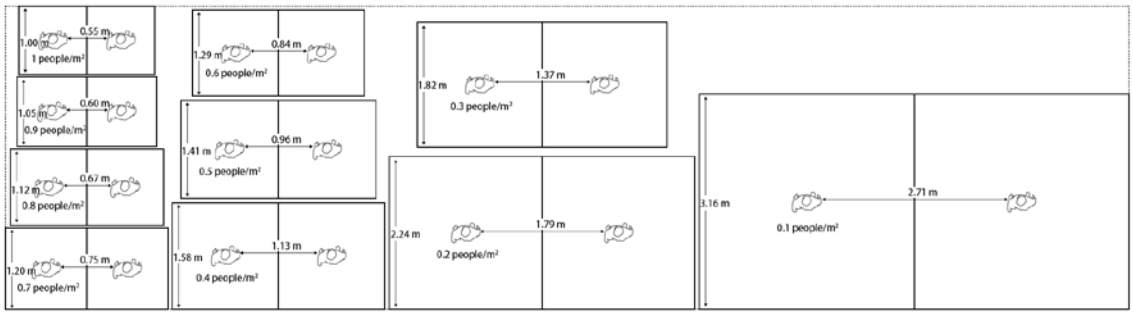

Figure 6 – Illustration of the crowd density of fewer than 1 person/m^2.

Table 1 – Pedestrian density terms.

Density (P: people/m^2)	Pedestrian density term
$0 \leq P \leq 1$	Low-density
$1 < P \leq 3$	Ordinary density
$3 < P \leq 5$	Relatively high-density
$5 < P \leq 6$	Higher-density
$6 < P \leq 8$	High density
$P > 8$	Extreme density

2.3.1.2 Dynamic Crowd Density

A walking person takes a larger space than a standing person. In unimpeded walking, the arms and legs should move freely to the extent the pedestrian feels comfortable (concluded based on Still, 2014). We repeated an experiment designed by Still, 2014, within Japanese and Chinese male adult groups. A 3.54 m long string is tied in a loop as an approximate area of one square meter. We put one to seven (or eight) people one by one into the loop and ask them to walk ten steps ahead. Even though much research has focused on graphing the crowd density and crowd flow relationship, this experiment gives an intuitive illustration of how crowd density and flow status are related.

In Figure 7, we conduct a walking pedestrian experiment with a group of Japanese male students age between 20 to 25 with their indoor clothes. The Akashi accident happened in the summertime, and we want this experiment to provide some intuitive side information for understanding the crowd congestion formation.

We can see that when there are two or three people in the loop, they can walk side by side unimpeded and remain comfortable. When a fourth person adds up to the loop, they can still keep a reluctant distance from each other, but the forward step of the back row person will be affected.

Higher-density (5 – 6 people/m^2): Usually, a pedestrian's body will naturally sway left and right during walking. When there are five people in the loop, not only the forward step but the swaying from left to right will also be restricted. However, there are still gaps between the individuals at this density level. This result is much different from Still's experiment conducted with British males, where 'the individuals are in a closer packing configuration' when the density is 4 people/m^2. When a six-person is

added to the loop, the movement is severely restricted, and the group is packed, and the walking steps stumble.

Figure 7 – Dynamic crowd density experiment with Japanese adults (age 20 – 25, male, indoor clothes).

High density (7 people/m^2): Still's experiment stopped at the density of 6 people/m^2 as it is very difficult to add another person, and people started to feel 'unsafe, no real control over their balance.' When the seventh person is added to the loop in our experiment, they can move forward by spontaneous unified footsteps. The group is closely packed, and the people on either side of the rope lean outward. When there are

no other people around, this density will not squeeze their bodies, and there is no tendency to lose their balance without external force.

This discussion helps us understand the crowd status and to reveal a crowd accident. No matter the body characteristic of the population, higher-density and high-density crowd status should be avoided during design and management.

In Figure 8, we conduct a pedestrian walking experiment with the same setup with a group of Chinese male students age between 20 to 35 with their winter cloth. This experiment provides side information for understanding the Shanghai Bund crowd accident, which happened in January.

We can see that when there are two to three people in the loop, the individuals walk side by side unimpeded and remain comfortable. Physical contact cannot be avoided when a fourth person is added to the loop, but they can stay in a group shape side by side.

Higher-density (5 – 6 people/m^2): when a fifth person is added to the loop, the group is in a closer packing configuration. There are still small gaps between the individuals. The person's walking pace in the front row is not affected obviously, but the other individuals are taking smaller steps. A six individual can quickly get into the loop with a configuration of three rows, but it is difficult for the individuals to control their steps and shake left and right slightly. People from the back row unintentionally push the people in the front row to maintain their balance. The people have to put their arms out of the loop to have enough space to stand.

Figure 8 – Dynamic crowd density experiment with Chinese adults (age 20 – 35, male, winter clothes).

High density (7 people/m^2 or higher): When seven people are in the loop, the individuals are arranged in three rows. The group can move forward with stumble paces,

and the two individuals in the back row have to do small jump steps to keep balance. The group can not move in a straight line but advance in the push of people. When there are eight people in the loop, the individuals are arranged in four rows. The group compacts closely and can only move forward cautiously with minimal and inconsistent steps. The whole crowd is shaking violently with this density. Everyone keeps their arms out of this loop.

2.3.1.3 Pedestrian Walking Stage

Evaluation criteria of crowd safety need to be identified before examing different space layouts and management plans. We reviewed the studies related to crowd safety and defined our evaluation criteria.

By comparing different research, we found that: 1) when the crowd density is less than 1 person/m^2, and the speed is close to free walking; 2) when the crowd density is close to 3 people/m^2, the highest pedestrian flow rate is achieved and speed gradually slows down; 3) when the crowd density is close to 4 people/m^2, the pedestrians move forward slowly, and congestion gradually forms (Japanese Architecture Society, 1980). To facilitate the high-density crowd analyses, we divided the following pedestrian walking stages in Table 2.

Table 2 – Pedestrian walking stages.

Density (P:people/m^2)	Pedestrian walking stages
$0 \leq P \leq 1$	The free walking stage.
$1 < P \leq 3$	The density accumulation stage.
$3 < P \leq 4$	The congestion-forming stage.
$P > 4$	The high-risk stage.

2.3.2 Considering Items of Safe Urban Public Spaces

2.3.2.1 Pedestrian Facilities

The goals of pedestrian urban public spaces are different in daily pedestrian facilities and MG events. The daily pedestrian facilities require maximizing pedestrian flows' efficiency and dividing the level of safety (for example, Level of Services, Fruin, 1971). Table 3 shows the evaluation items for pedestrian facilities that we concluded based on Helbing & Johansson, 2010. The scale of the evaluation items is descending with: general layout, design element layout, the shape of design elements, and the function and schedule of space.

Table 3 – Evaluation items for pedestrian facilities.

	Safety evaluation item	Requirement
General layout	The location and form of planned buildings	• Maximize the efficiency of pedestrian flows. • Divide the level of safety.
Design element layout	Walkways	
	Entrances and exits	
	Staircases	
	Elevators	
	Escalators	
	Corridors	
The shape of design elements	Entrances and exits	
	Rooms	
	Corridors	
The function and schedule	The function and schedule	

2.3.2.2 Mass Gathering Events

In contrast, MG events require avoiding extreme densities (Helbing & Johansson, 2013). Table 4 shows the evaluation items and reference requirements for MG events. The purpose of this table is to assess the criticality of conditions in the crowd

systematically. These items are divided by spatial design and crowd management into two categories (Helbing & Mukerji, 2012). Finally, the reference requirements and values are summarised from the crowd accident case studies above.

Table 4 – Evaluation items for mass gathering events.

Spatial design item	Requirement
Venue suitability	• The projected number of visitors should be used when planning flow control. • If the spatial layout suits the using plan should be checked.
Crowd density	• All areas where higher crowd density may occur must be analyzed. • A safe crowd condition can usually be assumed to be 2-3 people/m^2. • Once the density exceeds between 4-5 people/m^2, congestion can build up quickly. • High risks, for stumble or fall, mainly occur with uneven ground.
Capacity	• The capacity of a design element depends on the minimum usable width (the effective width).
Capacity reserve	• An event should be planned based on the number of expected people, not on capacity.
Capacity loss	• Bidirectional flows can reduce the capacity by 6-14%. • 90-degree turn • Walking group • Obstacles
Crowd management	Requirement
Control flow rate	• The maximum acceptable flow is 82 people per meter and minute.
Separation of flows	• Separating in- and outflows is necessary for evacuation to let people out without letting in people. • Separate other flows if necessary.
Avoid obstacles	• Should avoid the density accumulation around food stands, fences, police cars, and other places.
Separate route for emergency vehicles or evacuation	• The width of the route should be analyzed. • The evacuation time and pedestrian density should be analyzed.
Contingency plans	• Be prepared for the occurrence of various problems, especially the onset of congestion at bottlenecks.
Location of rescue units	• Rescue units should be assigned to the critical locations of the site.
Location of cordons	• The locations that require police cordons need to be analyzed in advance.
Event function and schedule	• Prepare flow separation plan for the functions with continuously frequented visitors. • Set up waiting areas. • Control the density of queuing area and prevent reverse flow o
Crowd communication	• Prepare loudspeakers, signs, maps, and other plans. • Decide the location of the loudspeaker vehicle.

2.3.3 Considering Items of Pedestrian Encounter

Based on the above literature, we define the concepts used in the following analysis: Pedestrian proximity probability measures the chance a pedestrian will be at a certain distance from a contagious pedestrian (Singhal, 2020), (Bourouiba, 2020), (Verma et al., 2020), (D'Orazio et al., 2020ab), (Fang et al., 2020). The considering items of pedestrian encounter are pedestrians' avoidance distance, lateral displacement offset, and avoidance rate of PSA and LRA behaviors.

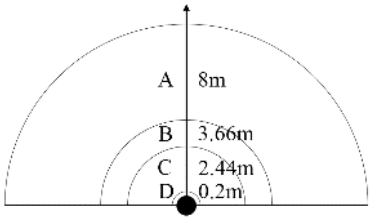

Figure 9 – Agent's proximity zones.

Table 5 – Pedestrian proximity zones.

Proximity zone	Description	Influence distance	Mask full protection	Source	Visualized color
A	A multiple turbulent gas cloud can reach when sneezing with face uncovered.	8.00 m	○	(Bourouiba et al., 2020)	Cyan
B	A heavy cough jet can reach with face uncovered.	3.66 m	○	(Verma, 2020)	Blue
C	Average cough jet distance with face uncovered.	2.44 m	○		Yellow
D	Average air leak can reach even wearing a non-woven mask.	0.20 m	×		Magenta

Pedestrian Proximity Zone is a concept we developed based on the public health studies we examined above. Contagious agents are visualized with the color red. An agent in Zone A is visualized with the color cyan, which means it is exposed to a sneezing contagious agent when neither of them is wearing a mask. An agent in Zone B is visualized with the color blue, which means it is exposed to a heavy cough contagious agent when neither of them is wearing a mask. An agent in Zone C is

visualized with the color yellow, which means it is exposed to an average cough contagious agent when neither of them is wearing a mask. An agent in Zone D is visualized with the color magenta, which means it is exposed to a contagious agent even though both are wearing masks. The agents out of all the above zones are in the exposure-free zone and visualized with green color. An agent's proximity zone can only be upgraded to a higher proximity zone. In the simulation results, each agent is only calculated once in its highest proximity zone.

2.4 Rule-Driven Agent-Based Models and Other Model Types

2.4.1 Models and Simulations of Crowd Behaviors

Pedestrian empirical studies can be traced back to the 1950s using direct observations. The main goals of pedestrian simulation studies were to develop a Level-of Serve concept (see Table 23 in Appendix B), design elements of pedestrian facilities, or build planning guidelines. The planning guidelines usually utilize regression relations, which are unsuitable for predicting pedestrian flows with exceptional spatial layouts. The complexity of pedestrian behavior, in addition to crowd psychology and the irreproducibility of accidents, simple observations cannot meet quantitative research's needs.

Computer simulation can be seen as an experimental technique for hypothesis testing and scenario analysis complementary to these real-life situations. Models and simulations can be utilized to determine the levels of comfort, safety, and security (Challenger et al., 2010). Furthermore, pedestrian and crowd simulation models can help prevent crowd accidents by predicting when, where, and why high-density crowd movements accumulated (Duives et al., 2013). In addition, the utilization of crowd simulation models makes it possible to assess the optimal grouping and scheduling

strategies and therefore facilitate crowd management and space engineering (Alaska et al., 2017). And to better understand how a design will influence user behavior (Dijkstra et al., 2001). Compared to pedestrian simulation, Crowd simulation involves replicating large numbers of pedestrians, which challenges computer efficiency.

2.4.2 Types of Crowd Simulation Models

There are generally two modeling attempts with different methods: slow but highly precise microscopic modeling attempts and fast but behaviorally questionable macroscopic modeling attempts. In addition, some hybrid models attempt to combine the advantages of both models (Duives et al., 2013).

Macroscopic crowd models include regression models, route choice models, gas-kinetics or fluid dynamics models and so on (Challenger et al., 2010). Early-stage simulation models most are macroscopic models and do not consider pedestrians' self-organization phenomena.

Microscopic crowd models include social force, cellular automata, activity-choice, velocity-based, and behavioral models. In addition, network models can either be in a microscopic or a macroscopic method (Duives et al., 2013). In the following, we only review several model types that are closely related to our model type. Microscopic pedestrian simulation models have been utilized in multiple heterogeneous contexts, such as transit stations, airports, sports venues, retails, other urban public spaces, and mass gathering events for non-evacuation purposes.

2.4.2.1 Social Force Models

The social force model (SFM) was initially developed by Helbing and colleagues (Helbing & Molnar, 1998). Social force models assume that a pedestrian in a crowd

moves due to combined socio-psychological and physical forces. Specifically, acceleration, repulsion and attractive forces are included in SFM. The initial social force model only includes homogeneous agents. Later scholars have contributed to calibrating the parameters in SFMs according to their research questions.

The advantage of SFM is that it provides continuous position representation and smooth movement, making the pedestrian model more realistic. In addition, the SFMs have successfully reproduced some observed pedestrian self-organization phenomena in both ordinary situations, such as the lane formation phenomenon, oscillation phenomenon, and various congestion phenomena in emergencies, such as arching phenomenon and fast-is-slower phenomenon (Helbing et al., 2002).

However, some researchers argue that even the social force models can capture the aggregate behaviors, they cannot fully capture the range or the subtleties of individual behaviors (Lerner et al., 2007). Blue and Adler also argue that the social force model did not investigate the fundamental flows of pedestrians (Blue & Adler, 2001). The force-driven method of SFMs also neglects the influence of individual decision making.

2.4.2.2 Cellular Automata Models

Cellular automata (CA) models divide the environment space into discrete cells, and each cell has a limited number of states. The CA model's automata (entities/agents) follow simple rules according to parameters such as density or speed and occupy or transit cells according to their surroundings (Blue & Adler, 2001). The cells can represent the free floor, obstacles, or the existence of other individuals.

CA models have a few advantages: they can approximate the more complicated models with a small ruleset. The simulations run fast (Blue & Adler, 2001) and therefore suits large-scale modeling. The characteristics of the rulesets and individual properties make CA models behavioral models (Blue & Adler, 2001). Cellular Automata can support a multi-agents approach (Dijkstra et al., 2001) (Bandini et al., 2007). Bandini and the others introduced the situated cellular agent model, where the agent's state is considered when interacting with the environment (Bandini et al., 2007).

The CA models are criticized for the similar speeds of agents and the restriction of the cells, which do not interpret pedestrian behaviors realistically (Owaidah et al., 2019). CA models are also criticized for lacking the representation of individual features.

2.4.2.3 Rule-Driven Agent-Based Models

Agent-based modeling (ABM), or multi-agent simulations (MAS), is modeled as a collection of one or multi types of autonomous decision-making agents. Each agent assesses its situation and makes decisions based on a set of behavioral rules (Bonabeau, 2002). Homogeneous and heterogeneous agents interact with each other, and the underlying simulation rules from the environment to suit their interests, characterized as boundary rationality (Al-Kodmany, 2013) (Challenger et al., 2010). Pedestrian self-organization phenomena have been reproduced by many studies using ABMs (Kurdi, 2017).

Helbing and colleges have concluded the advantages of rule-driven ABMs comparing to the early ABMs: Rule-driven ABM is a relatively new modeling method and can be seen as an extension of the CA model. The rule-driven ABM model adds extensibility, intelligence, behavior, and psychology to the CA model and can carry

more complex rules. The mobility of the agent allows the rule-driven ABM model to set many variables and parameters flexibly. Obstacles can be easily placed, enabling agents to make different perceptions and reactions according to obstacles. Rule-driven ABMs can also be well-combined with different model types and are suited for detailed hypothesis-testing (Helbing, 2012).

The scope of ABMs covers a wide range of pedestrian studies. ABMs have been utilized to evaluate pedestrian space under normal situations, such as city walkability, street structure, design layout, sign visibility, and universal design. The application of ABMs to combine geographical systems also has a considerable increase. In the traffic field, mixed traffic with cars, pedestrians, and trams are often studied. For emergency situations, ABMs are utilized to make evacuation plans considering pedestrian behavior in buildings and airports under natural disasters like earthquakes and tsunami. Large-scale pedestrian simulation has been emerging to deal with increasing crowd disasters.

The agents in ABMs can move individually or as a group. However, most ABMs still consider pedestrians as individuals. The group dynamic and modeling still lack research.

2.4.3 Evacuation Validation Guidelines and Tests

The first systematic guidance describing the verification and validation is the document MSC.1/Circ.1238, provided by the International Maritime Organization (IMO) in 2007. The guideline includes 11 IMO tests developed for passenger ship fire evacuation model analysis. They have been considered the benchmark of verification and validation for different evacuation fields out of their initial use. Derived from IMO tests, the Technical Note 1822, published by the National Institute of Standards and Technology (NIST) in 2003, contains 17 verification tests and a few possible

experimental data sources for the validation tests. The NIST tests are organized using five main core components of evacuation models: 1) pre-evacuation time, 2) movement and navigation, 3) exit usage, 4) route availability, and 5) flow conditions/constraints.

Figure 10 introduces the NIST test verif.2.9. as an example to show a validation test structure. Verif.2.9., group behaviors, examine the simulation model's reproduction ability of group behavior. This test scenario is set as five occupants (Group 1) walking from Zone 1, with different walking speeds, need to pass ten slower occupants (Group 2) in Zone 2 to exit the room. The expected results should demonstrate that the occupants of Group 1 will exit together within a limited time difference. It is worth mentioning that if the model does not permit group behavior, the tester is recommended to discuss this limitation in the related validation documentation.

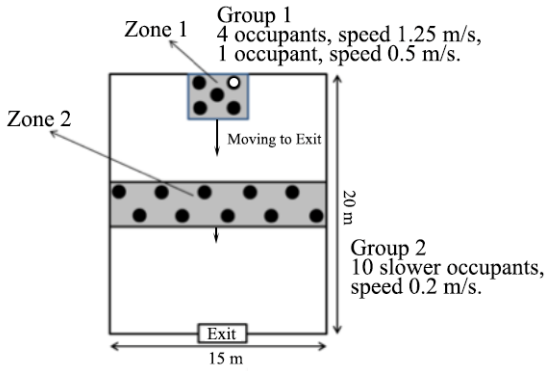

Figure 10 – Geometric layout of NIST verif.2.9. test: group behaviors.

The Second Edition of SFPE's Engineering Guide: Human Behavior in Fire is published in 2019, with the instruction of verification and validation operations intended for model users. The SFPE handbook does not suggest that the users perform all the verification and validation tests to avoid redundancy.

These three guidelines have a span of more than ten years, and it can be observed that they are moving towards broader application purposes and more open frameworks.

Table 6 – Existing verification and validation guidelines.

Organization	International Maritime Organization (IMO)	National Institute of Standards and Technology (NIST)	Society of Fire Protection Engineers (SFPE)
Guidance/ law	MSC.1/Circ.1238	Technical Note 1822	Guide to Human Behavior in Fire, 2nd Ed
Character	Intergovernmental organization	Government	Academia, industry, and government
Place, date	U.K., Oct 2007	U.S., Nov 2013	U.S., 2019
Purpose	Passenger ship fire evacuation	Building fire evacuation	Provide a common introduction of this field
Verification and validation	• Component testing • Functional verification • Qualitative verification • Quantitative verification	• Pre-evacuation time • Movement and navigation • Exit choice/usage • Route availability • Flow constraints	Verification: • Individual-level • Aggregate level • Scenario level Validation: • Outcome validity • Progress validity • Event validity

2.4.4 Qualitative and Quantitative Validation Assessments

Unlike an evacuation validation test that provides a standard scenario setting, researchers should choose and design their validation assessments accordingly. Campanella et al. proposed a simple validation procedure that combines qualitative and quantitative assessments. They argue that if no parameter set is calibrated for the specific task, the set to be used for prediction should perform well in various validation assessments to show their general usability. Guo et al., 2010 also give a similar statement that the validation method should be evaluated assuming a given purpose and environment. Lubas et al. mentioned that some requirements and tests are proper for all models, while each model type requires its specific test set. It stressed the primary source of Cellular Automata models' errors is from the discretization of space and time.

Dridi concluded the different verification and validation techniques and tests partially. Federici et al., 2014 designed a comprehensive checklist for the quantitative evaluation of pedestrian simulation software functionalities and proposed a set of criteria for evaluation. Seyfried et al. emphasized that even reproducing the fundamental diagrams is commonly used in validating simulation models, it does not necessarily result in the reproduction of microscopic pedestrian flow features. Federici et al. divided a simulation model's features into three subsets: scenario, pedestrian, and output. We divide the validation assessments following the same subsets.

Qualitative Validation Assessments:

Qualitative validation assessments judge the characteristic features of simulated pedestrians. Because pedestrian behaviors vary according to their purpose and surrounding environment, the simulation model's suitability should be considered before validation is started.

Scenario Level (subset 1)

Model usability: A simulation model's suitability should be considered according to pedestrian physical characteristics, pedestrian behavior purposes, and the walking environment before making any prediction (Guo et al., 2010)(Campanella et al., 2014).

Pedestrian avoidance with walking infrastructures: Qualitatively examines if there are pedestrians trapped with walking infrastructures, for example, corners and boundaries (Campanella et al., 2014).

Pedestrian Level (subset 2)

Uni-directional flow: Qualitatively examines if pedestrians can keep similar average distances with each other in a simulation. The frequency of a pedestrian collide with nearby pedestrians should also be reported. One should observe that pedestrians are staying in the simulated area during the simulation (Campanella et al., 2014).

Counterflow: Qualitatively examines if pedestrians in bi-directional flows can form self-organized lanes. The stability of the lanes should be reported. The frequency of a pedestrian collides with nearby pedestrians should be reported. It should also be observed how often a pedestrian is pushed backward when walking straight on other pedestrians. One should observe that pedestrians are staying in the simulated area during the simulation (Campanella et al., 2014).

Narrow corridor bottleneck flow: Qualitatively examines if there are zipper effects formed inside the corridor. One should also observe that if there is a funnel shape formed upstream of the bottleneck in the congested flow. The frequency of a pedestrian collide with nearby pedestrians should be reported. It should be observed that pedestrians are trapped outside the corridor, or pedestrians are being pushed towards the obstacles. One should observe that pedestrians are staying in the simulated area during the simulation (Campanella et al., 2014).

Output Level (subset 3)

Compare historical data/other actual events: Qualitatively compare the simulation results with historical data of the same site or other actual events to determine if they are similar (Dridi, 2014).

Graphic illustration of measured values: The simulation output values should be illustrated graphically while the model runs over time to ensure the simulation tools' correct performance (Dridi, 2014).

Face validity: Experts evaluate the model's suitability, such as the logic of the conceptual model and its input-output relationships (Dridi, 2014).

Quantitative Validation Assessments:

Quantitative validation requires that the tested phenomena can be reproduced in a quantitative method. This requirement makes quantitative assessments mainly examine simulation outputs. The data used for quantitative assessments come from different sources. Validation against empirical data uses data obtained through video analysis of pedestrians' movement in the natural environment, controlled laboratory experiments, natural disasters analysis, or other situations. Comparing the simulation results with fundamental diagrams is a commonly used method, even though this does not necessarily result in the reproduction of pedestrian flow features. Validation against theoretical data uses data obtained through expert opinion, bibliographic data, mathematical calculations, and so on.

Output Level (subset 3)

Travel time: Quantitively calculates the average of each pedestrian's travel time errors resulting from each simulation (Campanella et al., 2014)(Seyfried et al., 2006).

Bottleneck capacity: Quantitively calculates the maximum flow obtained at the bottleneck corridor entrance (Campanella et al., 2014)(Seyfried et al., 2006).

Fundamental diagrams: This assessment quantitively compares the slope, the scatter, and the maximum density of a fundamental diagram achieved in the simulation flows. Mainly the speed-density relation is used. However, it should be noted that reproduce the fundamental diagrams does not necessarily result in the reproduction of microscopic pedestrian features (Campanella et al., 2014)(Seyfried et al., 2006).

Compare with empirical models: Quantitively compares the simulation results of a simple test case with well-known results of empirical models (Dridi, 2014).

Compare with other validated models: Quantitively compares the simulation results with other validated models with the same properties (Dridi, 2014).

Extreme condition: Quantitively measures any extreme and improbable combination of factors in the simulation model to ensure the model structure and outputs are reliable (Dridi, 2014).

Sensitivity Analysis: Sensitivity analysis examines how the outputs will be affected due to the change of inputs. Both qualitative and quantitative properties in the simulation system can be assessed through sensitivity analysis. The sensitivity analysis observes how the outputs will be affected by changing the simulation model's inputs or internal parameters.

2.4.5 Microscopic Pedestrian Simulation Software

Pedestrian simulation models can be generated into computer software (Zainuddin et al., 2009). The simulation software in the market includes SimWalk,

AnyLogic, Arena, PanicSim, Exudox, Legion, ProModel, PedGo, Simul8, Kanbara Sim, and Pathfinder.

Artisoc This dissertation uses a multi-agent platform – Artisoc 4.0 (formerly KKMAS, Kozo Keikaku Engineering Inc., Japan). Artisoc is a flexible simulation platform developed for analyzing social phenomena and other complex systems based on human decision-making. It features GUI-based model definition, mapping, graphing and output, and Visual Basic-like description of behavior rules.

Legion is an ABM software first developed by Still as part of his Ph.D. dissertation and specializing in crowd behavior. Legion focuses especially on ingress and egress scenarios. This software has been utilized in modeling projects like airports, train stations, and stadiums (Still, 2000)(Legion.com)(Al-Kodmany, 2013).

Myriad 2 is also an ABM software developed by Still and colleagues (Crowd Dynamics Ltd). This software integrates network analysis, spatial analysis, and agent-based analysis to suit different purposes. Its advantages in predicting the best possible scenario according to given conditions (Al-Kodmany, 2013).

PedFlow is an ABM developed byLöhner Simulation Technologies International, Inc. (LSTI) (Dridi, 2014). It is more sophisticated in predicting crowd density and dynamics (Owaidah et al., 2019).

STEPS is an ABM crowd management simulation tool for predicting pedestrian dynamics under both normal and emergency conditions. Pedestrian movement in STEPS is based upon fundamental principles. STEPS predicts discrete individuals through 3D space (Fayoumi et al., 2011).

NetLogo is an ABM platform that can be used to simulate a complex system. NetLogo is utilized extensively in many domains and provides the basic building blocks. The NetLogo environment is a two-dimensional grid. Agents and their behavior depending on the underlying model (Ilyas, 2013).

PedGo is a microscopic simulation model (CA/multi-agent) with the ability to simulate large crowd evacuation (10.000 persons in real-time)(traffgo-ht.com). PedGo software package includes three different programs: PedGo, PedEd, and PedView.

Anylogic is a simulation environment that supports different modeling techniques such as Discrete Event, Agent-Based, and System Dynamics. Anylogic provides a Java-based development environment and a set of multipurpose component libraries to speed up modeling process. Anylogic pedestrian library (APL) deals with the modeling aspects of crowd simulation (Mahmood et al., 2017).

EXODUS buildingEXODUS is a CA-based simulation tool for the representation of pedestrian and evacuee movement. It can simulate the interaction between people, people to fire, and people to structure. The model outputs allow pedestrian or evacuee performance to be examined at individual, group, or population level (Siddiqui & Gwynne, 2012).

SimWalk is SFM based pedestrian movement simulation software. This software allows the architecture plan to be drawn in their program, SimDraw, or import from AutoCAD. SimWalk uses the shortest-path algorithm. This software is flexible in defining the density, destination, the range of speed for pedestrians, the level of service (LOS), time step, the radius of pedestrian, the interaction intensity, and the interaction distance (Zainuddin et al., 2009).

Pathfinder is an ABM egress simulator that uses steering behaviors to model pedestrian or evacuee movement. It provides two options for the pedestrian and evacuee motion: an SFPE mode and a steering mode. The SFPE mode conducts the concepts in the SFPE handbook, where the crowd density determines walking speeds. The steering mode is based on inverse steering behaviors and allows more complex behaviors (Pathfinder Technical Reference). The latest version of Pathfinder allows the social avoidance function, but this function has limitations when the crowd density is higher.

2.5 Development of an Agent-Based Modeling and Simulation Framework for Analyzing Pedestrian Spatial Problems

2.5.1 A Categorized Framework of Agent-Based Modeling

A classic ABM is consists of three elements: a set of agents with similar or different characteristics and behaviors, a set of agent relationships and interaction modes, an environment where agents can interact with each other and with the environment (Macal & North, 2014).

As shown in Figure 11, a general ABM framework can be categorized into four sub-elements: input, scenario, agent, and output. Under the designed scenario, the agents conduct their behavior within the input data limit while giving the simulation output.

The input data refers to those values that need to be entered before each simulation, such as pedestrian flow amount, speed, distance preference, and so on. The input data can be acquired through an empirical/experimental process or a theoretical hypothesis.

The scenario set includes both physical layout and other functions that can fulfill the simulation purpose. The physical layout can be 2D or 3D and is simply a spatial reproduction, while the space division decides how the agent recognizes the space. The space division in ABM can be discrete, continuous, or hybrid of both. Time setting refers to how long each simulation step represents the actual duration. It can be set as short as a few steps in one second or as long as one step for a few minutes, hours, or days, depending on the simulation scale. Time setting is closely related to the movement continuity and precision of an agent in space. The more the simulation is close to a personal scale, the more critical the body size and speed influence the simulation results. The environment variables constructed the essential and specific functions a simulation model needs. The routing of an agent includes two critical technique parts: the origin-destination (OD) pairs and the navigation towards the destination. The navigation of an agent towards its destination has multiple methods: shortest path method, waypoint method, vision-driven method, and so on. The shortest path method does not have redundancy to an agent's route, while the vision-driven method has maximum redundancy. The waypoint method compromises the former two methods by adding temporary destinations (waypoints) to an agent's route.

There could be a pedestrian agent type and other agent types in multiple-agent simulation platforms, such as obstacles, vehicles, wheelchairs, and so on. The pedestrian agent moves towards its destination while performing essential physical features, pedestrian behavior, and other advanced features.

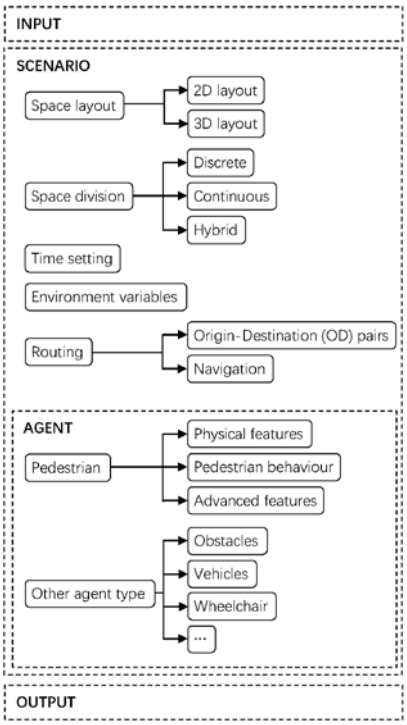

Figure 11 – A categorized framework of agent-based modeling.

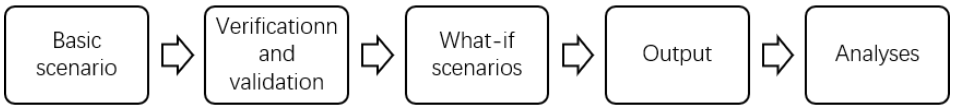

Figure 12 – The simulation process.

Figure 12 shows the simulation process of an ABM. After the verification and validation of the base scenario, other what-if scenarios can be simulated and analyzed. The output should include both numerical results and real-time illustrations to ensure the simulation process is normal.

2.5.2 Spatial Coordinate System and Parameter Setting

This section introduces how the agent recognizes the space in our ABM. The space division is a hybrid cell-based model combined with an absolute coordinate

system and a relative coordinate system. Figure 13 shows an illustration of the absolute and relative coordinate systems.

In the absolute coordinate system, the cell is set 40 by 40 cm square to get an essential setting considering the Japanese population's average speed is proximity around 1.2m/s. Following this setting, the time scale is set as three steps per second, close to the actual walking condition. The absolute coordinate system is a system with two decimal places real numbers. The 2D space layout and the location of stationary obstacles are reflected in the absolute coordinate system. The layout's right north direction is set to 0° on the Y-axis in this coordinate system. The real-time simulation animation is also reflected in this system

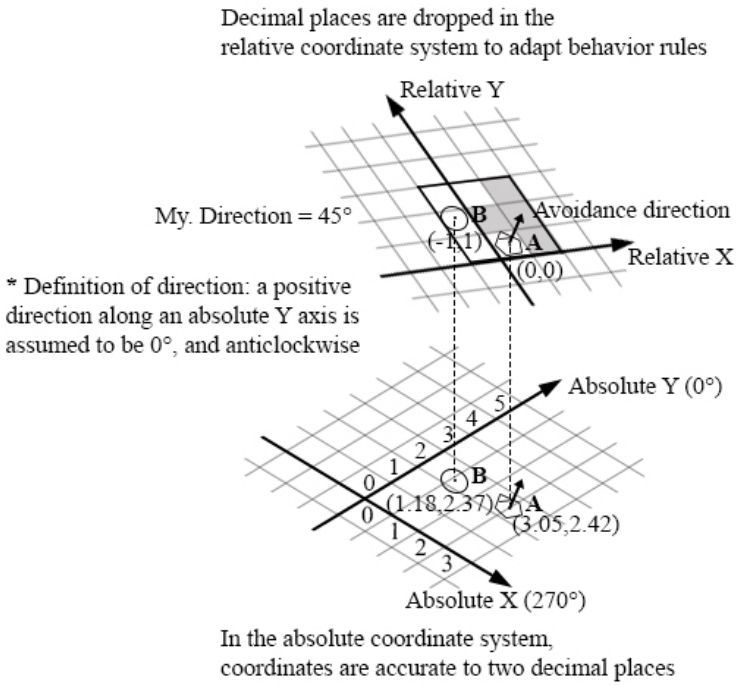

Figure 13 – Illustration of the absolute and relative coordinate systems (draw based on Kaneda et al., 2010).

In the relative coordinate system, the cell size is decided by each agent's step width that makes the agent able to have different speeds. In this system, the Y-axis

direction follows the agent's current direction. The agent avoids other agents following our defined pedestrian behavior rules. The decimal places are dropped in the relative coordinate system to adapt to the behavior rules and to know the avoidance direction.

Because the agent encounters other agents from different directions, the agent can deviate from its original direction for a short time and walk without the cell limitation in the absolute coordinate system. Every few steps, the agent fixes its direction according to its destination.

Figure 14 shows an outline of the conversion between coordinate systems.

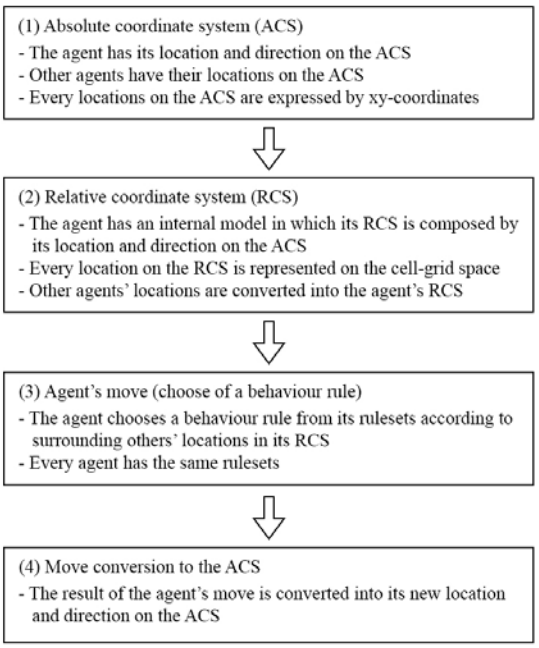

Figure 14 – Outline of conversion between coordinate systems (draw based on Kaneda & Okayama, 2007).

Environment Variables: The environment variables refer to the variables function in the scenario level, while the agent has its own variables. The essential environment variables for our ABM include:

- Pedestrian generation rate,
- Waypoint list,
- Entrance/exit choice rate,
- Density measurement area,
- Entrance pedestrian counter,
- Exit pedestrian counter.

Routing: Figure 15 shows an illustration of the routing of using waypoints. A pedestrian agent is generated with an input generation rate at each entrance and moves towards a preset exit in our ABM. The distribution of the preset exit follows the input entrance/exit choice rate. The pedestrian agent moves along with the waypoints, following the shortest path principle while avoiding other agents and obstacles until it reaches its destination. The waypoints are temporary walking targets set based on the directly visible principle. Around each waypoint, we set a choice-making sphere according to actual observation. An agent will update its temporary target to the next waypoint once it reaches the current target's choice-making sphere until it finds the exit. As the agent keeps avoiding other agents and obstacles, it will recalculate the direction between itself and the current target every few steps. The agent disappears when it reaches the sphere of the preset exit.

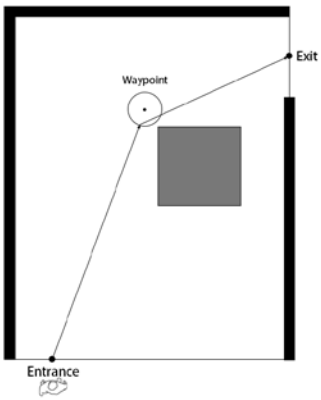

Figure 15 – Illustration of the routing.

2.5.3 Development of Agent Behavioral Rulesets

In a multi-agent simulation model, pedestrian agents and other agent types can interact with the environment and each other. Wall, standing pedestrians, generation objects, and other obstacles are all presented as different agent types for convenience. However, only pedestrian agents conduct complex behavior rules. The variables for an agent include:

- X coordinate,
- Y coordinate,
- Direction,
- Speed,
- Colour,
- Entrance,
- Exit,
- Origin ID,
- Destination ID,
- Step number.

To make a simulation realistic, additional parameters, such as psychological, physiological, and social parameters, need to be considered (Sarmady et al., 2008).

2.5.3.1 Physical Features

Speed is one of the critical physical features of our ABM. The initial speed of an agent is set with an average input value with deviations. The agent can reduce its speed in an overcrowded situation. Other physical features will be discussed in each case.

2.5.3.2 Pedestrian Behavior

Pedestrian behavior, mainly avoidance behavior between pedestrian agents, are functioned in the relative coordinate system. Rulesets adapt pedestrian behavior rules in our ABM. The rulesets are different in each case study and will be introduced in detail in the following chapters. In each simulation step, each agent selects one rule from the rulesets following the rulesets' priority order. Even though the adaptation of rulesets is sequential, our ABM is essentially implemented as a stochastic model. The right/left direction turn of agents in the rulesets is random with 50:50. The updating order of moves of each agent within each simulation step is also random sequential in Artisoc.

2.6 Chapter Conclusions

In Table 7 we concluded the findings from reviewing existing studies in summary. Based on the findings, section 2.3, the evaluation schema for safe pedestrian spaces, and section 2.5, the development of an ABMS framework, are developed.

Table 7 – Diagram for chapter conclusions.

Existing studies on	Section	Findings from reviewing existing studies	
		For relatively high-density crowds (3 - 5 people/m^2)	For lower-density crowds (0.1 - 0.5 people/m^2)
Crowd accidents	2.1.1 Crowd Motions and Phenomena	• Lane formation • Oscillatory flows at bottlenecks • Strip formation in intersecting flows • Herding • The faster-is-slower effect • Queueing behavior • Stop and go waves	—
	2.1.2 Mechanism of Crowd Accidents	• Trampling • Crushing	—
	2.1.3 Triggers of Crowd Accidents	Spatial design and crowd management: • Group conflict type • Construction collapse type • Accident fall type • Crowd turbulence type Irrational psychology: • Break limitation type • Penetration type • Panic type • Aggressive crowd type	—
	2.1.4 Case Study: Duisburg Love Parade Disaster (Germany, July 2010)	• The interdependent factors attributing to a failure of crowd system coordination are analyzed in details • Offered public accessible surveillance videos	—
	2.1.5 Case Study: the Hajj Experience	• Provided many research materials and revealed some crowd accident mechanisms • The new Jamarat Bridge is built based on ABMS analysis	—
	2.1.6 Case Study: Akashi Citizens' Summer Festival Disaster (Japan, July 2001)	• Offered a highly detailed accident investigation report	—
Public health	2.2.1 The Transmission Characteristics of the COVID-19	—	• Transmitted via large droplets and small droplets (aerosols) • Exhalations, sneezes, and coughs have different propagation distance
	2.2.2 Physical Distancing Policies and Advice Worldwide	—	• The policies and advice vary between 1 to 2 m.
	2.2.3 Pedestrian Avoidance Behavior	—	• Influential factors in defining pedestrian avoidance behavior

CHAPTER 3. AN ANALYSIS ON RELATIVELY HIGH-DENSITY SPATIAL SAFETY: USING AGENT-BASED SIMULATION FOR ANALYZING PUBLIC SPACE DESIGN BASED ON A CROWD DISASTER

3.1 Overview of the Shanghai Bund Crowd Accident

The Shanghai Bund Scenic Area is a downtown linear walking space along the Huangpu River. Exotic historical buildings, commercial leisure, and waterfront viewing attract one million tourists per day during holidays. From 2011, a New Year countdown, together with a light show, was held for three years in this area, and the number of visitors increased year by year. In 2014, the light show's location was changed into a nearby place that required tickets in the last few days of the year for safety considerations. However, large crowds were still unaware of the venue change or gathered at the previous site for the New Year countdown. At 23:35 on December 31, 2014, a severe crowd disaster occurred in front of a staircase which caused 36 deaths, and 49 injures. A media video recorded the moment the Shanghai crowd disaster happened, and the pedestrians were in a fluid condition (Nan-fang Metropolis Daily, 2015). An apparent human wave was forced by enormous pressure pushing down the staircase to cause people to fall on each other, although nobody was doing this on purpose.

The Bund Scenic Area In the past hundred years, the Bund waterfront has been reconstructed several times to adapt to the city's development. In 1990, the flood defense wall was shifted outwards, and the inside was converted to parking and its top to a viewing platform (Xi & Xu, 2011; Wu et al., 2011). This plan partially satisfied the

function of transportation, flood defense, and pedestrian activities. However, the city and the waterfront were separated by the height difference of the flood defense wall. Simultaneously, heavy vehicle traffic occupied a large part of the waterfront space, and the lack of public activity space made the area potentially dangerous for high pedestrian density. With the opportunity of the 2010 Shanghai World Expo and the building of the Bund Tunnel, reconstruction was possible again in the Bund area, intending to return more waterfront space to pedestrians. High-intensity vehicle traffic was channeled underground, and the ground roadways were reduced from 11 lanes to 4, plus 2 spare lanes, which increased the accessible pedestrian ground space by 40%.

Figure 16 – The Bund Scenic Area, A: Chen Yi Square, B: Waitan-Yuan, the actual event location (drawn by one of the authors based on the detailed plan of the urban design & site plan Shanghai Bund Waterfront by Xi & Xu, 2011).

Figure 16 shows the layout of the Bund Scenic Area. The Bund has an area of 3.1 km^2. Compared with the previous plan, a middle layer of 4.7 m squares was set between the 3.5 m sidewalk and the 6.9 m flood defense wall. Figure 17 shows the three layers of the Bund area, and they are designed to form three walking passages along the north and south to relieve the high-density flows in rush hours (Xi & Xu, 2011). The sidewalk

was widened from 2.5-9 m to 10-15 m. A facility belt is also set in the middle of the sidewalk to avoid obstruction. Squares are placed in the main pedestrian flow intersections and good viewing sites to accommodate large gatherings and provide event venues. Staircases and a few large slopes with angles between 3-5% were designed, combining the squares and the viewing platform, taking into account safety in high-density situations. Beside the staircases, the viewing platform on top of the flood defense wall was partially widened to provide better vision across the river and resting spaces.

Figure 17 – The three elevations of the road, square, and viewing platform of Chen Yi Square (snapshot from the survey video by one of the authors).

Chen Yi Square Chen Yi Square is located in the middle of the Bund Scenic Area (area A in Figure 16), and it was doubled in the 2010 reconstruction and now has a public activity area of 2877 m^2 (Xi & Xu, 2011). Chen Yi Square is connected to the viewing platform with staircases on both the north and south sides. The viewing platform in the Chen Yi Square section is considered the best viewing position of the Bund area. Besides, Chen Yi Square is around 580 m from subway lines 2 and 10 and is the area

with the highest crowd density and pedestrian flows. Waitan Yuan, about 550 m away from Chen Yi Square, was the actual event site for the New Year light show at night (area B in Figure 16).

The Accident Site The crowd accident happened in front and on the staircase in the southeast corner of Chen Yi Square. The staircase is made of two groups of 17 steps in total, and there is a 2.3m platform between them. The staircase is 6.2 m in width and 8.4 m in depth. The stair wall's highest point is 3.5m from the ground and is equipped with steel strip armrests on both sides. The original plan had no column to divide the up and downflows.

The Crowd Accident After the accident, the Shanghai Municipal Government, formed a Joint Investigation Team among different city departments. After a comprehensive analysis, an investigation report was released on January 20, 2015 (Shanghai Bund Chen Yi Square Crowd Accident Investigation Committee, 2015). We extract the crucial points of this report in our own words and conclude the accident's timeline in Table 8. The visitor number was obtained through a comprehensive data analysis of the communication department, the public security department, and the subway operating enterprise. There were around 120,000 people from 20:00 to 21:00, 160,000 people from 21:00 to 22:00, and 240,000 people from 22:00 to 23:00 in the Bund area. From 23:00 to 23:35, when the accident happened, there were around 310,000 people. However, since visitors are not distributed evenly in the Bund area, the accident area had extremely high density. According to a media report, witnesses estimated that the accident site's density was around 6-7 people/m^2 (Sohu News, 2015).

Table 8 – Timeline of the Bund crowd accident.

Time	Event
20:00	There are more inflows than outflows in the Bund. A large number of visitors gathered on the viewing platform, and the crowds were gathering.
20:27	Set one police every 10 m in Nanjing Road. A one-way belt was set on the entrance of the viewing platform.
22:37	One-way belt towards the viewing platform was broken, large numbers of visitors moved into the viewing platform.
22:44	Interception lines along Nanjing Road were set to reduce visitors.
23:23-23:33	After constant collisions, the upward and downward pedestrian flows stalemated in the middle of the stairs and then formed a "wave."
23:35	The downward pressure of the stalemate suddenly increased, causing someone at the bottom to fall. After the first person fell, people started to fall on each other. A stampede ensued.

* The authors summary based on the investigation report on Shanghai Bund Chen Yi square crowd accident, 2015.

In the investigation report, this accident was defined as a stampede caused by insufficient preparation and management. The main reasons were given as the following:

1) When the event location changed, there was no risk evaluation of possible crowd gatherings;

2) The change of the event was not well-enough publicized. The New Year countdown was officially announced on December 30, just one day before the event. The Bund's pronunciation is 'Waitan' in Chinese, while the new location is read as 'Waitan-Yuan.' Many of the visitors did not know about the change or could not tell the difference;

3) Since the actual event site was changed, the Bund's security was not set to the event level;

4) There was not enough monitoring of the pedestrian flow change.

After the accident, a few facility improvements and management plans were adopted and discussed in detail in the scenario development section.

3.2 Site Survey: Pedestrian Flow Data

An aerial view video survey was conducted from 15:00 to 16:00 on a weekday in September 2017 in the area shown in Figure 18 below. There are ten places the visitors can enter freely, and they are named entrance A to J.

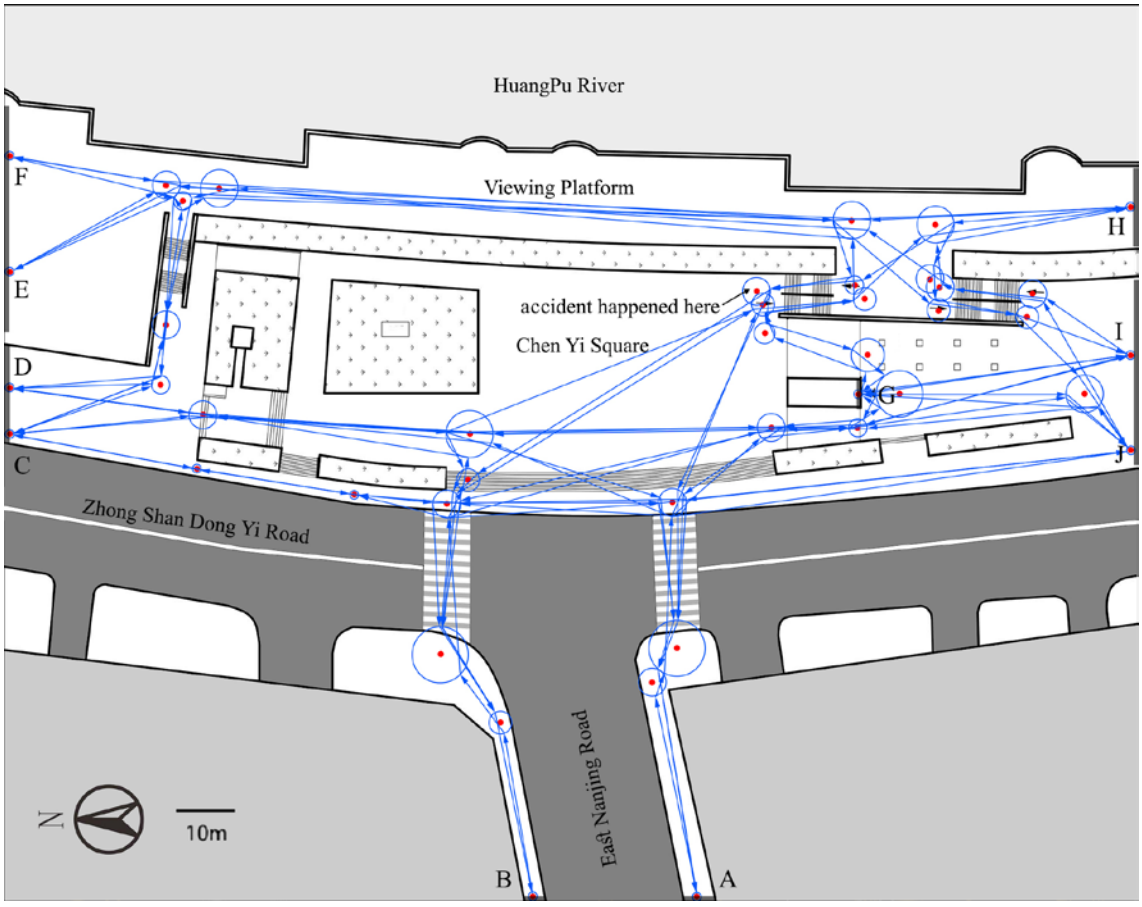

Figure 18 – Simulation area, agent generation areas (from A to J), and the waypoint network (drawn by one of the authors based on satellite map).

Table 9 below indicates the visitor numbers for each entrance.

Table 9 – Average entrance visitor number of the surveyed area (people/minute).

Entrance	A	B	C	D	E	F	G	H	I	J
Visitor	119	44	2	13	5	51	14	38	48	10
Width	4.4m	2.4m	2.8m	12m	24.4m	10.4m	3.6m	12m	24m	5.6m

Entrance A and B are on East Nanjing Road, which is in the subway station's direction. Almost half of the surveyed visitors were coming from this direction and went to the viewing platform. This main pedestrian stream was around 90 degrees to the viewing platform and was tightened by the staircase like an hourglass. Visitors from entrances E and F are from the north side of the viewing platform, accounting for 16.3% of the total visitors. Visitors from entrance H were from the south side of the viewing platform, accounting for 11% of the total visitors. These three directions of visitors were meeting at the platform beyond the stairs.

3.3 Development of an Agent-Based Simulator for Crowd Safety Analysis

3.3.1 Pedestrian Agent Algorithm

Figure 19 below explains the pedestrian agent's algorithm in the simulation model built for the Shanghai Bund crowd accident simulation. The algorithm contains four functions: route acquire function, target maintaining function, adapting walking behavior rules, and target renew function. An entrance in Artisoc is consists of many pedestrian generating objects and has width. A pedestrian is generated at the entrance (origin) A to J with an input generation rate and walking towards the preset exit (destination). We name the origin ID and destination ID from 1 to 10 accordingly. The route acquire function will calculate the waypoint list between the origin ID and destination ID. In the target maintaining function, the agent walking towards the current

target waypoint and avoid other pedestrian agents and obstacles. Every few steps, the agent reconfirms its walking direction. The avoidance of the other agents and obstacles following the ASPF walking rules will be introduced in detail in the next section. After reaching the current target waypoint sphere, the agent updates its target waypoint on the acquired waypoint list until it reaches its destination.

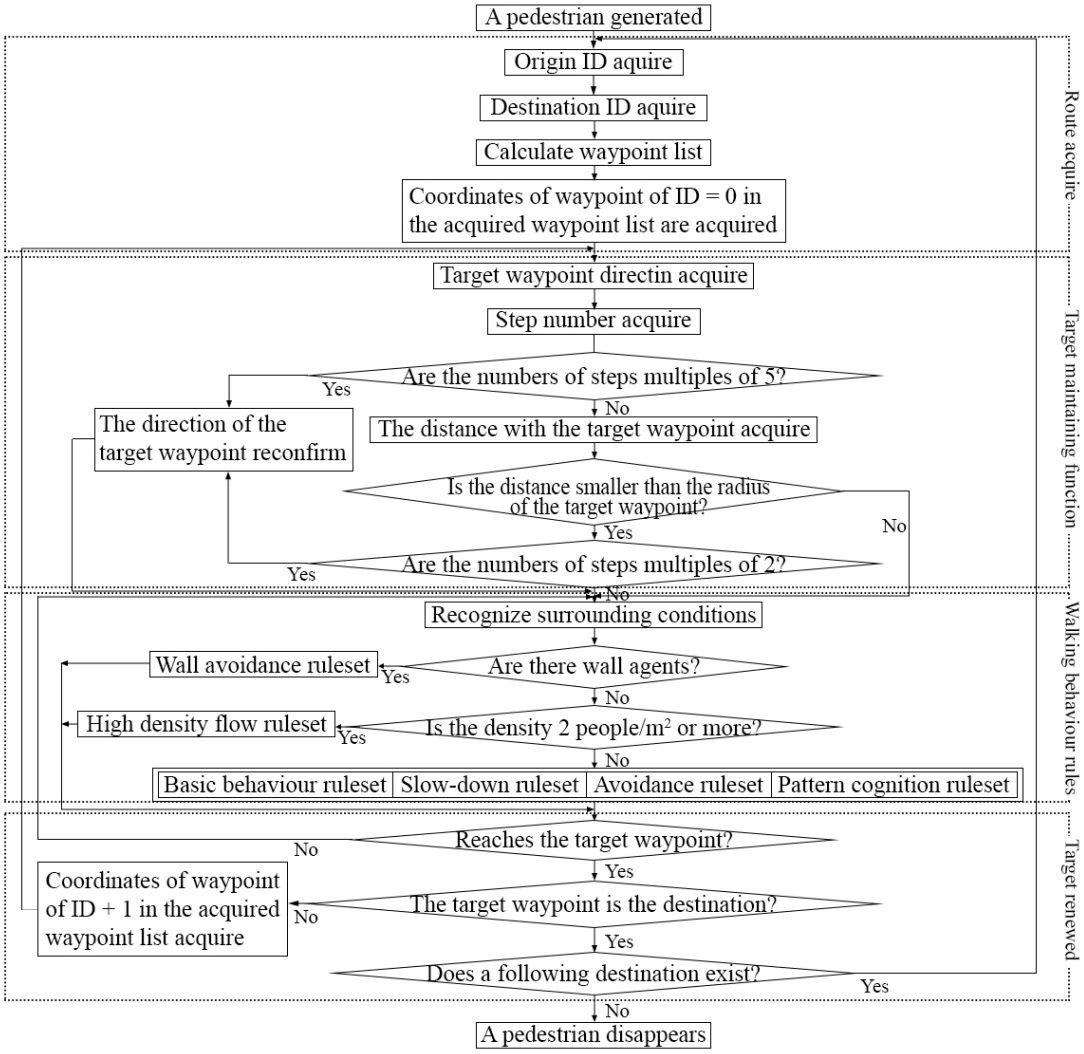

Figure 19 – Pedestrian agent's algorithm.

3.3.2 Pedestrian Behavior Rulesets: ASPFver4.0

ASPF (Agent Simulator of Pedestrian Flows), developed by Kaneda and others,

is introduced as behavioral rules in this model (Kaneda, 2007)(Kaneda & Okayama, 2007)(Kaneda & He, 2009)(Kaneda et al., 2010).

ASPFver.4.0 has a total of 36 rules: six basic behavior rules, eight slow-down rules, four avoidance rules, three high-density flow rules, one pattern cognition rule, and 14 wall avoidance rules. In each step, each agent selects one rule from the ASPF ruleset by following the given priority order. Rule explanations and adaptation priorities are shown in Table 10, and the rule illustration is shown in Figure 20. The ASPF model is essentially implemented as a stochastic simulation model. The updating order of moves of each agent within each simulation step is random sequential in Artisoc. The right/left direction turn of agents in ASPE rules is random with 50:50.

Table 10 – Explanations of ASPF rulesets and rule adapt priorities.

Ruleset (rule number)	Adapt priority	Explanation
Basic behavior rules (6)	1	- Applied when an agent is walking in a low-density situation (density $\leq$ 2 people/m^2). - Not to overlap with one another. - To decide the speed according to the surrounding density.
Slow-down rules (8)	2	- When slowing down in response to other agents, the agent keeps a distance from agents behind and in front in low-density.
Avoidance rules (4)	3	- When avoiding agents, the rules maintain a distance between agents on the left and right sides in low-density.
High-density flow rules (3)	4	- In case of density $\geq$ 2 people/m^2, to reduce span to front and backward agents rather than the right and left.
Pattern cognition rule (1)	5	Scanning the sight zone, decide to follow or avoid the crowd.
Wall avoidance rules (14)	6	To avoid a wall by changing the direction of movement.

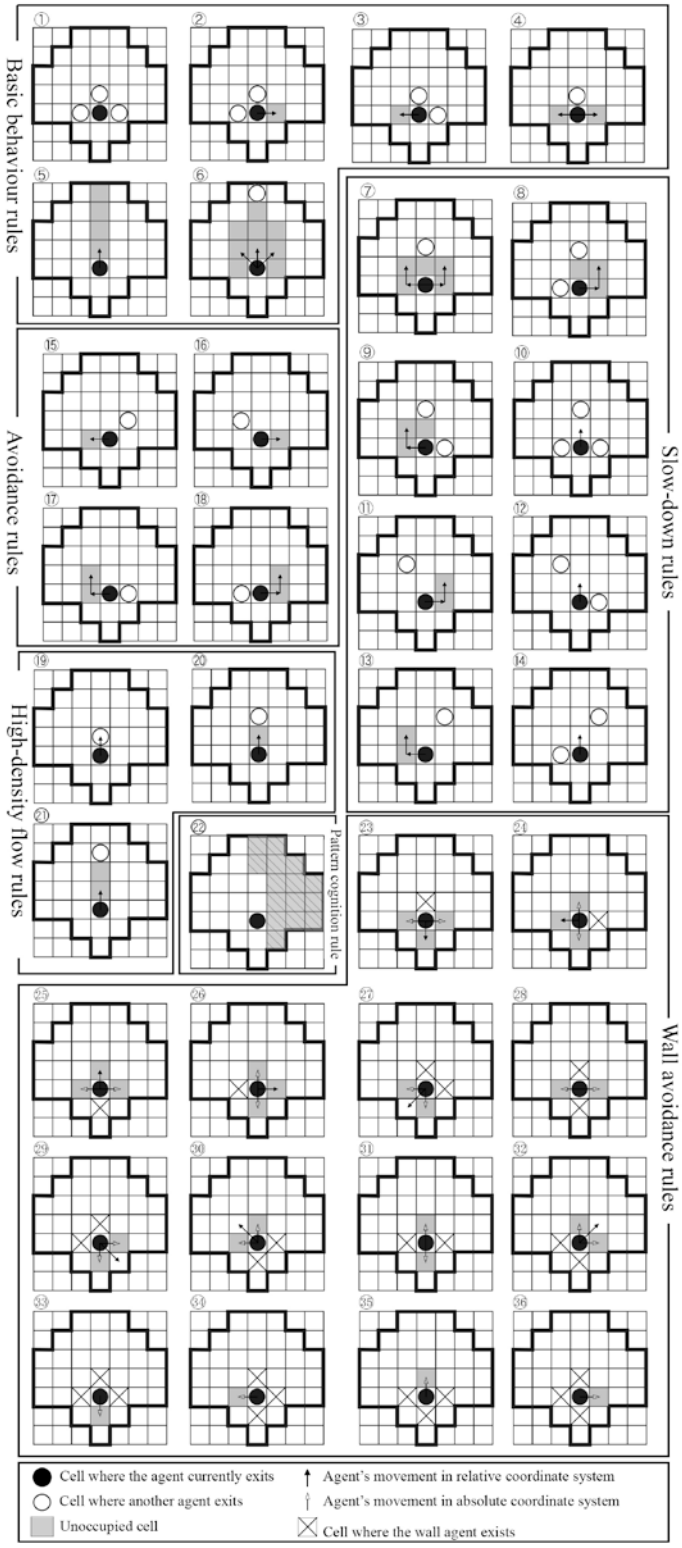

Figure 20 – Explanation of pedestrian behavior rules of ASPFver4.0 (Kaneda & Okayama, 2007).

The pedestrian agent walks following the absolute and relative coordinate system, as described in chapter 2. With the absolute coordinate system's capability and the 0.4m cell-grid space in the current model, density under 6.25 people/m^2 can be calculated accurately. Because of the relative coordinate system's application, a density above 6.25 people/m^2 can be simulated. However, since the current model does not consider body deformation in high density, the density values higher than 6.25 people/m^2 are listed as trends. The agents' speed setting follows Henderson's survey result of casual base distribution of an average speed of 1.34 m/s and a standard deviation of 0.26 m/s (Henderson, 1971).

3.4 Development of Simulation Scenarios

We developed six scenarios, including the original Shanghai Bund space layout in 2014, three designs with different separation facilities, one plan with reserve capacity, and one management plan with proper route control measures. Those scenarios can be seen in Table 11 and Figure 21. Each scenario has a waypoint network accordingly.

Table 11 – Simulation scenario settings.

		Columns on the staircase	Short fences on the viewing platform	Pillars	Iron belt	Warning line (soft)
The original layout	Sc.1 Base case	×	×	×	×	×
Separation facilities	Sc.2 Rotary traffic	√	√	×	×	×
	Sc.3 Pillar	√	×	√	×	×
	Sc.4 Belt separation	√	×	×	√	×
Reserve capacity	Sc.5 Reserve capacity	×	×	×	×	√
Management plan	Sc.6 Route control	×	×	×	×	×

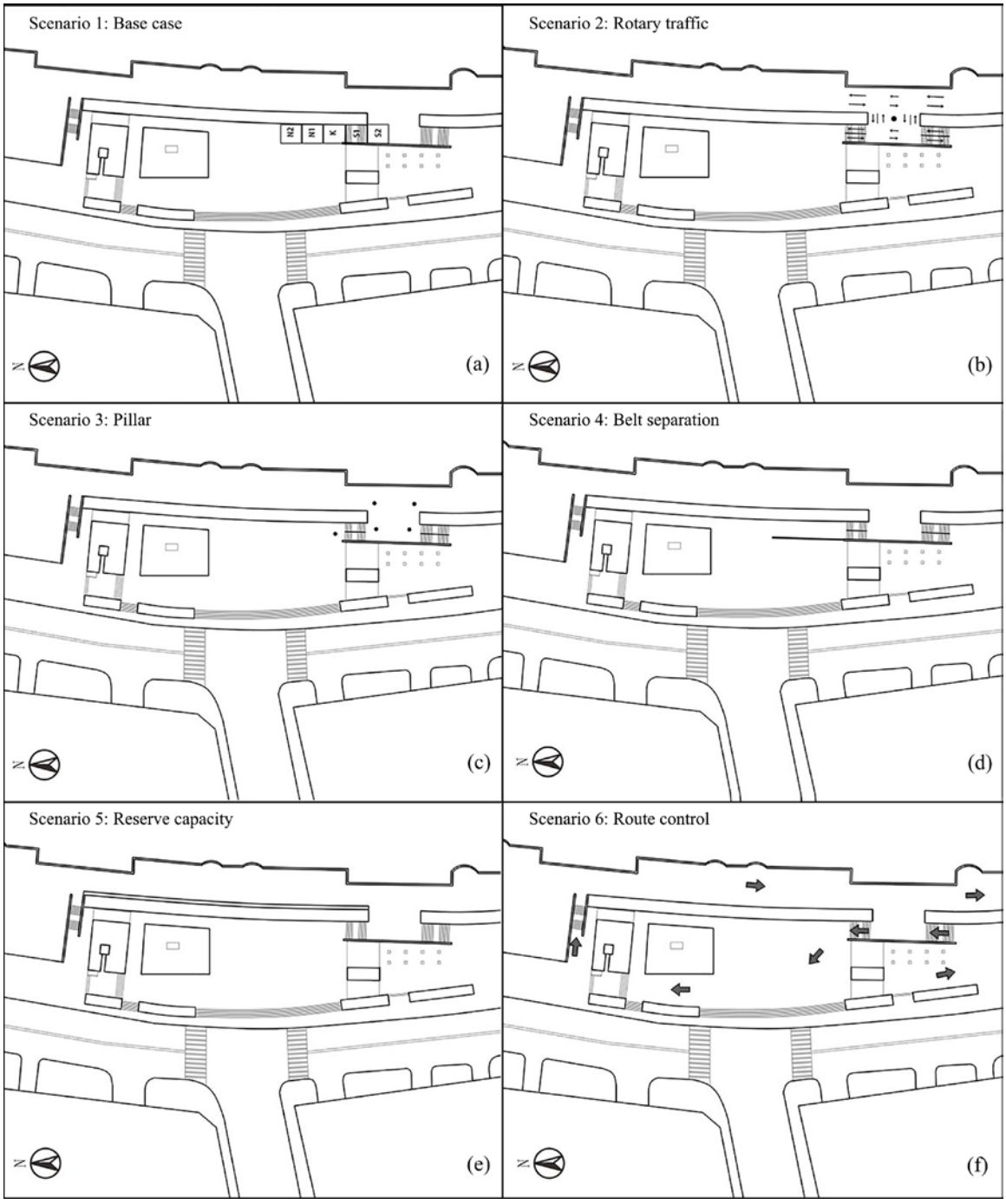

Figure 21 – Scenario settings (a. the original space layout in 2014; b. use separation facilities to form rotary traffic; c. add pillars to divide pedestrian traffic; d. add belt separation facilities after the crowd accident; e. set capacity reserve area and the viewing platform; f. the route control plan implemented after the crowd accident).

• (Sc.1) Scenario 1: Base case

The original space plan is set as the base case, as shown in Figure 21 (a). The staircase has no column to divide the up and down pedestrians. The density will be measured in area K and four density spread zones and each scenario.

• (Sc.2) Scenario 2: Rotary traffic

Research has shown that when two pedestrian streams intersect, pedestrian streams will form stripes to facilitate both sides' movement. However, when three or more flow directions intersect, there will be chaos rather than any kind of stripes (Helbing et al., 2005). As can be seen from Figure 17, the survey shows that many pedestrian streams in different directions meet on the square platform on top of the stairs. Scenario 2 aims to form rotary traffic to avoid congestion, as shown in Figure 21 (b). A few short fences are added to divide pedestrians from different directions.

• (Sc.3) Scenario 3: Pillar

Research has shown that in evacuation experiments, the arching phenomenon is observed because everyone tends to move faster. When an obstacle is added in front of the exit, the evacuation speed increases, pillars can also be considered similar to conventional wave breakers and absorb pressure in the crowds (Helbing et al., 2005). To examine if adding obstacles to divide pedestrian flows is useful in open space and evacuation experiments, scenario 3 situates five pillars in the positions where congestion easily forms, as shown in Figure 21 (c).

• (Sc.4) Scenario 4: Belt separation

After the accident, expandable iron fences were added in the position shown in Figure 21 (d), and stone divisions were added on the staircase to divide up and down pedestrians. This design improvement directly blocked the funnel shape of pedestrian flows in front of the staircase. This scenario is set to examine the current space layout's crowd safety performance, as shown in Figure 21 (d).

• (Sc.5) Scenario 5: Reserve capacity

The Hajj management experience shows that reserve capacity in locations where pedestrians easily accumulate and open the space when the crowd situation is growing risky will be a solution (Al-Kodmany, 2013). Capacity reserve area can also be designed to combine with an emergency aid route. A few days after the accident, a reserve capacity area with a width of around 2 meters was set along the green belt on the viewing platform, as shown in Figure 21 (e). The evacuation route function is unquestioned; however, this area is relatively far from the congestion area, and the ability to lower crowd density is still under testing. In this scenario, the capacity reserve area's fences disappear at the 900-second mark, half of the simulation period.

• (Sc.6) Scenario 6: Route control

Scenario 6 set more proper route control measures than other design improvements, as shown in Figure 21 (f). The visitors are led to the north staircase to go up to the viewing platform, while the south staircase where the accident happened is only used by visitors going downwards.

3.5 Simulation Results and Discussion

As previously mentioned, the surveyed visitor data considered to be a safety coefficient were input into the simulation models from one to four times to examine the

crowd performance. Each scenario was run twenty times to achieve a 95% confidence interval. One simulation step was set as 0.5 seconds, and each simulation was run for 1800 seconds.

The local densities are analyzed according to four stages we divided in the evaluation criteria section: free walking stage (lower than 1 person/m^2), density accumulation stage (from 1 to 3 people/m^2), congestion-forming stage (from 3 to 4 people/m^2) and high-risk stage (over 4 people/m^2).

Figure 22 shows the simulation results of local density by measurement areas, and it is easy to compare the density value. The density areas are: (a) N2 and N1 areas, the space in front of the accident area; (b) K area, to see the density of the accident area; (c) S1 area, to know the density on the staircase; (d) S2 area, to know the density on top of the staircase, which is the platform.

Figure 23 shows the results by scenarios, and it is easy to compare the density difference around the accident spot. The focused density differences are: (a) N2, N1, and K areas, to see if the areas in front of the accident areas are fully applicable as density release areas; (b) K and S1 areas, to see if pressure comes from lack of balance in front of the staircase; (c) S1 and S2 areas, to see if pressure comes from the congestion on top of the stairs.

Figure 24 shows the snapshots of simulations run at twice the surveyed pedestrian flow-in value of each scenario. When the simulation ends, many agents are left in the simulation map, caused by different congestion levels and other route choices. A space that has a higher passing ability is relatively safer. The average visitor number results are shown in Table 12 as a reference.

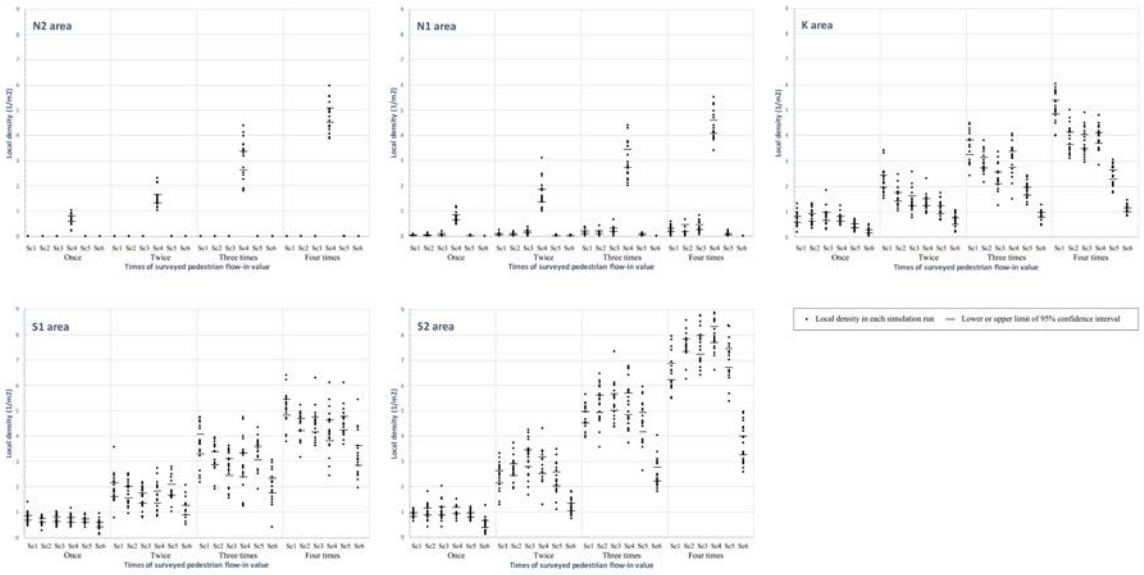

Figure 22 – Local density simulation results shown by density measurement areas.

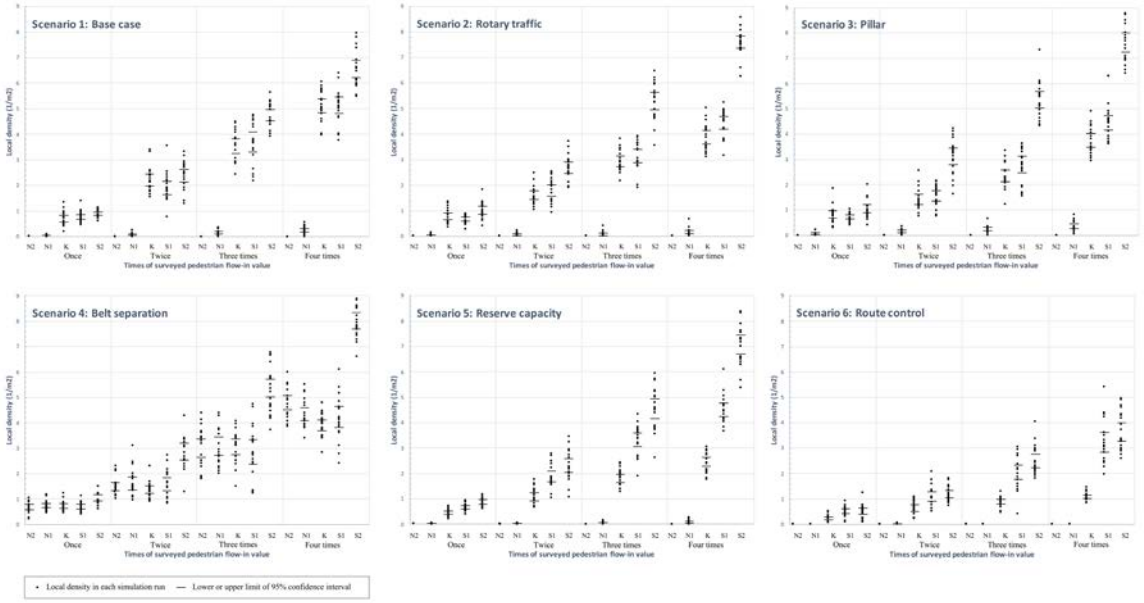

Figure 23 – Local density simulation results shown by scenarios.

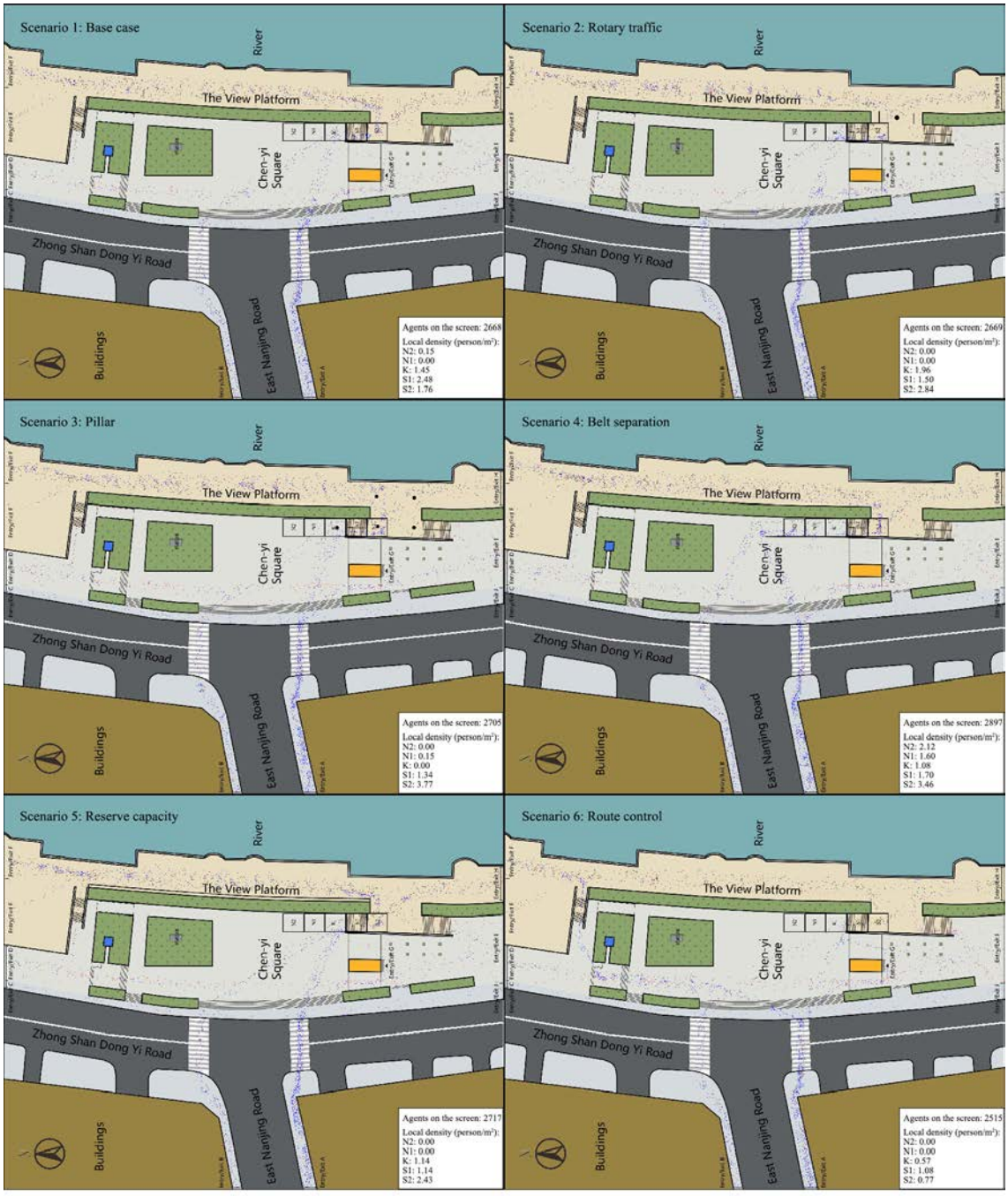

Figure 24 – Snapshots of simulations in two-times surveyed pedestrian flow-in value in different scenarios.

Table 12 – Agent amount in different scenarios.

	Surveyed pedestrian entering value			Twice surveyed value			Three times surveyed value			Four times surveyed value		
	Avg. enter	Avg. exit	On the field	Avg. enter	Avg. exit	On the field	Avg. enter	Avg. exit	On the field	Avg. enter	Avg. exit	On the field
Sc.1	11245	10193.4	1051.6	22479	19751.2	2727.8	33843	28879.4	4963.6	44978.8	37128.2	7850.4
Sc.2	11238.8	10187.8	1051	22554.6	19797.4	2757.2	33908.8	29026.2	4882.6	45082.2	37309.8	7772.4
Sc.3	11237.8	10114.8	1123	22493.8	19700.8	2793	33844	29111.4	4732.6	45054.8	37371.2	7683.6
Sc.4	11242.8	10139.2	1103.6	22601.2	19768.2	2833	33860.2	28771	5089.2	45041.8	36761.6	8280.2
Sc.5	11210.4	10158.8	1051.6	22622.6	19877.6	2745	33920	28985.6	4934.4	45144	37336.6	7807.4
Sc.6	11153.2	10126.2	1027	22505.4	19922	2583.4	33684	28958.6	4725.4	45020.6	37314.8	7705.8

* According to simulation results in this research, average value for 20 times.

From Figure 22, we can see that:

In the N2 and N1 areas, belt separation (Sc. 4) is the only scenario that stopped pedestrians' funnel shape in front of the staircase. While in other scenarios, N2 and N1 areas are always in the free walking stage.

In the K area, all the scenarios reduced the accident spot's density as the flow-in value increased. The route control scenario (Sc. 6) as a management plan has the best ability to reduce the density in the K area, followed by the reserve capacity scenario (Sc. 5) and separation facility scenarios (Sc. 2-4).

In the S1 area, all the scenarios reduced the density on the staircase. The route control scenario (Sc. 6) as a management plan has the best ability to reduce the density on the staircase, followed by the separation facility scenarios (Sc. 2-4) and the reserve capacity scenario (Sc. 5). This result differs from the K area figure, possibly because the capacity reserve area is too close to the congestion area on the platform.

In the S2 area, all the scenarios except the route control scenario increased the platform's density on top of the staircase compared with the base case. This result

demonstrates that special attention should be paid to not making the already congested area worse when adding hard facilities to separate the pedestrians.

From Figure 23, we can see that:

In Sc.1, the base case, the significant density difference between N2, N1, and K means they did not function as a density release area for the critical location. The absence of a significant difference between the K and S1 areas means that the density in front of and on the staircase is quite balanced. The density difference between S1 and S2 areas increases as the flow-in value grows. The high density accumulating on top of the staircase is possibly caused by chaotic flows coming from different directions and will lead to downward pressure. When the people in front of the stairs can no longer sustain the pressure, someone will ultimately fall and cause a domino effect. The video recorded by the media confirmed this inference (Nan-fang Metropolis Daily, 2015).

In Sc.2, rotary traffic, the density difference between N2, N1, and K is not as significant as the base case. The density difference between K and S1 increases compared to the base case. S2 area (platform) accumulated higher densities, which will lead to a higher downward pressure than the base case and makes the crowd situation even riskier. This scenario, designed to make the congestion area orderly, proved to be a dangerous solution.

In Sc.3, Pillar, the density difference between N2, N1, and K is much lower than in the base case. The density difference between K and S1 is more significant than the base case, which will cause pressure from a lack of balance in front of the staircase. S2 area (platform) accumulated a higher density than the S1 area compared with the base case, which will lead to a higher downward pressure and makes the crowd situation risky. This result could be that in evacuation experiments with pillars, occupants move

in the same direction to the exit, and the number of evacuees is limited. The arching effect can be avoided in this way. In an open public space, visitors move in different directions and form more complicated congestion than an arch while new visitors keep flowing into the area. Along with the densities increasing, the pillar may increase congestion, and the uneven distribution of visitors then cause fatalities.

In Sc.4, belt separation, more visitors are led to N2 and N1 areas and the densities in N2, N1 and K areas from one to three times flow-in value are pretty balanced. The density difference between K and S1 is pretty balanced within three times of flow-in values. S2 area (platform) reaches the congestion-forming stage and the high-risk stage first and increases significantly compared to the S1 area with three times the flow-in value. Comparing Sc. 2-4 shows that density accumulates very quickly when over 4 people/m^2. No matter what density release plan is chosen, crowds in the high-risk stage should not last long. This scenario results are a good combination of not overly-high density on the staircase and a not overly-large density difference between the top of the staircase and the front of the staircase. This result shows that the current separation fences added after the crowd disaster positively improve the original space plan.

In Sc.5, reserve capacity, the density difference between N2, N1, and K are much lower than the base case. The density difference between K and S1 is higher than the base case, leading to downward pressure from a lack of balance. The density difference between S1 and S2 areas is getting higher than the base case, which will lead to downward pressure coming from congestion on top of the staircase. There is no doubt the current capacity reserve plan is functional to reduce over-density and function as an emergency plan, but when deciding a location for capacity reserve space, the already congested area should be avoided.

In Sc.6, route control, N2 and N1 are always in the free walking stage, and the K area in front of the staircase maintains a stable low density at around 1 person/m^2. All the areas are generally under 4 people/m^2. The density on the staircase (S1) and on top of the staircase (S2) mirror each other, which means there is no apparent downward pressure.

In conclusion, in the Shanghai Bund crowd disaster, the reason for the accident technically may not have been caused by the upward and downward flows of the pedestrians on the staircase, but because the multi-direction flows meeting on the platform created a fatal downward pressure.

Compared with the ability to lower the densities in crucial areas, like the staircase and the high-density mixed flows area, more efficient crowd management measures such as planning capacity reserve in advance (Sc.5) and changing the route planning (Sc.6) will have a better effect than design improvement measures. However, this does not mean that design improvement should be neglected. The reasons for this are as follows:

(Sc.1) Safety design utilizing computational simulation can help find a space plan's weakness, making more proper crowd management planning possible. In this case, experts tend to consider the approximately 90-degrees relationship between the mainstream from the subway to the Bund led to a contraction in front of the stairs. Still, the simulation results from Sc.1-5 show that the density on top of the stairs is the main reason for the accident.

(Sc.2) Even knowing that high-density flows are dangerous, it is unavoidable in some mass-gathering and limited space environments. When making detour plans,

increasing the congestion of the crucial area should be avoided. The best way is always to keep the density low in the first place.

(Sc.3) An improper detail in a high-density crowd can be fatal. The evacuation approaches should be subjected to adaptability testing before being applied in an open public space. For example, using pillars to divide crowds will increase the congestion and the instability of the crowds.

(Sc.4) It is also essential to maintain a stable overall density. It can be very dangerous if a low-density area is located in a disadvantageous location, worse than having equally high density on both sides.

In the Shanghai case, the separation belt facilities added after the accident have been proven to improve. Reserve capacity and route control measures can be applied as a management plan, together with spatial modification. Any stationary obstacles and stoppers in the areas where congestion forms easily should be avoided in high-density situations. Moreover, the conditions on top of the stairs should be monitored closely. When congestion forms in this area, the downward-moving pedestrians should be led to leave the viewing platform from the south exit to reduce the downward pressure on the stairs.

3.6 Chapter Conclusions

This chapter presented research about improving the crowd congestion condition based on a previous crowd disaster. An agent-based simulation model was built to make the analysis quantifiable, making it easier to consider crowd science in urban space design. The results revealed a different possible reason for the crowd disaster, which may have been caused by the congestion on top of the staircase instead of the

contraction in front of it. By comparing the local density in each scenario, we generalized some common aspects that need to be avoided in public space design dealing with mass gatherings. However, simulation examination is still necessary for specific public spaces dealing with specific crowds to discover the hidden risks. High-density crowds are a magnifier for hidden dangers in urban space. Sometimes, with only a few separation facilities and a more proper crowd management plan, significant life losses can be avoided. It also means that fatalities can happen because of minor improper design details.

The current model cannot consider the spread of force among pedestrians in high-density conditions, and this is the main reason why many current models are invalid for high-density crowd simulations. Moreover, due to the non-reproducibility and ethical issues regarding crowd accidents, the verification and validation of many crowd accident analyses still need improvement.

CHAPTER 4. AN ANALYSIS ON LOW-DENSITY SPATIAL SAFETY: USING AGENT-BASED SIMULATION FOR ESTIMATING PEDESTRIAN PROXIMITY PROBABILITY DURING THE COVID-19 PANDEMIC

4.1 Overview of the COVID-19 Pandemic

With the recent global COVID-19 pandemic, physical distancing measures have been commonly applied. Recent research shows that physical distancing may be necessary into 2022 or even longer (Kissler et al., 2020). Therefore, policymakers must tighten and relax public gathering policies according to the pandemic to balance the economy and health.

This chapter develops an ABM tool to estimate proximity probability with a contagious pedestrian in an atrium inside a station during the COVID-19 pandemic using agent-based simulation. Even though many infectious models have been made to estimate the transmission of COVID-19, there are not enough models estimating people's interactions in a specific space. While keeping people at a distance is more accessible in a stationary scenario, it is harder to follow the distancing regulations since the pedestrian environment is ever-changing. In addition, the pedestrian planning and capacity design for most spaces use standards from the pre-pandemic period, and there is no published quantitive study considering pedestrian proximity probability in public space. This chapter conducted a comparative video analysis before and during the pandemic and divided the pedestrian avoidance behavior into personal spacing avoidance (PSA) behavior and long-range avoidance (LRA) behavior. Based on the findings, an Agent Simulator of Contagious Pedestrian Proximity (ASCPP) was

developed. The pedestrian proximity probability to a contagious agent will be examined under free walking and similar flow conditions within the specific space layout. The influence of the presence/absence of pedestrians' 'distancing' awareness, mask-wearing, and standing pedestrians are simulated and analyzed.

This chapter first conducted a video analysis of pedestrian avoidance behavior in an atrium inside Nagoya Station in June 2020, under the COVID-19 pandemic situation. Then, a video in the same location in June 2015 from different research was analyzed as an ordinary situation. As will be detailed in a later section, we extracted pedestrians' avoidance distance, lateral displacement offset, and avoidance rate of PSA and LRA behaviors from videos taken from both years. Based on the extracted data, we build an Agent Simulator of Contagious Pedestrian Proximity (ASCPP), with pedestrian walking rulesets extracted from the pandemic and ordinary situations. The concept of pedestrian proximity zone is developed by examining the relevant studies. Pedestrian proximity probability with a contagious agent is estimated in each pedestrian proximity zone. Simulation scenarios were designed considering the presence/absence of pedestrians' 'distancing' awareness, the mask-wearing population, and standing pedestrians as influential factors. The results are discussed, focusing on each scenario's degree of effect on an agent's proximity probability.

4.2 Site Survey: Pedestrian Avoidance Behavior Before and During the COVID-19 Pandemic

4.2.1 Data Collection

This section introduces the data collection location and time. The Golden Clock atrium is an indoor public space inside Nagoya Station. Figure 25 shows the spatial layout of this atrium and the video-recording spot. The atrium contains four

entrances/exits, named A to D in this chapter, and has an entire area of 32 × 34 m. Figure 26 is a snapshot of the sight field from the video-recording spot from an overhanging space on the second floor. We recorded a five-minute video clip from 8:00 to 20:00 every two hours on a weekday and a weekend in June 2020. Our comparative video clips are from a different study recorded in the same atrium in 2015 (Mizuno et al., 2016). We excluded the commuting hours and pedestrians congested video clips after comparing the pedestrian walking behaviors and the density levels. There are two reasons for this exclusion: 1) The 2015 video clips were recorded in non-commuting hours and had no apparent pedestrian congestion; 2) Our analysis focuses on the microscopic behavioral difference in the COVID-19 pandemic when pedestrians are under free walking and similar conditions of 0.0 – 0.5 people/m^2. Eventually, two five-minute videos recorded between 14:00 to 15:00 on June 8, 2020, and the comparison video recorded between 19:00 to 20:00 on June 5, 2015, were selected as main video clips. The video clips recorded from other time zones are kept as supplementary video clips.

Table 13 presents a full sampling origin-destination (OD) matrix of the two main video clips in 2015 and 2020. This table presents the number of pedestrians in fields initially, and the pedestrians can be tracked to the OD matrix and the pedestrians in fields at the end of the video clips. The OD matrix shows that a large ratio of pedestrians moves between entrance/exit A to C, and the pedestrian flow is mainly bidirectional. This bi-directional flow with a low possibility of walking conflict is easier to distinguish between pedestrians' 'distancing' behavior within the pandemic context. That is why we chose the area between entrance/exit A and C instead of the area between entrance/exit B and D, which has a diagonal flow of pedestrians walking from entrance/exit A and D. A density-speed measurement area is set in the middle of the atrium.

We also counted the mask-wearing ratio among the population in the pandemic case. Among the 100 pedestrians selected randomly, 90% were wearing a mask. Most of them were commercial non-woven masks, and a small percentage were handmade masks.

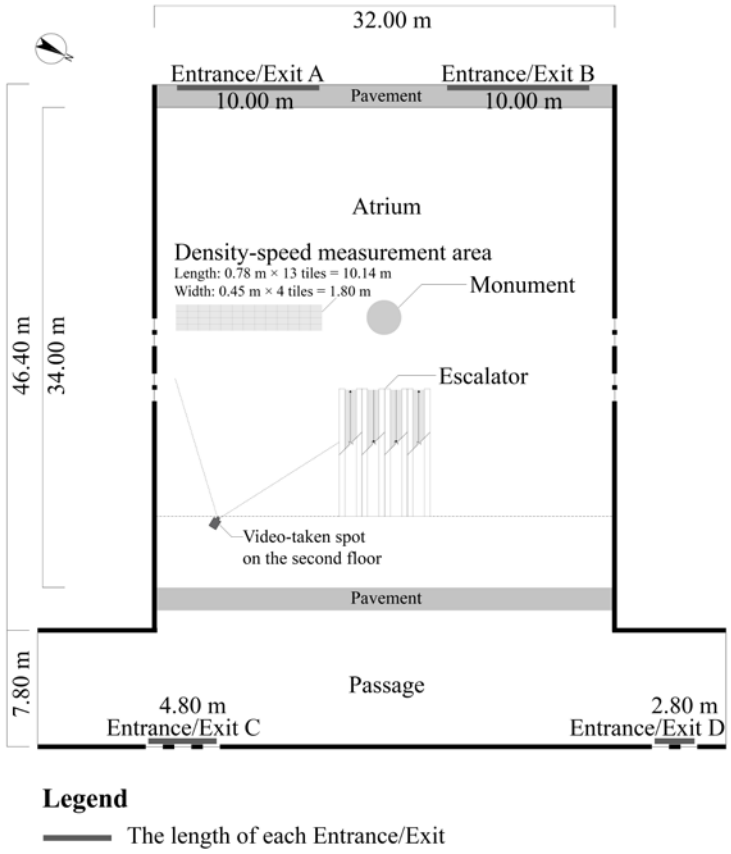

Figure 25 – Spatial layout of the atrium in Nagoya Station.

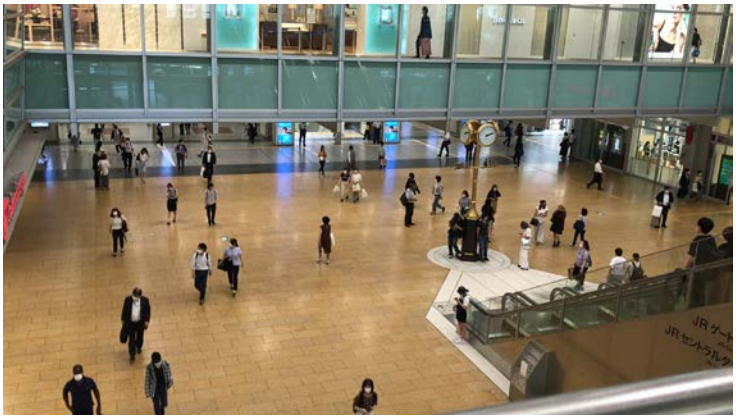

Figure 26 – Sight field from the video-recording spot in 2020.

Table 13 – Pedestrian origin-destination matrix measured in 2015 and 2020.

2015 ordinary situation (five-minute measured value)											2020 pandemic situation (five-minute measured value)										
To / From		In fields α*	Inflow β	Outflow γ: Exit					Other**	In fields δ	To / From		In fields α	Inflow β	Outflow γ: Exit						In fields δ
				A	B	C	D	Total							A	B	C	D	Total	Other	
Entrance	A	71	148	—	1	103	10	114	122	73	Entrance	A	40	127	—	0	90	8	98	101	42
	B		139	0	—	35	73	108				B		96	0	—	21	30	51		
	C		126	74	21	—	1	96				C		84	59	15	—	0	74		
	D		96	21	45	1	—	67				D		43	10	12	2	—	24		
Total		71	509	95	67	139	84	385	122	73	Total		40	350	69	27	113	38	247	101	42

* Infield α + inflow β – outflow γ = infield δ

** Pedestrians exit the atrium through the escalator or retail stores.

Pedestrian passed density-speed measurement area	West to east	East to west	Total	Pedestrian passed density-speed measurement area	West to east	East to west	Total
	106	105	211		93	79	172

4.2.2 Measured Speed in Each Density Level

We compare how the COVID-19 influences pedestrian walking speed and avoidance behaviors. The video clips recorded from 2015 and 2020 can not have precisely the same pedestrian flow conditions to make the comparison. To control the variable, we classify five density levels to compare pedestrian speed and avoidance behavior within the same local density level. We also conducted ANCOVA and ANOVA analysis to exclude the influence of density but focus on the influence of COVID-19.

In this section, we compare pedestrian speed before and during the pandemic. The samples for speed measuring are selected with the following steps: 1) A snapshot is taken every 30 seconds (enough time for a pedestrian to pass the atrium to avoid sample duplication) from the two main video clips and supplementary video clips; 2) In each snapshot, the pedestrians between entrance/exit A and C are assigned ID numbers. 155 pedestrians in 2015 and 140 pedestrians in 2020 are assigned ID numbers; 3) We then go to each ID pedestrian's time frame when his body centerline touches the west/east line of the density-speed measurement area. We count the frames (one frame of video clip = 1/30 second) each pedestrian spends to pass the measurement area.

When the pedestrian's body centerline touches the centerline of the measurement area, we count how many other pedestrians are existing in the measurement area. In this way, the density-speed pair for each ID pedestrian is acquired; 4) We classify all the ID pedestrians by their density levels. Steps 2 and 3 are repeated a few times to ensure twenty samples in each density level. Among each density level, ten samples passed the measurement area from west to east inside each density level, and ten samples passed from east to west. In total, 100 samples each from the ordinary situation and the pandemic situation are selected.

Figure 27 shows all the measured speeds in each density level, the average values, and the 95% confidence intervals. In the hours the videos were recorded, density above 0.50 people/m^2 is scarce. Therefore, the average speed in the ordinary situation is 1.15 m/s with a standard deviation of 0.27 m/s, while the average speed in the pandemic situation is 1.14 m/s with a standard deviation of 0.22 m/s.

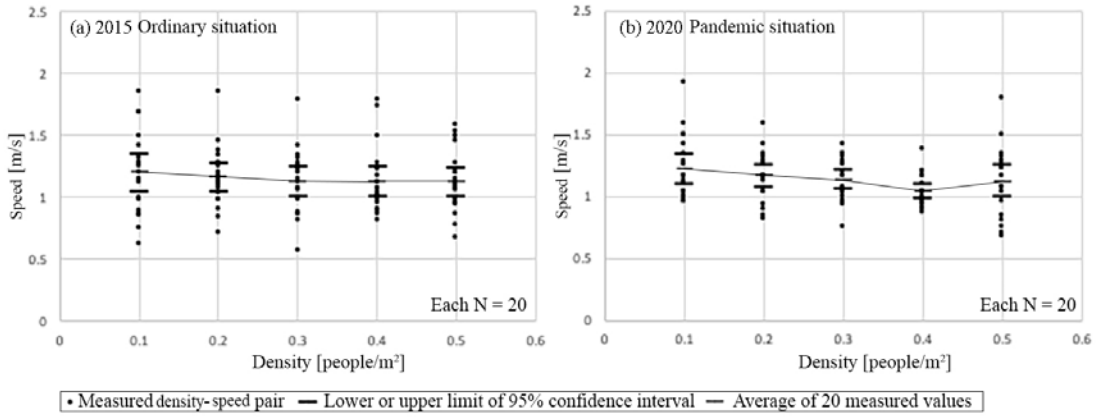

Figure 27 – Measured speed in each density level.

To examine if COVID-19 has influenced pedestrian walking speed, we conducted an analysis of covariance (ANCOVA). ANCOVA evaluates whether the means of a dependent variable (DV) are equal across levels of a categorical independent variable

(IV) while statistically controlling for the effects of other continuous variables that are not of primary interest, known as covariates (CV) (Keppel, 1991). All statistic analysis in this paper is conducted using data analysis software SPSS (SPSSAU, 2021).

This research analyzes the influence of the COVID-19 (IV) on pedestrian speed (DV). The data set includes two groups, 100 samples in the ordinary situation and 100 samples in the pandemic situation. The pedestrian density is considered in the analysis model as a covariate. This set of data passed the parallelism test that the interactive item: COVID-19*Density does not show significance ($F = 0.302$, $p = 0.583 > 0.05$). Table 14 shows the results of ANCOVA. The density factor shows significance ($F = 4.198$, $p = 0.042 < 0.05$) on its influence on speed, which is an obvious result. However, ANCOVA aims to exclude the influence of density and focus on the influence of COVID-19 on speed. The COVID-19 factor does not show significance ($F = 0.138$, $p = 0.711 > 0.05$). It means whether or not the pedestrian is walking during the COVID-19 pandemic does not significantly affect pedestrian speed.

Table 14 – Analysis of covariance on speed.

Source of differences	Sum of squares	df	Mean square	F	p
Intercept	54.288	1	54.288	922.095	0.000**
COVID-19 (pandemic/ordinary)	0.008	1	0.008	0.138	0.711
Density	0.247	1	0.247	4.198	0.042*
Residuals	11.598	197	0.059		
R^2: 0.022					
* p < 0.05 ;** p < 0.01					
ANCOVA for the ‘measured speed’ samples plotted in Figure 27; Ordinary samples n = 100, Pandemic samples n = 100.					

4.2.3 Personal Spacing Avoidance (PSA) and Long Range Avoidance (LRA)

In this section, we compare the avoidance behavior before and during the pandemic. As mentioned before, we define avoidance behavior starting at a distance of

less than 3.66 m as PSA, or else as LRA. Figure 28 shows the illustration of PSA and LRA in the opposite direction. We measure four variables: the avoidance distance and the lateral displacement offset (after this referred to as offset) of avoidance behavior, the encounter number and the avoidance times while a pedestrian transit the atrium. The avoidance distance is the distance from an avoided object when the avoidance subject starts a direction change, marked as L. The avoidance subject and object's avoidance distance can differ depending on if they start avoidance simultaneously. The offset is the lateral displacement of a subject/object since the avoidance starts and is measured when the distance between the avoidance subject and object is the nearest. The encounter number counts how many other pedestrians one passes by while traversing the atrium. The avoidance times measure how many avoidance behaviors one makes while transiting the atrium.

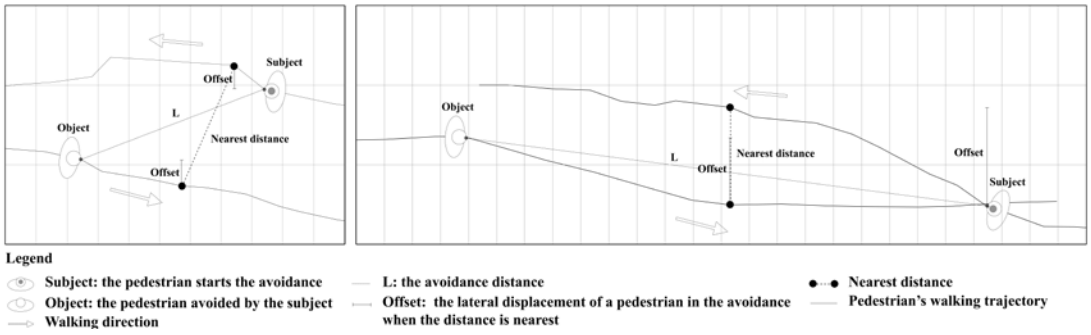

Figure 28 – Pedestrian's personal spacing avoidance (PSA) behavior and long-range avoidance (LRA) behavior.

The samples selected for the density-speed measurement are continued to use in the avoidance analysis. If one sample has multiple PSA and LRA behaviors in the trip, only the first PSA and LRA are extracted to get a more accurate value among the population. Some pedestrians do not make avoidance during the transit. In total, 61 samples from the ordinary situation and 60 samples from the pandemic situation are

selected. Figure 29 shows the avoidance distance distribution in each density level of the selected samples.

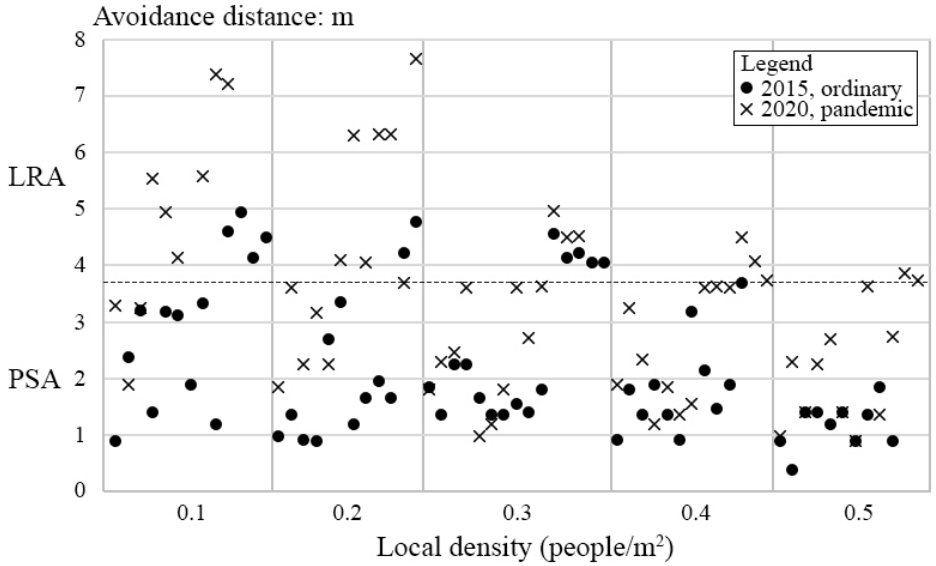

Figure 29 – Pedestrians' avoidance distance in each density level.

Table 15 and Table 16 show using two-way analysis of variance (ANOVA) to study the influences of COVID-19 and density on avoidance distance. PSA and LRA are analyzed separately. In ANOVA for PSA, COVID-19 shows significance ($F = 19.670$, $p = 0.000 < 0.05$), and it means COVID-19 influences the PSA avoidance distance; the density also shows significance ($F = 3.463$, $p = 0.012 < 0.05$), and it means density influences the PSA avoidance distance. In ANOVA for LRA, COVID-19 shows significance ($F = 4.679$, $p = 0.041 < 0.05$), and it means COVID-19 influences the LRA avoidance distance, while the density does not show significance, means density does not cause a difference in long-range avoidance distance.

Table 15 – Analysis of variance on avoidance distance (PSA).

ANOVA on personal spacing avoidance distance					
Source of differences	Sum of squares	df	Mean square	F	p
Intercept	350.060	1	350.060	586.323	0.000**
COVID-19	11.744	1	11.744	19.670	0.000**
Density	8.270	4	2.068	3.463	0.012*
Residuals	48.360	81	0.597		
R^2: 0.268; * p < 0.05; ** p < 0.01					
Mean ± Standard deviation					
Density (people/m^2)	0.1 (n=12)	0.2 (n=15)	0.3 (n=20)	0.4 (n=20)	0.5 (n=20)
Ordinary	2.29 ± 0.97	1.67 ± 0.81	1.69 ± 0.35	1.69 ± 0.66	1.17 ± 0.41
Pandemic	2.81 ± 0.80	2.62 ± 0.73	2.40 ± 0.98	2.42 ± 0.99	1.96 ± 0.89

Table 16 – Analysis of variance on avoidance distance (LRA).

ANOVA on long-range avoidance distance					
Source of differences	Sum of squares	df	Mean square	F	p
Intercept	666.193	1	666.193	340.684	0.000**
COVID-19	9.150	1	9.150	4.679	0.041*
Density	5.781	2	2.891	1.478	0.248
Residuals	46.931	24	1.955		
R^2: 0.283; * p < 0.05; ** p < 0.01					
Mean ± Standard deviation					
Density (people/m^2)	0.1 (n=11)		0.2 (n=9)	0.3 (n=8)	
Ordinary	4.54 ± 0.34		4.49 ± 0.39	4.20 ± 0.21	
Pandemic	6.51 ± 2.22		5.49 ± 1.53	4.66 ± 0.26	

Table 17 shows the analysis results of PSA and LRA in both situations. In LRA, two types of offset are observed, designated as a small offset when the offset is smaller than 0.40 m (around one step distance) or else as a large offset. PSA/LRA rate is the number of the PSA/LRA avoidance behavior divided by the total encounter number; it means the frequency one avoids other pedestrians.

Table 17 – Analysis results of personal spacing avoidance (PSA) behavior and long-range avoidance (LRA) behavior.

Year	Local density (people/m²)	Personal spacing avoidance (PSA)			Long-range avoidance (LRA)				Total avoidance times		Avoidance rate		
		Ave. distance*1 (m)	Ave. offset (m)	Ave. times	Ave. distance (m)	Ave. offset (m)	Ave. times	Small: large offset*2	Ave. encounter (people)	Ave. times	Ave. PSA rate*3	Ave. LRA rate	Ave. total rate
2015	0.10	2.29	0.50	1.90	4.54	1.37	0.40	0.50: 0.50	5.50	2.30	0.35	0.07	0.42
	0.20	1.67	0.44	2.40	4.49	0.20	0.30	0.00: 1.00	5.30	2.70	0.45	0.06	0.51
	0.30	1.69	0.41	2.10	4.20	0.78	0.50	0.60: 0.40	5.60	2.60	0.38	0.09	0.47
	0.40	1.69	0.51	2.70	3.68	0.59	0.20	1.00: 0.00	6.30	2.90	0.43	0.03	0.46
	0.50	1.17	0.35	2.80	—	—	—	—	7.00	2.80	0.40	0.00	0.40
	Average	1.70	0.44	2.38	4.23	0.74	0.35	0.53: 0.47	5.94	2.66	0.40	0.05	0.45
2020	0.10	2.81	0.33	0.30	6.51	0.61	0.70	0.29: 0.71	4.30	1.00	0.07	0.16	0.23
	0.20	2.62	0.55	1.00	5.49	0.45	0.90	0.20: 0.80	5.00	1.90	0.20	0.18	0.38
	0.30	2.40	0.51	3.40	4.66	0.78	0.30	0.67: 0.33	6.70	3.70	0.51	0.04	0.55
	0.40	2.42	0.51	3.40	4.10	0.46	0.30	0.33: 0.67	6.80	3.70	0.50	0.04	0.54
	0.50	1.96	0.51	3.30	3.79	0.59	0.20	0.50: 0.50	6.40	3.50	0.51	0.04	0.55
	Average	2.44	0.48	2.28	4.91	0.58	0.48	0.40: 0.60	5.84	2.76	0.36	0.09	0.45

*1 Each average value of this table is an average of 20 pedestrian samples.

*2 Offset: LRA small offset≤0.4m; LRA large offset>0.4m.

*3 The 20 pedestrian samples for each density level include the pedestrians who do not make any avoidance. They are only included for calculating PSA/LRA rates.

PSA and LRA avoidance distance In Table 17, we divide the avoidance distance difference by one ladder for 0.40 m, around one walking step. PSA avoidance distance in both ordinary and pandemic situations show three ladders. In the pandemic situation, PSA's average distance is 2.44 m, which is much higher than the average distance of 1.77 m in the ordinary situation. LRA distance in the ordinary situation shows three ladders, while in the pandemic situation, the distance in each density level varies from the others. In the pandemic situation, the average distance for LRA is 4.91 m, which is much higher than the average distance of 4.23 m in the ordinary situation. In the ordinary situation, pedestrians stop LRA behavior when the density reaches 0.50 people/m^2.

PSA and LRA offset In the ordinary situation, PSA offset decreases obviously when the density reaches 0.50 people/m^2. In the pandemic situation, the PSA offset stays stable as the density goes higher. The exception at 0.10 people/m^2 is because

pedestrians take longer LRA avoidance distance. Also, because of the longer LRA avoidance distance under the pandemic situation, the average LRA offset of 0.74 m in the ordinary situation is larger than 0.58 m in the pandemic. In the ordinary situation, 0.47 of the LRA takes a larger offset, while in the pandemic situation, this number increases to 0.60.

PSA and LRA rate The average total avoidance rate of PSA and LRA keeps unchanged at 0.45. However, in the pandemic situation, the rate of LRA behavior increases from 0.05 to 0.09.

Big gestures (BG) When a pedestrian can not make avoidance in advance, the pedestrian starts and finishes the avoidance in one or two walking steps. We found big gesture avoidance behaviors quite often in the videos. The observed BG includes: 1) A pedestrian encounters a few other pedestrians side by side; 2) A fast-walking pedestrian wants to pass a slow walking pedestrian in front of him; 3) Crossing pedestrians choosing conflicting walking directions.

Conclusions of comparative analysis The analysis results show that under the pandemic conditions: 1) Pedestrian walking speed does not have significant changes; 2) Pedestrians have significant longer avoidance distance; 3) The lateral displacement offset of avoidance behavior is slightly higher in PSA; 4) Pedestrians conduct LRA more often. Also, pedestrians will conduct sudden avoidance when they realize they are too close to one another (BG). These findings are thought to reflect pedestrian's 'distancing' awareness.

4.3 Development of an Agent Simulator of Contagious Pedestrian Proximity

4.3.1 Pedestrian Agent Algorithm

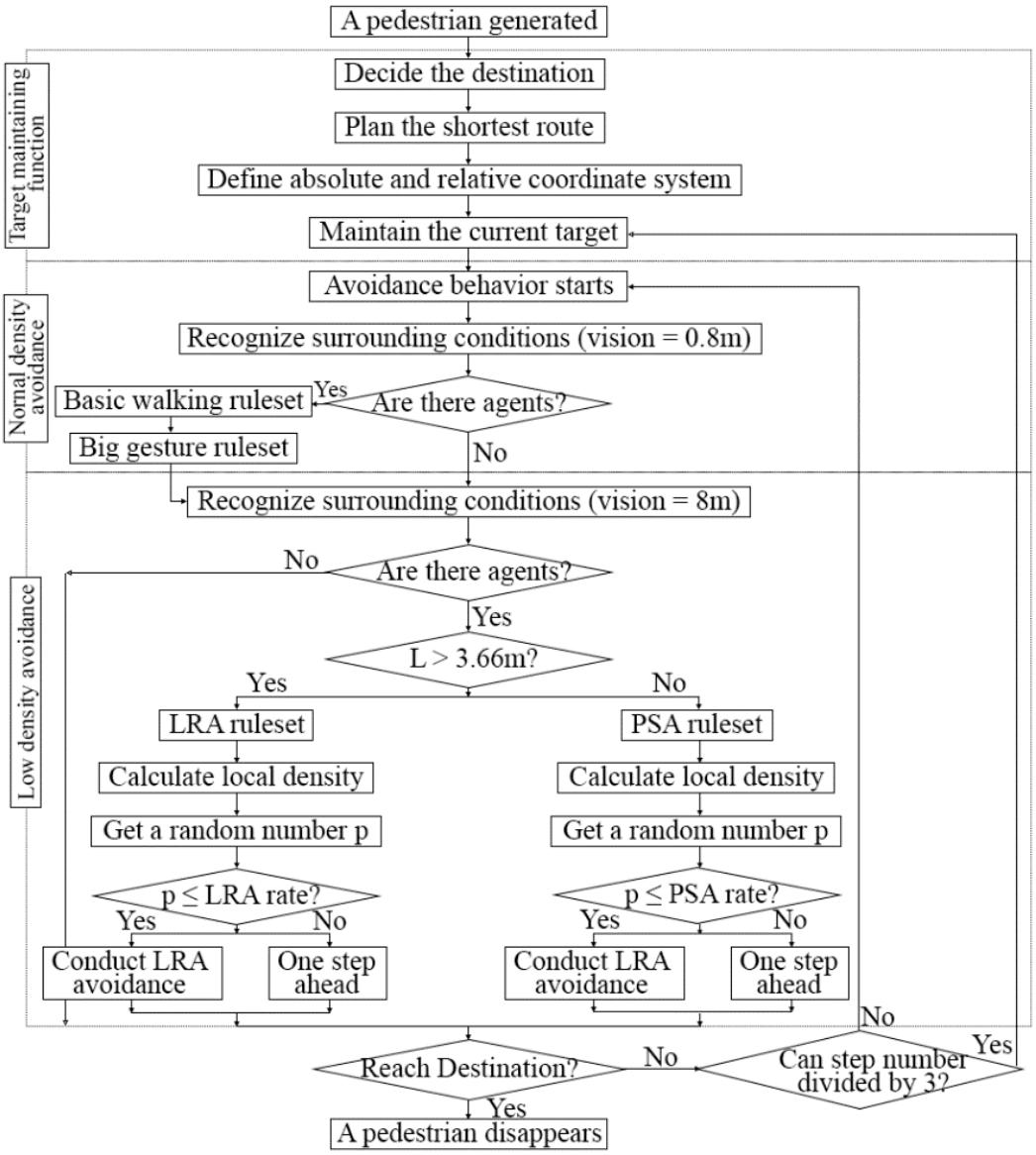

Figure 30 – Pedestrian agent's algorithm.

Figure 30 shows the pedestrian agent's algorithm. A pedestrian agent is generated according to the setup generation rate and origin-destination matrix at its entrance. The agent's trip towards its destination moves following the shortest path principle on our preset waypoints while avoiding other agents and obstacles. The waypoints are temporary targets while walking towards the destination exit and are set based on the directly visible principle. When an agent moves into the sphere of its target, it updates its target. The waypoint and the sphere around it are set up intuitively according to

observation and simulation test run. The waypoint network and the sphere of each waypoint are shown in Figure 32. The agent will confirm its direction towards the target every three steps. In each step, the pedestrian agent will scan agents in the close-by cells and apply normal density avoidance rules. If there are not agents in the close-by cells, the agent will continue to scan its personal space and long-range space to apply low-density avoidance rules. This algorithm repeats every simulation step until the agent reaches its destination. Each simulation runs for 2700 steps.

4.3.2 Pedestrian Behavior Rulesets: ASCPP

Figure 31 shows the ASCPP rulesets. The bold frame denotes the vision of the agent. The shaded cell means this cell needs to judge that another agent does not exist. The merged cells mean the existence of other agents in any of those cells is equal. The left-right inverted states are omitted. We know from the video analysis that some pedestrian avoidance takes more than one step to finish when the offset is large. The step number reflects the simulation steps need to complete the avoidance. ASCPP includes four behavioral rulesets extracted from the video analysis results: 8 basic behavior rules for the ordinary case and 7 basic behavior rules for the pandemic case, 1 big gesture rule, 2 long-range avoidance rules, and 6 personal spacing avoidance rules. In each simulation step, each agent selects only one rule from the ASCPP rulesets by the sequential order of rule number, according to its surroundings. The updating of each agent's movement inside one simulation step is random sequential. The right/left turn in a rule is random with 50:50. The PSA and LRA avoidance follow the extracted avoidance rate and avoidance distance according to the local density level in Table 17. The offset of LRA behavior also has a probability of being a large or small offset.

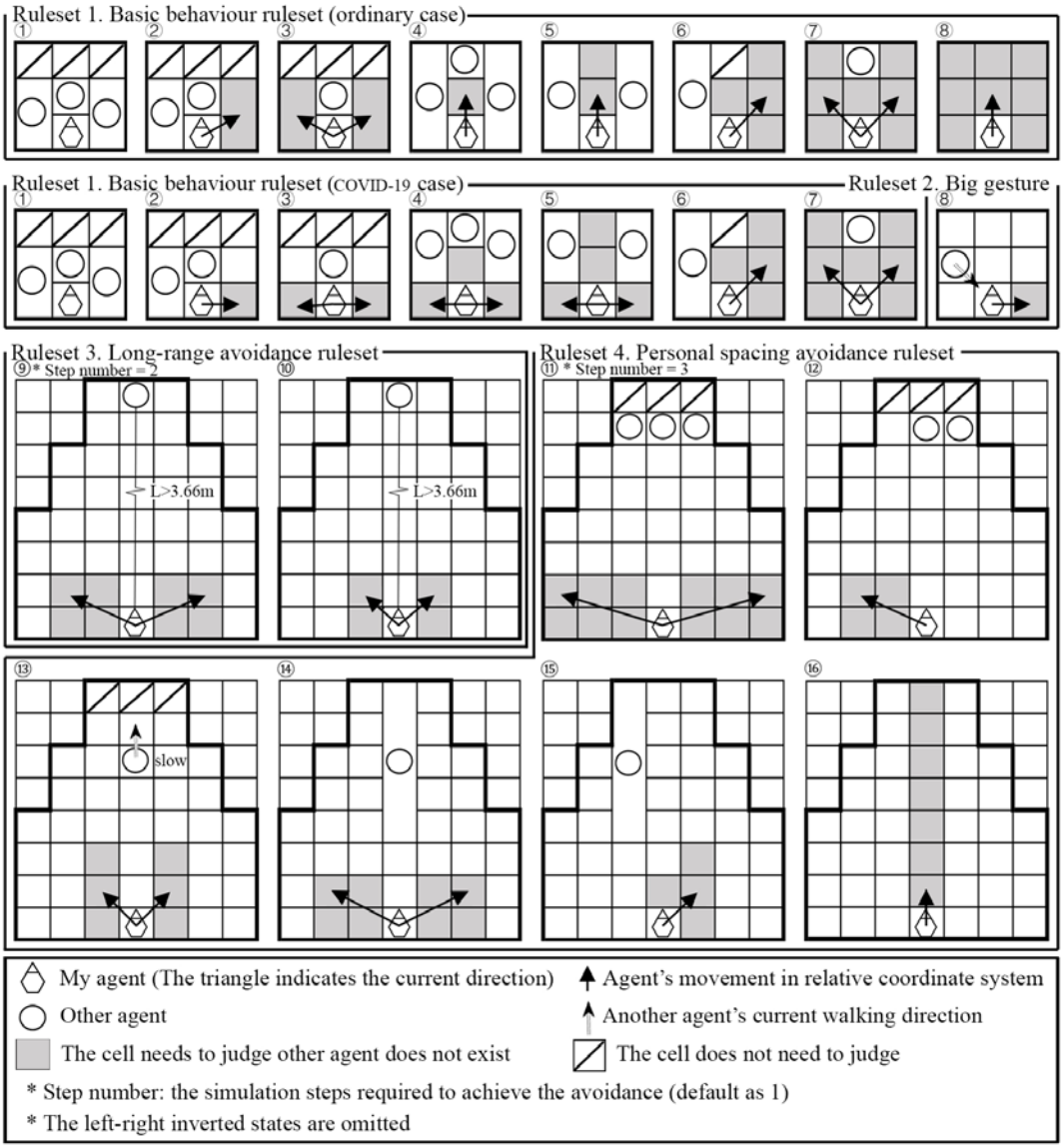

Figure 31 – ASCPP pedestrian behavior rulesets.

4.3.3 Variable Settings

Our simulator includes three variable categories: the general variables, pedestrian variables, and input variables. The general variables include variables for the generators, origin-destination settings, waypoint settings, proximity zone settings, and different counters. The pedestrian variables, including coordinate system, direction, speed, destination, target, health, encounter, and mask-wearing condition. The input variables, including pedestrian generation rate for each entrance, the contagious rate among the

population, the mask-wearing rate among the population, the avoidance distance for each density level (PSA and LRA), PSA and LRA rate.

The speed of each agent is set from our video analysis results: in the ordinary situation, the average speed is 1.15 m/s, and the standard deviation is 0.27 m/s with normal distribution, while in the pandemic situation, the average speed is 1.14 m/s, and the standard deviation 0.22 m/s with normal distribution.

4.3.4 Model Validation

Table 18 – Model validation results.

	Ordinary case (2015)					Pandemic case (2020)				
	PSA times	LRA times	Ave. encounter (people)	PSA rate	LRA rate	PSA times	LRA times	Total encounter (people)	PSA rate	LRA rate
Ave. measured value*1	2.70	0.20	6.30	0.43	0.03	3.40	0.30	6.80	0.50	0.04
Ave. simulation value*2	2.25	0.58	6.38	0.35	0.09	2.67	0.28	4.78	0.55	0.06
Error	-0.45	0.38	0.08	-0.08	0.06	-0.73	-0.02	-2.02	0.05	0.02

*1 The survey video analysis data from Table 17, in the density level 0.4 people/m^2.
*2 Each average value results from 20 simulation runs; the average local density of 20 simulation runs is in the density level of 0.4 agent/m^2.

As a validation of the model, we ran 20 simulation trials with an average local density of 0.4 people/m^2 for both ordinary case and pandemic case. From the output of the trials, we calculated PSA and LRA rates by dividing the values of PSA and LRA times by Average Encounter. Table 18 shows the comparison with the measured values with the same density level in Table 17. The PSA rate was found to have an error of -0.08 (measured value 0.43, simulation value 0.35) for the ordinary case and 0.05 (measured value 0.50, simulation value 0.55) for the pandemic case. On the other hand, the error in the LRA rates was found to be 0.06 (measured 0.03, simulation 0.09) for the ordinary case and 0.02 (measured 0.04, simulation 0.06) for the pandemic case. The

simulation outputs relatively well-reproduced pedestrian survey data. This validation result shows that the model can reproduce the PSA and LRA behaviors and make further predictions.

4.4 Development of Simulation Scenarios

Table 19 shows the simulation scenario design. In total, five scenarios are considered. These scenarios range from the ordinary case without the mask-wearing population (Sc.000) to the pandemic case with the different mask-wearing population (Sc.100-Sc.120) and the pandemic case with standing pedestrians (Sc.101). Sc.120 reflects the actual pedestrian flowrate and mask-wearing rate, as in the 2020 video.

Table 19 – Scenario design.

Scenario name	Scenario settings		
	Pandemic	Mask	Standing pedestrian
Sc.000	×	×	×
Sc.100	○	×	×
Sc.110	○	50%	×
Sc.120	○	90%	×
Sc.101	○	×	○

In Sc.101, two standing agents are located in the pedestrian flow between entrance/exit A and C. The golden clock atrium is a customary waiting area for pedestrians in Nagoya Station. While most waiting pedestrians are standing by the walls or the escalator, a few standing pedestrians are often present on other pedestrians' walking paths.

In each scenario, 1% of the population is set as contagious and does not wear masks. This is a hypothetical condition to show the influence of each influential factor. Under different flowrate settings, the total population vary from around 1500 to 2100.

1% is a value decided from the simulation test run to ensure there is no more than one contagious agent on the map simultaneously, and the contagious agents occupy the same proportion of the total population. The contagious agents appear on the map at even time intervals and travel from entrance/exit A to C. Each scenario was run 20 times in the video taken flowrates from 2015 and 2020 to reduce the error caused by different pedestrian flowrate. At the end of each simulation run, the number of agents in each proximity zone is divided by the total population to get a proximity zone rate.

4.5 Simulation Results and Discussion

This section presents the application of our ASCPP model to estimate the pedestrian proximity probability with a contagious agent. According to the survey videos, the densities in all the scenarios are lower than 0.5 people/m^2. Figure 32 shows the simulation snapshots.

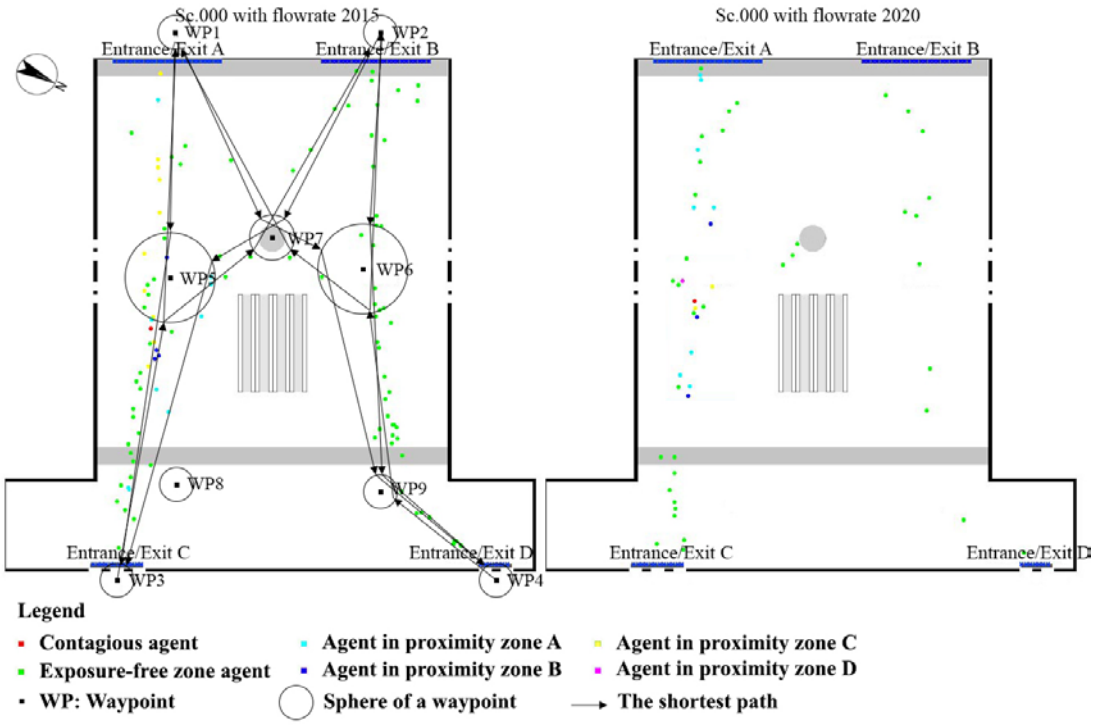

Figure 32 – Waypoint network and simulation snapshot.

Table 20 shows the simulation results of the agent distribution in each proximity zone. Figure 33 shows the agent number in each proximity zone with the means and 95% confidence intervals. After plotting the above data, we can compare the relationships across scenarios with the spans of the confidence intervals based on 20 times simulation runs.

Table 20 – Simulation results of the agent distribution in each proximity zone.

Scenario name	Flowrate (year)	Population (agent)	Distribution of agents in each proximity zone					Density (agent/m²)	Violation of physical distancing
			Exposure-free zone	Zone A	Zone B	Zone C	Zone D		
Sc.000	2015	2113.15	69.94%	10.18%	2.64%	15.75%	1.49%	0.46	17.25%
	2020	1526.75	75.93%	8.49%	1.95%	11.36%	1.29%	0.48	12.66%
Sc.100	2015	2102.25	71.85%	10.21%	2.37%	14.53%	1.04%	0.41	15.57%
	2020	1509.65	77.77%	8.24%	2.01%	10.09%	0.90%	0.45	10.99%
Sc.110	2015	2097.80	85.35%	5.02%	1.21%	7.27%	1.14%	0.46	8.42%
	2020	1504.50	87.70%	4.05%	1.02%	5.19%	1.04%	0.41	6.23%
Sc.120	2015	2089.40	96.27%	1.03%	0.22%	1.44%	1.04%	0.43	2.48%
	2020	1502.40	95.79%	0.87%	0.25%	1.07%	1.02%	0.43	2.10%
Sc.101	2015	2100.15	71.71%	10.25%	2.35%	14.55%	1.14%	0.40	15.69%
	2020	1490.70	77.01%	8.22%	1.95%	10.79%	1.02%	0.41	11.81%

* The results for each scenario represent an average value of 20 simulation runs.

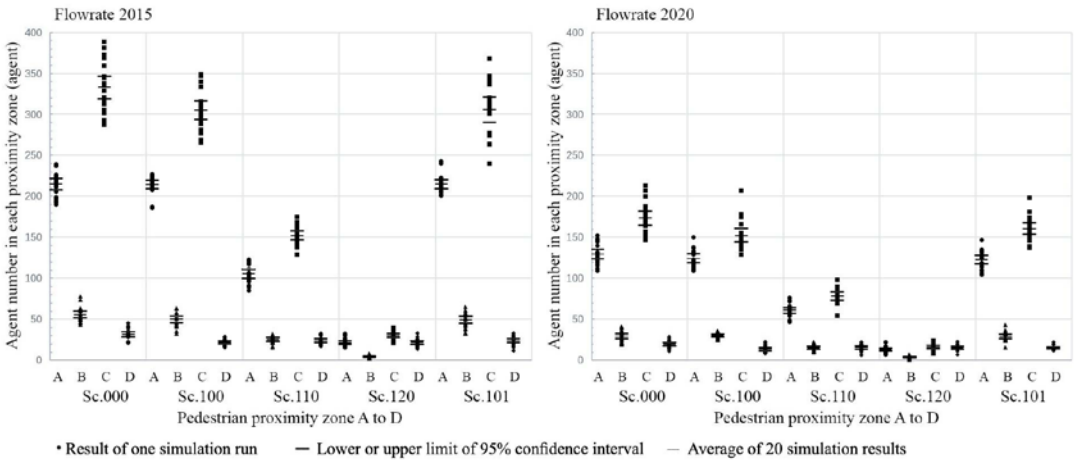

Figure 33 – Agent number in each proximity zone.

4.5.1 Influence of Pedestrians' 'Distancing' Awareness

Comparing Sc.000 and Sc.100 reveals the influence of pedestrians' 'distancing' awareness during the COVID-19 pandemic. The t-test results in Table 21 show that the numbers of agents in proximity Zone C and D are significantly different. This result shows that pedestrians' 'distancing' awareness influences pedestrian exposure within the range of proximity Zone C.

Table 21 – T-test of Sc.000 and Sc.100 simulation results.

Flowrate (year)	Proximity zone	Scenario (Agent number, Mean ± Std. Deviation)		t	p
		Sc.000 (n=20)	Sc.100 (n=20)		
2015	Zone C	332.90 ± 29.29	305.40 ± 24.04	3.246	0.002**
2020	Zone C	173.50 ± 18.79	152.35 ± 17.76	3.658	0.001**
2015	Zone D	31.55 ± 6.14	21.90 ± 3.63	6.050	0.000**
2020	Zone D	19.75 ± 4.81	13.60 ± 4.60	4.130	0.000**
* p<0.05 ** p<0.01					

4.5.2 Influence of Mask-Wearing Population

Comparing Sc.100 with Sc.110, Sc.120 reveals the influence of the mask-wearing population, with a ladder of 0%, 50%, and 90%. In the flowrate for 2015, the exposure-free agents increased by 13.50% and 24.42%, respectively. In the flowrate for 2020, the exposure-free agents increased by 9.93% and 18.02%. Because wearing a non-woven mask cannot protect from air leaks in proximity Zone D, the increase of exposure-free agents is non-linear. Pedestrians' personal spacing avoidance behavior mainly happens in the 2.44 m range of Zone C. The mask-wearing ratio among the population affects the number of agents in Zone C directly. In flowrate 2015, the agents in proximity Zone C reduced by 7.76% and 5.83%, respectively, and in flowrate 2020, the agents in proximity Zone C reduced by 4.90% and 4.12%. In both flowrate 2015 and 2020, the

agents in proximity Zone D change minorly. This result shows that the mask-wearing population has an important influence on pedestrian proximity probability.

4.5.3 Influence of Standing Pedestrians

Comparing Sc.100 and Sc.101 reveals the influence of standing agents on proximity probability. In flowrates 2015 and 2020, the exposure-free agents reduced by 0.14% and 0.76%. This result shows that standing pedestrians influence proximity probability to a minor degree.

4.5.4 Violation of Physical Distancing with A Contagious Person

Zone C and Zone D together have a range of 2.44 m, which covers a loose range of physical distancing. Comparing the results of Sc.000 and Sc.100 of flowrate 2020 shows that by improving pedestrians' 'distancing' awareness, the violation of physical distancing with a contagious agent can be reduced by 1.67%. Comparing the results of Sc.100, Sc.110, and Sc.120 of flowrate 2020 shows that, by encouraging 90% of the population to wear a face mask, the exposure within the physical distancing to a contagious agent can be reduced by 8.89%. Comparing the results of Sc.000 and Sc.101 of flowrate 2020 shows that by removing the standing pedestrians, the violation of physical distancing with a contagious agent can be reduced by 0.85%.

4.6 Chapter Conclusions

This chapter aimed to develop an ABM tool for estimating pedestrian proximity probability in public space and explore an agent-based modeling and simulation framework for emergency space planners and designers.

We first analyzed pedestrian walking behavior before and during the COVID-19 pandemic from video clips recorded in 2015 and 2020. The analysis results show that under the influence of COVID-19 pandemic: 1) Pedestrian walking speed does not show the difference; 2) Pedestrians have significant longer avoidance distance; 3) The lateral displacement offset of avoidance behavior is slightly higher in PSA; 4) Pedestrians conduct LRA more often. These findings are thought to reflect pedestrian's 'distancing' awareness.

Based on the above analysis results, an ABM, ASCPP, was developed to model pedestrian behavior in ordinary and pandemic situations. This model included four rulesets, 16 rules in total, and was validated by reproducing PSA and LRA rates with the video analysis results in ordinary and pandemic situations. Then simulations were conducted for five scenarios under both situations considering the presence/absence of 'distancing' awareness, the different face-mask wearing rate, and the obstruction of flows by people standing still. In each scenario, the average probability of pedestrian proximity was estimated. The simulation results show that: 1) T-tests have been conducted for the presence/absence of the 'distancing' awareness, and significant differences were confirmed; 2) The influential factors affect pedestrian proximity probability with a contagious agent in the sequential order of face-mask wearing rate, 'distancing' awareness, and the presence of standing pedestrians; 3) Quantitively estimated the violation of physical distancing with a contagious pedestrian in a hypothetical scenario in a facility-level space as a tool to help future policymaking.

Under the worldwide pandemic, the need to reduce physical contact in public spaces is increasing. Through this study, we have gained the prospect to develop a feasible methodological framework for pedestrian agent modeling and simulation that

is consistent with the data survey to contribute to spatial considerations during the pandemic. The future challenge concerns larger-scale data collection in commuting hours and different space types.

CHAPTER 5. CONCLUSIONS

This dissertation mainly discussed how to utilize ABMS for analyzing and countermeasure complex spatial safety problems, such as crowd accident and infection problems. There are two aspects to consider when trying to solve or alleviate such problems: spatial design and crowd management. Based on the literature review, an evaluation scheme for analyzing different spatial safety problems has been summarised, and a research framework for developing corresponding ABMS has been established.

5.1.1 Evaluation Scheme for Pedestrian Spatial Safety Problems

Our evaluation scheme for pedestrian spatial safety problems includes three parts: 1) a detailed division and explanation of static and dynamic crowd density; 2) considering items of safe urban public spaces, and 3) considering items of pedestrian encounter.

We utilized pedestrian body array maps and pedestrian experiments to identify the different crowd statuses between static and dynamic crowd density. Because pedestrian and crowd dynamics will have different characteristics, distinguish the density range is necessary. So we divided pedestrian density terms, such as the density range for lower-density, relatively high-density, higher-density, referring to related literature.

The considering items for evaluating safe urban public spaces are different between daily pedestrian facilities and MG events. The daily pedestrian facilities require maximizing pedestrian flow's efficiency and dividing the level of safety. The evaluation items for pedestrian facilities include four scale descending categories: general layout, design element layout, the shape of design elements, and the function

and schedule of the space. In contrast, the evaluation items for MG events require assessing the criticality of the crowd conditions. We reviewed the lessons learned from past crowd accidents and summarised the evaluation items by spatial design and crowd management in two categories. The requirements and part of the reference value are provided.

The considering items for evaluating pedestrian encounter is for quantitatively measure the contact probability from a contagious pedestrian. The requirement of physical distancing policies under the pandemic added new considerating items in addition to physical contact safety and social distance comfortable requirements. The evaluation items are the four pedestrian proximity zones we divided based on the infectious characteristics of COVID-19.

5.1.2 ABMS Framework for Analyzing Two Specific Spatial Safety Problems

An ABMS framework can be categorized into four sub-elements: 1) input, 2) scenario, 3) agent, and 4) output. Here we conclude the significant characteristics of our framework briefly:

1) The input data can be acquired through the empirical/experimental process or theoretical hypothesis.

2) Scenario setting decides many characteristics of a simulation model, such as space division, time setting, and routing strategy. The space division of our ABMS framework is a hybrid cell-based model combined with an absolute coordinate system and a relative coordinate system. In the absolute coordinate system, the cell is set as 40 cm square to get an essential setting, considering the walking speed is approximately 1.2 m/s with three steps per second. The absolute coordinate system is a 2D space layout

with two decimal places real numbers. While the relative coordinate system, the cell size varies by each agent's step pace. In the relative coordinate system, the agent avoids other agents following our defined behavioral rules. The above settings ensure the agents in our framework can move at 360° and different speeds. The routing in our framework follows the preset waypoints, but the agent can deviate from its direction for short steps to make avoidance.

3) The agent in our framework has its physical features, pedestrian behavior rules, and other advance features according to the research topic. Besides the main agent type, other agent types can also be introduced into the simulation environment.

4) The outputs of our simulation results vary according to the research purpose.

This developed ABMS framework has been utilized in creating the specified simulators for the following case studies.

5.1.3 Case Study: Shanghai Bund Crowd Accident

We investigated and analyzed a crowd accident that happened in the Shanghai Bund Waterfront. This case study aims to introduce analyzing dangerous space layouts dealing with MG events and explore countermeasures. We investigated publicly available documents, videos, and materials. Based on the investigation, we conducted a site survey to get the pedestrian flow date of the site. With the above findings, we build an agent-based simulator following the previously validated ASPFver4.0 pedestrian walking rules. Together with five other comparison scenarios, the basic space layout scenario, including three space designs and two crowd management improvements, is tested. The analysis results show that even simple crowd control measures such as capacity reserve and more proper route planning will improve crowd

safety for MG events. General suggestions to urban public space safety under relatively high-density are also proposed.

5.1.4 Case Study: Pedestrian Encounter Under COVID-19

With the global pandemic of COVID-19, physical distancing has become a recommended practice in public spaces. Since the planning standards for indoor space use are based on pre-pandemic situations, there are no quantitative studies considering the pedestrian proximity probability in public spaces. With this background, agent-based modeling (ABM) that takes into account the dynamic characteristics of pedestrian behavior is promising. This study aims to develop an ABM tool for estimating pedestrian proximity probability in a station atrium and explore an agent-based modeling and simulation framework for emergency space planners and designers.

First, we reviewed relevant studies on the general characteristics of the COVID-19 pandemic, global physical distancing policies and recommendations, and the application of ABM in the field of density control in indoor public spaces and established pedestrian proximity zones from proximity levels A to D from these studies.

Next, we conducted a comparative analysis of pedestrian avoidance behavior in low-density conditions filmed during non-commuting hours on weekdays in the atrium of Nagoya Station in June 2020 during the pandemic, with video footage taken in the same location in 2015 during the ordinary period. As a result, even the pedestrian walking speed at both time periods do not show the difference, it was found that the average starting distance of pedestrians' avoidance behavior is longer during a pandemic (with a significant difference in ANOVA), which may reflect people's awareness of 'distancing'. Therefore, we divided avoidance behavior into two categories,

PSA (personal spacing avoidance) and LRA (long-range avoidance), using 3.66 m as the threshold for the avoidance distance, and then we analyzed these behaviors in details.

Then, ASCPP was developed to handle pedestrian behavior in ordinary and pandemic situations and has 16 behavioral rules based on ASPF. The model was validated by reproducing the times of PSA and LRA occurrences at both time periods. Next, we simulated the counter flows in the station atrium with five scenarios that dealt with the 'distancing' awareness, facial masks, and the obstruction of flow by the presence of people standing still, and estimated the effect of each scenario on the probability of proximity under the condition of 1% contagious people in the population. In particular, a t-test was conducted for the 'distancing' awareness, and a significant difference was confirmed.

The conclusion summarizes the findings from the series of works. Through this study, we have gained the prospect to develop a feasible methodological framework for pedestrian agent modeling and simulation that is consistent with the data survey to contribute to spatial considerations during the pandemic. The future challenge concerns larger-scale data collection.

APPENDIX A. ANTHROPOMETRIC DATA

Table 22 concluded the anthropometric data of the world's population, mainly the population between the ages of 20-60 (Pheasant, 2003). The data covers 5%, 50%, and 95% of the population are given, and the researchers should select relevant data according to the research topic.

Table 22 – Anthropometric sizes of the world's population (adults).

Population	Breadth (mm)			Depth (mm)		
	5th%ile	50th%ile	95th%ile	5th%ile	50th%ile	95th%ile
British male	420	465	510	215	250	285
British female	355	395	435	210	250	295
Swedish male	420	465	510	185	220	255
Swedish female	355	390	425	185	241	300
Dutch male	430	475	520	240	285	330
Dutch female	355	400	445	230	290	350
French male	425	470	515	210	245	280
French female	380	425	470	205	250	295
Polish male	405	440	475	215	245	275
Polish female	350	380	410	205	245	285
US male	425	470	515	220	255	290
US female	360	400	440	210	255	300
Brazilian male	400	445	490	205	235	275
Sri Lankan male	330	370	400	145	170	205
Sri Lankan female	300	330	360	130	170	210
Indian male	375	410	440	145	170	205
Hong Kong Chinese male	380	425	470	155	195	235
Hong Kong Chinese female	335	385	435	160	215	270
Japanese male	405	440	475	180	205	230
Japanese female	365	395	425	175	205	235
Average	378.5	418.75	458.25	191.25	229.8	270.25
Maximum	430	475	520	240	290	350

APPENDIX B. LEVEL OF SERVICES

Fruin's Level-of-Services (LoS) concept is one of the earliest evaluation standards to define the comfort and safety level for crowd gathering in public places. Table 23 shows a summary of the LoS standards. In the LoS standards, when the density is over 0.7 people/m^2 on horizontal roads and 1.1 people/m^2 on stairs, free walking speed cannot be guaranteed. However, the LoS standards have some problems when dealing with the high-density environment. Figure 34 shows the body template Fruin adopted for the New York subway's standing capacity design - an ellipse of 600mm and 450 mm. This ellipse covers 95% of an adult male's body size. The body ellipse is designed to be large, enable to consider the personal belongings and the psychology of keeping a distance from others and body swings, which is questioned about being too loose (Still, 2000).

Moreover, the LoS standards stop in service level F, at 2.5 people/m^2, where people are not closely connected to each other. Unlike the flow paralysis or stoppage described in service level F by Fruin, we can often see the high-density and high-speed pedestrian movements in public transportation facilities and the stadiums' exits. This condition proves that even in service level F, the pedestrian movement does not stop, and the density will continue to increase. Those reasons make the risk of high-density pedestrian movement far exceed the measurement of the LoS.

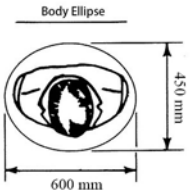

Figure 34 – Fruin Body Ellipse.

Table 23 – Relationships between pedestrian status and density in Level-of-Services.

LoS*	Density (persons/m2)		Pedestrian walking status			
-	Horizontal	Stairs	Free walking speed	Free to exceed the others	Possibility of conflicts	Flow status (Uni-direction, stairs)
A	0.3	0.5	Completely guaranteed	Free	None	-
B	0.3-0.45	0.5-0.7	Mostly guaranteed	Free movement in the same direction/ some difficulty on stairs	Crossroads/counterflow, occur slightly	5 steps space in front and back, 0.9-1.2m gap in left and right
C	0.45-0.7	0.7-1.1	Some restrictions	Some restrictions	Crossroads/counterflow, very likely to occur	4-5 steps space in front and back, 0.9m gap in left and right
D	0.7-1.1	1.1-1.5	Mostly cannot be guaranteed	Mostly cannot be guaranteed/ very difficult on stairs	Crossroads/counterflow, high possibility to occur	3-4 steps space in front and back, 0.6-0.9m gap in left and right
E	1.1-2.0	1.5-2.5	All people cannot	All people cannot	Very likely to occur	2-4 steps space in front and back, 0.6m gap in left and right, intermittent flow
F	>2.0	>2.5	Extremely restricted	All people cannot	Cannot move without touching others	Unstable paralysis or cessation, very dangerous

*LoS: Level-of-Services concept developed by Fruin, 1971.

REFERENCES

Akashi Citizen's Summer Festival Accident Investigation Committee. (2002). Report on the Investigation of the Fireworks Display Accident at the 32nd Akashi Citizen's Summer Festival, 2002.1, last update: March 28, 2019, Accessed at: June 14, 2021 (in Japanese) https://www.city.akashi.lg.jp/anzen/anshin/bosai/kikikanri/jikochosa/dai32hokoku.html

Al-Kodmany, K. (2013). Crowd Management and Urban Design: New Scientific Approaches, *URBAN DESIGN International*, *18*(4), 282–295

Alaska, Y. A., Aldawas, A. D., Aljerian, N. A., Memish, Z. A., & Suner, S. (2017). The Impact of Crowd Control Measures on the Occurrence of Stampedes During Mass Gatherings: The Hajj Experience, Travel Medicine and Infectious Disease, *15*, 67–70

Alshammari, S., & Mikler, A. R. (2015). Modeling Disease Spread at Global Mass Gatherings: Hajj as a Case Study, 2015 International Conference on Healthcare Informatics, 574–577

Artisoc, Kozo Keikaku Engineering Inc., Accessed at June 14, 2021 https://www.kke.co.jp/en/solution/theme/artisoc.html

Bandini, S., Federici, M. L., & Vizzari, G. (2007). Situated Cellular Agents Approach to Crowd Modeling and Simulation, Cybernetics and Systems, 38(7), 729–753

Bar-Yam, Y. (2002). General Features of Complex Systems, Encyclopedia of Life Support Systems, EOLSS UNESCO Publishers, Oxford, UK, 2002

Bonabeau, E. (2002). Agent-based modeling: Methods and techniques for simulating human systems, Proceedings of the National Academy of Sciences, 99, 7280–7287

Bourouiba, L. (2020). Turbulent Gas Clouds and Respiratory Pathogen Emissions: Potential Implications for Reducing Transmission of COVID-19, JAMA - Journal of the American Medical Association, 323(18), E1–E2

Blue, V. J., & Adler, J. L. (2000). Modeling Four-Directional Pedestrian Flows, Transportation Research Record, 1710(1), 20–27

Campanella, M., Hoogendoorn, S., & Daamen, W. (2014). Quantitative and Qualitative Validation Procedure for General Use of Pedestrian Models, Pedestrian and Evacuation Dynamics 2012, In Weidmann, U., Kirsch, U. & Schreckenberg, M. (Eds.), Springer International Publishing, 891–905

Centers for Disease Control and Prevention, Travelers From Countries with Widespread Sustained (ongoing) Transmission Arriving in the United States, Last updated February 18, 2021, Accessed February 26, 2021 https://www.cdc.gov/coronavirus/2019-ncov/travelers/after-travel-precautions.html

Challenger, R., Clegg, C., Robinson, M., & Leigh, M. (2010). Understanding Crowd Behaviours: Supporting Theory and Evidence, 2, Centre for SocioTechnical Systems Design (CSTSD), Leeds University Business School, London, UK

Dijkstra, J., Jessurun, J., Timmermans, H. (2001). A multi-agent cellular automata model of pedestrian movement, Physical Chemistry Chemical Physics - PHYS CHEM CHEM PHYS, 173–181

D'Orazio, M., Bernardini, G., & Quagliarini, E. (2020a). How to restart? An agent-based simulation model towards the definition of strategies for COVID-19 "second phase" in public buildings, e-prints, Accessed June 14, 2021 https://arxiv.org/abs/2005.12547

D'Orazio, M., Bernardini, G., & Quagliarini, E. (2020b). Sustainable and resilient strategies for touristic cities against COVID-19: an agent-based approach, e-prints, Accessed June 14, 2021, https://arxiv.org/abs/2005.12547

Dridi, M. H. (2014). Pedestrian Flow Simulation Validation and Verification Techniques, arXiv:1410.0603 [physics.data-an], http://arxiv.org/abs/1410.0603

Duives, D. C., Daamen, W., & Hoogendoorn, S. P. (2013). State-of-the-art crowd motion simulation models, 37, 193–209

Fang, Z., Huang, Z., Li, X. et al. (2020). How many infections of COVID-19 there will be in the "Diamond Princess"-Predicted by a virus transmission model based on the simulation of crowd flow, e-prints, Accessed June 14, 2021 https://arxiv.org/abs/2002.10616

Fayoumi, A., Al-Ghoraibi, S., Fadel, A., Al-Aswadi, F., Mujallid, F., & Wazzan, M. (2011). A Simulator to Improve the Pilgrims Performance in Stoning Ritual in Hajj, IJCSNS International Journal of Computer Science and Network Security, *11*(5), 141–144

Federici, M. L., Manenti, L., & Manzoni, S. (2014). A Checklist for the Evaluation of Pedestrian Simulation Software Functionalities, arXiv:1404.7717 [cs.MA] https://arxiv.org/abs/1404.7717

Fruin, J. J. (1971). Pedestrian Planning and Design, New York: Metropolitan Association of Urban Designers and Environmental Planners, Inc.

Golas, A., Narain, R., Curtis, S., & Lin, M. C. (2014). Hybrid Long-Range Collision Avoidance for Crowd Simulation, *IEEE* Transactions on Visualization and Computer Graphics, 20(7), 1022–1034

Guo, R.-Y., Wong, S. C., Huang, H.-J., Zhang, P., & Lam, W. H. K. (2010). A microscopic pedestrian-simulation model and its application to intersecting flows, Physica A: Statistical Mechanics and Its Applications, 389(3), 515–526

Hall, E. T. (1966). The Hidden Dimension, Anchor Books.

Helbing, D., & Molnar, P. (1998). Self-Organization Phenomena in Pedestrian Crowds, Understanding Complex Systems, arXiv:cond-mat/9806152 [cond-mat.stat-mech], https://doi.org/10.1007/978-3-642-24004-1_3

Helbing, D. (2012). Agent-Based Modeling, Social Self-Organization, D. Helbing (ed.), Springer Berlin Heidelberg, 25–70

Helbing, D., Buzna, L., Johansson, A., Werner, T., Johansson, A., & Werner, T. (2005). Self-Organized Pedestrian Crowd Dynamics: Experiments, Simulations, and Design Solutions, Transportation Science, 39(1)

Helbing, D., Farkas, I., Molnar, P., & Vicsek, T. (2002). Simulation of pedestrian crowds in normal and evacuation situations, Pedestrian and Evacuation Dynamics, 21–58

Helbing, D., & Johansson, A. (2010). Pedestrian, Crowd, and Evacuation Dynamics, arXiv:1309.1609 [physics.soc-ph], https://arxiv.org/abs/1309.1609

Helbing, D., Johansson, A., & Al-Abideen, H. Z. (2007a). Crowd turbulence: the physics of crowd disasters, arXiv:0708.3339 [physics.soc-ph] https://arxiv.org/abs/0708.3339

Helbing, D., Johansson, A., & Al-Abideen, H. Z. (2007b). Dynamics of crowd disasters: An empirical study, Physical Review E - Statistical, Nonlinear, and Soft Matter Physics, 75(4), 1–7

Helbing, D, & Balietti, S. (2011). From social data mining to forecasting socio-economic crises, The European Physical Journal Special Topics, 195(1), 3

Helbing, D., & Mukerji, P. (2012). Crowd disasters as systemic failures: analysis of the Love Parade disaster, EPJ Data Science, 1(1), 7

Henderson, L. F. (1971). The Statistics of Crowd Fluids, Nature, 229(5284), 381–383

Ilyas, Q. M. (2013). A NetLogo Model for Ramy al-Jamarat in Hajj, Journal of Basic and Applied Scientific Research, 3(12), 199–209

Imam, A., & Alamoudi, M. (2014). Mina: the city of tents origination and development, International Conference Virtual City and Territory, 1351-1365

International Maritime Organization, London. (2007). MSC.1/Circ.1238: Guidelines for Evacuation Analysis for New and Existing Passenger ships, Annex 3

International Standards Organization. (2008). Fire Safety Engineering Assessment, Verification and Validation of Calculation Methods, ISO 16730

Japanese Architecture Society. (1980). Integration of Architectural Design 3, Unit Space I, Maruzen Publishing Co., Ltd, 50–57 (in Japanese)

Kaitsuji, M. (2012). A Study on Measures to Prevent a High-Density Crowd Stagnation To Trigger a Crowd Accident at Large-Scale Events, Ph.D. thesis, Kobe University (in Japanese)
http://www.lib.kobe-u.ac.jp/handle_kernel/D1005471

Kaitsuji, M., & Hokugo, A. (2014). Venue Suitability for Large-Scale Events from the Viewpoint of Safety Measures, Pedestrian and Evacuation Dynamics 2012, In Weidmann, U., Kirsch, U. & Schreckenberg, M. (Eds.), Springer International Publishing, 1405–1416

Kaneda, T. (2007). Developing a Pedestrian Agent Model for Analyzing an Overpass accident, Pedestrian and Evacuation Dynamics 2005, In Waldau, N., Gattermann, P., Knoflacher, H. & Schreckenberg, M. (Eds.), Springer Berlin Heidelberg, 273–284

Kaneda, T., & He, Y. (2009). Modeling and Development of an Autonomous Pedestrian Agent — As a Simulation Tool for Crowd Analysis for Spatial Design, Agent-Based Approaches in Economic and Social Complex Systems V,

In Terano, T., Kita, H., Takahashi, S., & Deguchi, H. (Eds.), Springer Japan, 107–118

Kaneda, T., & Okayama, D. (2007). A Pedestrian Agent Model Using Relative Coordinate Systems, Agent-Based Approaches in Economic and Social Complex Systems IV, In Terano, T., Kita, H., Deguchi, H. & Kijima, K. (Eds.), Springer Japan, 63–70

Kaneda, T., Yoshida, T., He, Y., Tamada, M., & Kitakami, Y. (2010). Adding Higher Intelligent Functions to Pedestrian Agent Model, Pedestrian and Evacuation Dynamics 2008, In Klingsch, W. W. F., Rogsch, C., Schadschneider, A. & Schreckenberg, M. (Eds.), Springer Berlin Heidelberg, 529–535

Keppel, G: Design and Analysis: A Researcher's Handbook (3rd ed.), Englewood Cliffs: Prentice-Hall, Inc., 1991

Khan, I., & McLeod, R. D. (2012). Managing Hajj Crowd Complexity: Superior Throughput, Satisfaction, Health & Safety, Kuwait Chapter of the Arabian Journal of Business and Management Review, 2(4), 45–59

Kim, S., Guy, S. J., Hillesland, K., Zafar, B., Gutub, A., & Manocha, D. (2015). Velocity-based modeling of physical interactions in dense crowds, The Visual Computer, 31(5), 541–555

Kissler, S., Tedijanto, C., Lipsitch, M., & Grad, Y. H. (2020). Social distancing strategies for curbing the COVID-19 epidemic, MedRxiv, 2020.03.22.20041079 https://doi.org/10.1101/2020.03.22.20041079

Krausz, B., & Bauckhage, C. (2012). Loveparade 2010: Automatic video analysis of a crowd disaster, Computer Vision and Image Understanding, 116(3), 307–319

Kurdi, O. (2017). Crowd modelling and simulation, Doctoral Thesis of the University of Sheffield, Department of Computer Science

Lerner, A., Chrysanthou, Y., & Lischinski, D. (2007). Crowds by Example, Computer Graphics Forum, 26(3), 655–664

Lee, R. S. C. & Hughes, R. L. (2005). Exploring Trampling and Crushing in a Crowd, Journal of Transportation Engineering, 131(8), 575–582

Low, S. M. (2003). Embodied Space(s): Anthropological Theories of Body, Space, and Culture, Space and Culture, 6(1), 9–18

Lubaś, R., Porzycki, J., Wąs, J. and Mycek, M. (2016). Validation and Verification of CA-Based Pedestrian Dynamics Models, Journal of Cellular Automata, 11(4), 285–298

Macal, C., & North, M. (2014). Introductory tutorial: Agent-based modeling and simulation, Proceedings of the Winter Simulation Conference 2014, 6–20

Mahmood, I., Haris, M., & Sarjoughian, H. (2017). Analyzing Emergency Evacuation Strategies for Mass Gatherings Using Crowd Simulation And Analysis Framework: Hajj Scenario, Proceedings of the 2017 ACM SIGSIM Conference on Principles of Advanced Discrete Simulation, 231–240

Ministry of Health, Labour and Welfare, Information on Health and Medical Consultation, Accessed February 26, 2021, https://www.mhlw.go.jp/stf/covid-19/kenkou-iryousoudan_00006.html

Mizuno, T., Shohmitsu, M. and Kaneda, T. (2016). A Study on the Agent-Simulation of Waiting Behaviours Inside a Transfer Station Space, 2016 IEEE 40th Annual Computer Software and Applications Conference (COMPSAC), 2, 111-116

Nan-fang Metropolis Daily. (2015). Accessed at June 14, 2021 https://www.iqiyi.com/w_19rxvc0zed.html

Okada K. (2011). Safety Technology for Crowd, Kajima Institute Publishing CO., LTD (in Japanese)

Owaidah, A., Olaru, D., Bennamoun, M., Sohel, F. & Khan, N. (2019). Review of Modelling and Simulating Crowds at Mass Gathering Events: Hajj as a Case Study, Journal of Artificial Society and Social Simulation, 22(2)9

Pheasant, S. (2003). Bodyspace: Anthropometrey, Ergonomics and the Design of Work, Second Edition, Taylor & Francis, ISBN 0-7484-0326-4

Pretorius, M., Gwynne, S., & Galea, E. R. (2015). Large crowd modelling: an analysis of the Duisburg Love Parade disaster, Fire and Materials, 39(4), 301–322

Ronchi, E., Kuligowski, E.D., Reneke, P.A., et al. (2013). NIST Technical Note 1822: The Process of Verification and Validation of Building Fire Evacuation Models

SFPE Task Group on Human Behavior in Fire (2019). SFPE Guide to Human Behavior in Fire, 2nd Edition

SPSSAU, QingSi Technology Ltd., Accessed September 9, 2020, Accessed at June 14, 2021, https://spssau.com/en/index.html

Sarmady, S., Haron, F., & Talib, A. Z. H. (2008). Multi-Agent Simulation of Circular Pedestrian Movements Using Cellular Automata, 2008 Second Asia International Conference on Modelling & Simulation (AMS), 654–659

Shanghai Bund Chen Yi Square Crowd Accident Investigation Committee. (2015). Investigation report on Shanghai Bund Chen Yi square crowd accident (in Chinese), Accessed at June 14, 2021 http://cpc.people.com.cn/n/2015/0121/c64387-26424620.html

Seyfried, A., Steffen, B., & Lippert, T. (2006). Basics of modelling the pedestrian flow, Physica A: Statistical Mechanics and Its Applications, 368(1), 232–238

Siddiqui, A. A., & Gwynne, S. M. V. (2012). Employing pedestrian observations in engineering analysis, Safety Science, 50(3), 478–493

Singhal, T. (2020). A Review of Coronavirus Disease-2019 (COVID-19), The Indian Journal of Pediatrics, 87(4), 281–286

Sohu News. 2rd January 2015, Accessed at June 14, 2021 http://news.sohu.com/20150102/n407479756.shtml

Still, G. K. (2000). Crowd Dynamics, Ph.D. thesis, University of Warwick, BSc Physical Sciences

Still, G. K. (2014). Introduction to Crowd Science, CRC Press, Taylor & Francis Group, ISBN-13: 978-1-4665-7965-1

Tang, S., Kwak, D. and Kitahara, T. (2012a). A Study of a Distance Modle of People-To-People Avoiding Behavior in a Station Square: Correlative Factors of People-To-People Avoidance Behavior Distance, Journal of Architecture and Planning (Transactions of AIJ), 77(679), 2101–2107

Tang, S., Kwak, D. and Kitahara, T. (2012b) A Study of Pedestrian Personal Space in a Station Square: People-To-People Avoidance Behavior in Nishi-Chiba Station Square, Journal of Architecture and Planning (Transactions of AIJ), 77(681), 2569–2575

Tatebe, K. and Nakajima, H. (1990). Avoidance Behavior Against a Stationary Obstacle under Single Walking: A Study on Pedestrian Behavior of Avoiding

Obstacles (I), Journal of Architecture, Planning and Environmental Engineering (Transactions of AIJ), 418, 51–57 (in Japanese)

Tatebe, K., Tsujimoto, M. and Shida, K. (1994). Methods for Judging the Beginning Point of Avoiding Behavior and Avoidance Distance between A Pedestrian and a Standing Obstacle: A Study on Pedestrian Behavior of Avoiding Obstacles (II), Journal of Architecture and Planning (Transactions of AIJ), 59(465), 95–104 (in Japanese)

Verma, S., Dhanak, M., & Frankenfield, J. (2020). Visualizing the effectiveness of face masks in obstructing respiratory jets, Physics of Fluids, 32(6), 61708

World Health Organization (2021). Coronavirus Disease (COVID-19) Advice for the Public, Last updated February 24, 2021, Accessed February 26, 2021 https://www.who.int/emergencies/diseases/novel-coronavirus-2019/advice-for-public

Wu, W., Xi, W., & Xi, D. (2011). To return the space to the public – landscape transformation design of Shanghai bund waterfront, Chinese Landscape Architecture 2011(7), 22–25 (in Chinese)

Xi, W., & Xu, W. (2011). Remodeled classic, the centenary Shanghai bund: detailed plan of the urban design & site plan of Shanghai bund waterfront, Urbanism and Architecture 2011(2), 42–45 (in Chinese)

Zainuddin, Z., Thinakaran, K., & Abu-Sulyman, I. (2009). Simulating the Circumambulation of the Ka'aba using SimWalk, European Journal of Scientific Research ISSN, 38, 1216–1450